Technical Report

T - 3

Prepared for

National Aeronautics & Space Administration

Electronics Research Center

Under

NASA GRANT NGR-33-006-020

Prepared by

Allan Guida, Research Fellow

Donald L. Schilling, Associate Professor

Department of Electrical Engineering

Polytechnic Institute of Brooklyn

ABSTRACT

The maximum likelihood equation for demodulating an FM signal corrupted by additive gaussian noise is derived and examined. Asymptotic formulae for the signal-to-noise ratio of the maximum likelihood estimate are calculated for high carrier-to-noise ratio and infinite observation time. The results show that the FM discriminator is approximately equivalent to the maximum likelihood estimator at high carrier-to-noise ratios. An iterative method for solving the maximum likelihood equation at any carrier-to-noise ratio is presented. The method consists of generating a sequence of test solutions by varying the parameter ε in the following equation:

Test Solution = Approximate Solution +

ε [Solution error due to the Approximate Solution]

where the solution error is defined as the error produced by substituting the approximate solution in the maximum likelihood equation. For each value of ε, the likelihood function of the associated test solution is evaluated; the test solution for which the likelihood function is a maximum replaces the approximate solution and the process is repeated. Computer evidence of the convergence of the series of approximate solutions to a solution with high likelihood is presented.

It is noted that the difference between optimum FM receivers and non-optimum FM receivers (FM discriminator, phase-locked loop, FM with feedback) lies mainly in the number of spikes per second present in the output of these receivers. The problem of spike detection is considered and a spike detector is designed for an FM discriminator. Computer

results on the capability of the spike detector are presented.

Two simple FM receivers are analyzed using appropriate auto-correlation functions and spectral densities. The results are compared to the FM discriminator.

TABLE OF CONTENTS

TABLE OF FIGURES

Chapter 1

Introduction

1.1 Statement of the problem

The problem of designing optimum receivers for demodulating analog signals subject to additive gaussian noise has been handled satisfactorily in the case of linear modulation (AM) but the cases of nonlinear modulation (FM, PM) are still, for the most part, unsolved. (Numerous articles have been written on the PLL and FMFB but none of the designs lead to devices which are optimum in some commonly accepted sense (least mean square error or minimum variance (MV) maximum likelihood (ML), etc.). Some may, in actuality, be very close to optimum devices, but this fact has not yet been demonstrated). In order to extend the present knowledge of optimum FM reception, the ML estimator for FM will be investigated. The primary objective will be the solution of the ML equation for FM. In addition, the output signal-to-noise power ratio obtainable with the ML estimator at high input carrier-to-noise power ratios will be examined.

An alternate approach to the optimization problem is to consider those characteristics of the present receivers (particularly FM receivers) which make them sub-optimum. It can be shown (1.9) that the difference lies mainly in the number of "spikes" present in the output of FM receivers. These spikes are sharp pulses present in the unfiltered FM receiver output noise. When we examine the outputs of FM receivers, those with a smaller mean square error have fewer spikes. Theoretically, there must be some maximum number of spikes which can be detected and removed; the corresponding FM receiver would then be optimum in a spike detection sense. The spike detection approach will be investigated by designing a spike detection and correction system for an FM receiver.

A third approach to the optimization problem is to examine various FM

receivers which can be completely analyzed to determine those characteristics which tend to improve output signal-to-noise power ratio. Two elementary FM receivers will be examined.

1.2 Summary of prior work

The first step toward solving the problem of designing an optimum PM receiver was made by Lehan and Parks (1.1) in 1953, when they considered the problem from the point of view of statistical estimation theory. Unfortunately, the mathematics presented in their paper is not clear enough for a complete understanding of their work, although the equations they derive appear to be correct. In 1954 Youla (1.2) placed their work on a firm mathematical basis. He derived a pair of non-linear integral equations whose solution is the ML estimate of the modulation in the PM case. Subsequently in 1964, Becker and Lawton (1.3) extended the results to the FM case, again reducing the problem to one of solving a pair of non-linear integral equations. In 1964, Schwartz (1.4) demonstrated that the Youla equations could be derived using vector space concepts, which simplified the derivation considerably.

However, in none of these studies did the authors show how to solve the integral equations, other than to state that the equations closely resembled the phase-locked loop. In 1963, Van Trees (1.5) suggested an iterative technique for solving the equations in the white noise case where the two equations can be reduced to a single equation. However, this technique has never been successfully demonstrated.

The alternate approach to the optimum FM receiver problem, i.e., spike detection, was first investigated experimentally by Schilling (1.6) in 1966. Schilling designed a spike detector for an FSK system based on the facts demonstrated by Rice (1.7) in 1963. However, no other work appears to have been done in the area of spike detection.

1.3 Summary of results obtained

The SNR at the output of the linearized ML estimator for FM was evaluated for high CNR and it was found that the result is the same as for the FM discriminator. The difference between the two devices lies entirely in the number of spikes present in their respective outputs, which represents a minor contribution to the noise power at high CNR. Thus, we conclude that the FM discriminator is nearly an optimum receiver for analog FM signals at high CNR. It should be noted that for digital signals, where the probability of error is a more significant quantity than the SNR, spike noise cannot be neglected and the FM discriminator is a poor approximation to an optimum receiver even at high CNR.

Van Trees' (1.5) simple iteration procedure for solving the ML equation was improved upon by employing an additional function called the likelihood function, which provides a measure of the likelihood of a test solution. The new procedure consists of generating a sequence of test solutions by varying the parameter ϵ in the following equation:

Test Solution = Approximate Solution + ϵ•[Solution error due to the Approximate Solution]

where the solution error is defined as the error produced by substituting the approximate solution in the ML equation. For each value of ϵ selected, the likelihood function of the associated test solution is evaluated; the test solution for which the likelihood function is a maximum replaces the approximate solution. The solution error and the integrated absolute value of the solution error (called the total solution error) are evaluated and the process is repeated. When the total solution error goes below some preset value, the process stops. Otherwise, the process is stopped after a preset number of iterations. The last test solution is then an approximate solution to the ML equation.

There are several advantages obtained with the new process:

1. The process can be used at any CNR. [The simple iteration procedure is limited to low CNR].

2. The process requires fewer iterations than the simple iteration procedure; however, the iterations in the new process are more complex.

3. The computer time required for this process should be less than the simple iteration computer time when the initial test solution is far from the final solution because this process can accept large test solution increments without diverging.

4. The likelihood associated with the solution found by this process must be greater than or equal to the likelihood of the solution found by the simple iteration process. It has not been demonstrated, however, that the solution obtained is the absolute maximum likelihood solution.

A computer simulation of the process for solving the ML equation provided evidence that the technique leads to a convergent series of approximate solutions. A number of sequences of signal and noise values were tested and the SNR-CNR results were plotted on a graph along with the asymptotic SNR-CNR curves. However, an attempt to measure the threshold of the ML estimator was unsucessful because the amount of computer time required to perform this task was found to be excessive.

In the area of spike detection, a technique was developed which permitted spike detection to be applied to an analog FM system. For a particular CNR and β, and with sinewave modulation, a system was developed which was capable of detecting 57% of the spikes at the output of an FM discriminator. The basic technique used was to measure the difference between the short term and long term averages of the discriminator output and look for large values of this difference, indicating the presence of a large disturbance of short duration (a possible spike).

In an attempt to learn more about various explicit functions of FM data which, when filtered, lead to FM receivers, two simple cases were analyzed. The results indicated that the receivers were not optimum but it was interesting to compare them to the discriminator.

1.4 Definitions and approximations

The FM signal, S(t), is defined by the equation

$$S(t) = A \cos \left(\omega_c t + \int_0^t m(t)dt\right) \qquad (1.1)$$

where t = time

ω_c = carrier frequency, radians/second

m(t) = modulation

The following types of modulation are used:

1. gaussian (random): $p(m) = \frac{1}{2\pi\sigma^2} e^{-m^2/2\sigma^2}$

   where σ^2 = modulation power = $E(m^2)$

2. sinusoidal (deterministic): $m(t) = \beta\omega_m \sin \omega_m t$

   where $\beta = \omega_n/\omega_m$

   ω_m = modulation bandwith, radians/second

   ω_n = one sided bandwidth of S(t), radians/second

3. pulse (deterministic): $m(t) = \sigma[u(t) - u(t-T)]$

   where u(t) = unit step

Gaussian modulation is used in deriving all theoretical results. Sinusoidal modulation and pulse modulation are used in the computer simulation of spike detection and the solution of ML equation respectively.

It will be assumed in all cases that

$$\omega_c \gg \omega_r \gg \omega_m$$

and that

$$\omega_n \doteq \sigma\sqrt{2} \qquad (1.2)$$

The latter approximation is often used for sinusoidal modulation; see for example, Rice (1.7). [A paper by Stewart (1.8) in 1954 indicates that for gaussian modulation, the 3db bandwidth of S(t) is approximately 1.2σ].

There are two types of input noise that will be considered in this thesis.

A. White Gaussian Noise, $n_w(t)$

This refers to gaussian noise with double sided spectral desnity

$$S_{nw}(\omega) = N_o, \quad -\infty \leq \omega \leq +\infty$$

and autocorrelation function

$$R_{nw}(t) = N_o\, \delta(t)$$

This noise can be separated into two components using the equation

$$n_w(t) = x_w(t) \cos \omega_c t - y_w(t) \sin \omega_c t \qquad (1.3)$$

Each of the two noises, $x_w(t)$ and $y_w(t)$ are also gaussian and have the same spectral density and autocorrelation as $n_w(t)$.

B. Band Pass Gaussian Noise, n(t)

This refers to gaussian noise with the spectrum shown in Fig. 1.1. This noise can also be separated into two components using the equation

$$n(t) = x(t) \cos \omega_c t - y(t) \sin \omega_c t \tag{1.4}$$

The two noises, x(t) and y(t) have the spectral density shown in Fig. 1.2.

The input signal power-to-noise power ratio will be called the carrier-to-noise ratio and will be designated CNR. For the case of FM, the carrier is

$$A \cos (\omega_c t + \int m)$$

having a power equal to $A^2/2$. For determining input noise power, only the noise contained in the region of frequencies ω such that

$$|\omega - \omega_c| \leq \omega_n$$

will be considered. Hence, the carrier-to-noise ratio is

$$\text{CNR} = \frac{\text{Carrier Power}}{\text{Input Noise Power}} = \frac{\frac{A^2}{2}}{\frac{1}{\pi}\int_{\omega_c-\omega_n}^{\omega_c+\omega_n} N_\theta \, d\omega} = \frac{A^2 \pi}{4 N_o \omega_n} \tag{1.5}$$

The output signal power-to-noise power ratio will be called the signal-to-noise ratio and will be designated SNR. If e_o is the output of the FM receiver, then the signal-to-noise-ratio is given by

$$\text{SNR} = \frac{\text{Modulation Power}}{\text{Output Noise Power}} = \frac{\sigma^2}{E(e_o - m)^2} \tag{1.6}$$

The term threshold will be used in connection with the SNR versus CNR curves of FM receivers. These curves generally approach an asymptotic line from below as the CNR increases. The CNR at which the SNR on the FM receiver curve differs from the SNR on the asymptotic line by 1 db will be defined as threshold. Fig. (4.4) is a good example

of the type of curves under consideration. The graph shows that the 1 db threshold point for the FM discriminator with modulation is approximately at a CNR = 9.5 db.

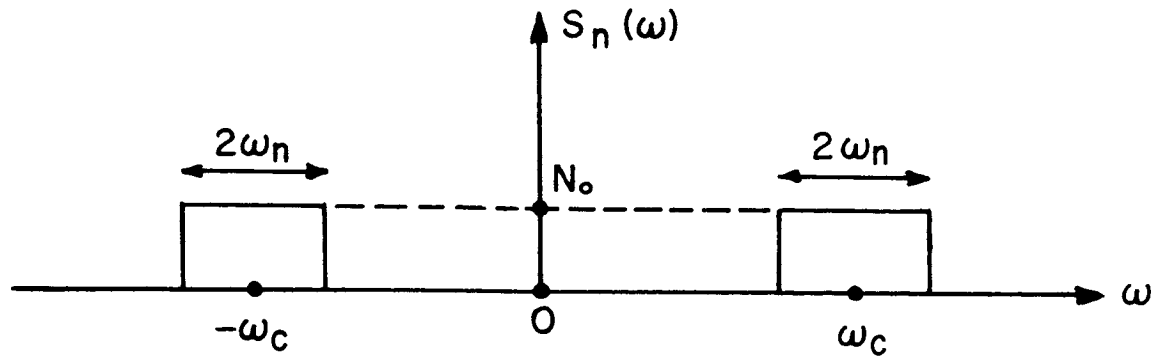

Fig. I.1 Spectrum of the gaussian noise centered at ω_c

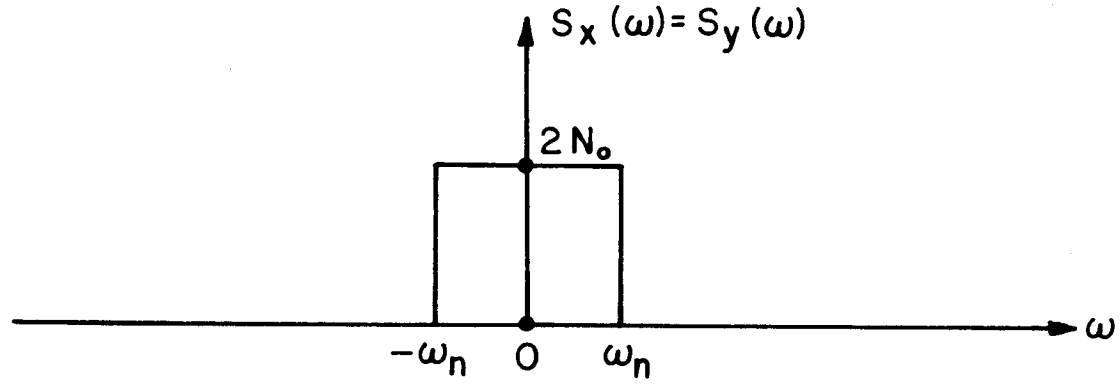

Fig. I.2 Spectrum of the gaussian noise centered at $\omega=0$

Chapter 2

MAXIMUM LIKELIHOOD

2.1 Derivation of the maximum likelihood estimate

The modulation in a general communications system, during a time interval 0 to T, can be regarded as a particular sequence of voltages taken from the set of all possible sequences that could occur. From a knowledge of the modulation source, one can assign a probability of occurrence to each sequence. Similarly, the noise in the system, during the time interval 0 to T, can be regarded as a particular sequence of voltages taken from the set of all possible sequences that could occur. Again, knowing the properties of the noise source, one can assign a probability of occurrence to each noise sequence. At the receiver, in this communications system, one has a received voltage sequence consisting of a noise sequence plus a particular function of a modulation sequence. The ML estimate of the modulation sequence is then the most likely modulation sequence to have produced the received voltage sequence. In mathematical terms, the maximum likelihood estimate is that modulation sequence which maximizes the conditional probability of all possible modulation sequences given a particular received voltage sequence.

If $m(t)$ = modulation

$\int m = \int_0^t m(\lambda)d\lambda$ (for an FM system)

$S(t) = S(t, m)$ = function of the modulation - AM, PM, FM

$n(t)$ = noise

$v(t)$ = received voltage

$= S + n = A \cos(\omega_c t + \int m) + n$ (for an FM system)

$a(t)$ = ML estimate of $m(t)$

$p(m|v)$ = condition probability of the modulation m, given a received voltage v

then

$a(t)$ = the solution of the equation

$$\frac{\partial}{\partial m} p(m|v) = 0 \qquad (2.1A)$$

for which

$$p(a|v) = \text{an absolute maximum} \qquad (2.1B)$$

If Eq. (2.1A) has more than one solution, then $a(t)$ must be found by evalvating $p(m|v)$ at each solution. Note also, that minimum likelihood estimates of m are also solutions to Eq. (2.1A).

The first step in finding $a(t)$ is to determine $p(m|v)$. From Bayes' Rule, one finds that

$$p(m|v) = \frac{p(m, v)}{p(v)} = \frac{p(v|m)\, p(m)}{p(v)} \qquad (2.2)$$

where $p(m, v)$ = joint probability density function of m and v

$p(v)$ = probability density of v

$p(m)$ = probability density of m

$p(v|m)$ = conditional probability of v given m

These probabilities can be put into convenient mathematical form if one assumes the time functions $m(t)$ and $n(t)$ are gaussian distributed and can be represented as vectors in N dimensional sample space, i.e.,

$$m(t) \text{ in sample space} = \begin{bmatrix} m(\Delta t) \\ m(2\Delta t) \\ \cdots \\ m(N\Delta t) \end{bmatrix} = \begin{bmatrix} m_1 \\ m_2 \\ \\ m_N \end{bmatrix} = [m] \qquad (2.3)$$

$N\Delta t = T$

= a column vector

$$n(t) \text{ in sample space } = \begin{bmatrix} n(\Delta t) \\ n(2\Delta t) \\ \cdots \\ n(N\Delta t) \end{bmatrix} = \begin{bmatrix} n_1 \\ n_2 \\ \\ n_N \end{bmatrix} = [n] \qquad (2.4)$$

$$= \text{a column vector}$$

Then if

$$R_m(\tau) = E(m(t)\, m(t+\tau))$$

$$R_n(\tau) = E(n(t)\, n(t+\tau)),$$

$$R_m(\tau) \text{ in sample space } = \begin{bmatrix} R_m(0) & R_m(\Delta\tau) & \cdots & R_m[(N-1)\Delta\tau] \\ R_m(\Delta\tau) & R_m(0) & \cdots & \cdots \\ \cdots & \cdots & \cdots & \cdots \\ R_m[(N-1)\Delta\tau] & \cdots & \cdots & R_m(0) \end{bmatrix}$$

$$= [R_m] = \text{a square matrix} \qquad (2.5)$$

$$\text{and } R_n(\tau) \text{ in sample space } = \begin{bmatrix} R_n(0) & R_n(\Delta\tau) & \cdots & R_n[(N-1)\Delta\tau] \\ R_n(\Delta\tau) & R_n(0) & \cdots & \\ \cdots & \cdots & \cdots & \\ R_n[(N-1)\Delta\tau] & \cdots & \cdots & R_n(0) \end{bmatrix}$$

$$= [R_n] = \text{a square matrix,} \qquad (2.6)$$

one can write p(m) and p(n) as follows:

$$p(m) = C_1 \exp\left[-\frac{1}{2}\, [m]^T\, [R_m]^{-1}\, [m]\right] \qquad (2.7)$$

$$p(n) = C_2 \exp\left[-\frac{1}{2}\, [n]^T\, [R_n]^{-1}\, [n]\right] \qquad (2.8)$$

Furthermore, since

$$v(t) = n(t) + s(t, m(t))$$

when m(t) is given, the samples of v(t) have the same density function as n(t) except for the mean values which vary as s(t, m).

Hence,

$$p(v|m) = C_3 \exp\left[-\frac{1}{2}\, [v-S]^T\, [R_n]^{-1}\, [v-S]\right] \qquad (2.9)$$

Combining Eqs. (2.2), (2.7) and (2.9), one finds that

$$p(m|v) = \frac{C_1 C_3}{p(v)} \exp\left[-\frac{1}{2}[v-S]^T [R_n]^{-1} [v-S] - \frac{1}{2}[m]^T [R_m]^{-1} [m]\right] \quad (2.10)$$

The second step in finding a(t) is to evaluate the partial derivative of $p(m|v)$ with respect to m and set that derivative equal to zero. Let

$$f(m) = -\frac{1}{2}\left[[v-S]^T [R_n]^{-1} [v-S] - [m]^T [R_m]^{-1} [m]\right] \quad (2.11)$$

Then

$$\frac{\partial}{\partial m} p(m|v) = \exp[f(m)]\left[\frac{\partial}{\partial m}\left(\frac{C_1 C_3}{p(v)}\right) + \frac{C_1 C_3}{p(v)} \frac{\partial f(m)}{\partial m}\right]$$
$$= 0$$

Since v is a given received constant vector, p(v) is a constant; C_1, C_3 are also constant. Hence, the derivative of these quantities with respect to m is 0. Since exp (f(m)) is not zero, except in the trivial case $f(m) = -\infty$, we conclude that

$$\frac{C_1 C_3}{p(v)} \frac{\partial f(m)}{\partial m} = 0$$

Therefore,

$$-\frac{1}{2}\left[\frac{\partial}{\partial m}\right][v-S]^T [R_n]^{-1} [v-S] + [m]^T [R_m]^{-1} [m] = 0 \quad (2.12)$$

where

$$\left[\frac{\partial}{\partial m}\right] = \begin{bmatrix} \partial/\partial m_1 \\ \partial/\partial m_2 \\ \vdots \\ \partial/\partial m_N \end{bmatrix}$$

because the meaning of $\partial/\partial m$ in N-dimensional sample space is the partial derivative with respect to each component of m. The operator $\partial/\partial m$ corresponds to the del operator commonly used in electromagnetic theory

and $[\partial f/\partial m]$ is the gradient of f(m). [Note that for exp (f(m)) to be a maximum, f(m) must be a maximum].

In order to evaluate the partial derivative of f(m) with respect to the ith component of m, it is necessary to expand f(m). The first term becomes

$$[v-S]^T \; [R_n]^{-1} \; [v-S] = \sum_{j,k} (v_j-S_j) \; (R_n^{-1})_{jk} \; (v_k-S_k)$$

where $(R_n^{-1})_{jk}$ = j, k component of $[R_n]^{-1}$ matrix.

Therefore,

$$\frac{\partial}{\partial m_i} [v-S]^T \; [R_n]^{-1} \; [v-S] = \sum_{j,k} \frac{\partial}{\partial m_i} (v_j-S_j) \; (R_n^{-1})_{jk} \; (v_k-S_k) \tag{2.13A}$$

$$+ \sum_{j,k} (v_j-S_j) \; (R_n^{-1})_{jk} \; \frac{\partial}{\partial m_i} (v_k-S_k)$$

$$= -2 \sum_{j,k} \frac{\partial S_j}{\partial m_i} (R_n^{-1})_{jk} \; (v_k-S_k) \tag{2.13B}$$

if $(R_n^{-1})_{jk}$ is replaced by $(R_n^{-1})_{kj}$ and j and k are interchanged in the last term in Eq. (2.13A). The replacement is possible because R_n and, therefore, its inverse, $[R_n]^{-1}$ are symmetric matrices. The terms

$$\frac{\partial}{\partial m_i} v_j \; , \; \frac{\partial}{\partial m_i} v_k = 0$$

because [v] is a constant vector.

The term $[m]^T \; [R_m]^{-1} \; [m]$ is evaluated in a similar manner and one gets

$$\frac{\partial}{\partial m_i} [m]^T \; [R_m]^{-1} \; [m] = 2 \sum_k (R_m^{-1})_{ik} \; m_k \tag{2.14}$$

Writing Eqs. (2.13B) and (2.14) in matrix form, one has

$$\left[\frac{\partial}{\partial m}\right][v-S]^T \; [R_n]^{-1} \; [v-S] = -2 \left[\frac{\partial S}{\partial m}\right][R_n]^{-1} \; [v-S] \tag{2.15}$$

$$\left[\frac{\partial}{\partial m}\right] [m]^T \; [R_m]^{-1} \; [m] \; = \; 2 \; [R_m]^{-1} \; [m] \tag{2.16}$$

where

$$\left[\frac{\partial S}{\partial m}\right] = \begin{bmatrix} \frac{\partial S_1}{\partial m_1} & \frac{\partial S_2}{\partial m_1} & \cdots & \frac{\partial S_N}{\partial m_1} \\ \frac{\partial S_1}{\partial m_2} & \frac{\partial S_2}{\partial m_2} & \cdots & \cdots \\ \cdots & \cdots & \cdots & \cdots \\ \frac{\partial S_1}{\partial m_N} & \cdots & \cdots & \frac{\partial S_N}{\partial m_N} \end{bmatrix} \tag{2.17}$$

Substituting Eqs. (2.15) and (2.16) in Eq. (2.12) gives

$$\left[\frac{\partial S}{\partial m}\right] [R_n]^{-1} \; [v-S] \; - \; [R_m]^{-1} \; [m] \; = \; 0 \tag{2.18}$$

Thus, [m] or the solution, [a], is given by

$$[a] = [R_m] \left[\frac{\partial S}{\partial m}\right] [R_n]^{-1} \; [v-S] \; \Big| \; _{[m]=[a]} \tag{2.19}$$

In order to bring this equation back into real time, various authors have found it convenient to define a new column vector $[g]\Delta t$ such that

$$\left[\frac{\partial S}{\partial m}\right] [g]\Delta t \; = [R_m]^{-1} \; [a] \quad , \quad \Delta t \; = \; \frac{N}{T} \tag{2.20}$$

and

$$\left[\frac{\partial S}{\partial m}\right] [g]\Delta t \; = \left[\frac{\partial S}{\partial m}\right] [R_n]^{-1} \; [v-S] \tag{2.21}$$

Then one has

$$[a] = [R_m] \left[\frac{\partial S}{\partial m}\right] [g] \; \Delta t \tag{2.22}$$

and

$$[v-S] = [R_n] \; [g] \; \Delta t \tag{2.23}$$

For the case in which S(t, m) is a no-memory function of m (AM, PM), the matrix $\left[\frac{\partial S(t, m)}{\partial m}\right]$ is a diagonal matrix. [The off-diagonal terms are

zero]. Consequently, if the ith component of the matrix Eqs. (2.22) and (2.23) is written out, the following sums are obtained:

$$a_i = \sum_j (R_m)_{ij} \left.\frac{\partial S_j}{\partial m_j}\right|_{m_j = a_j} g_j \, \Delta t \tag{2.24}$$

$$v_i - S_i = \sum_j (R_n)_{ij} \; g_j \, \Delta t \tag{2.25}$$

In the limit as $N \longrightarrow \infty$, $\Delta t \longrightarrow 0$, and $i\Delta t = t$, $j\Delta t = \lambda$, one gets

$$a(t) = \int_0^T R_m(t, \lambda) \left.\frac{\partial S(t, m)}{\partial m}\right|_{m = a(\lambda)} g(\lambda) \, d\lambda \tag{2.26}$$

$$v(t) - S(t, a(t)) = \int_0^T R_n(t, \lambda) \; g(\lambda) \, d\lambda \tag{2.27}$$

However, in the case of an FM signal, memory is involved and the matrix $\frac{\partial S(t, m)}{\partial m}$ is not a diagonal matrix. Writing the column vector $[S(t, m)]$ for an FM signal, one finds that

$$[S] = \begin{bmatrix} A \cos (\omega_c \Delta t + m_1 \Delta t) \\ A \cos (2\omega_c \Delta t + (m_1 + m_2) \Delta t) \\ \cdots \\ A \cos (N\omega_c \Delta t + \sum_{j=1}^{N} m_j \Delta t) \end{bmatrix}$$

Taking the partial derivative of $[S]^T$ with respect to m, one obtains the matrix $\left[\frac{\partial S}{\partial m}\right]$ (Eq. 2.17):

$$\left[\frac{\partial S}{\partial m}\right] = -A\Delta t \begin{bmatrix} \sin (\omega_c \Delta t + m_1 \Delta t) & \sin (2\omega_c \Delta t + (m_1+m_2)\Delta t) & \cdots & \sin (N\omega_c \Delta t + \sum_j m_j \Delta t) \\ 0 & \sin (2\omega_c \Delta t + (m_1+m_2)\Delta t) & \cdots & \cdots \\ \cdots & \cdots & \cdots & \cdots \\ 0 & 0 & \cdots & \sin (N\omega_c \Delta t + \sum_j m_j \Delta t) \end{bmatrix} \tag{2.28}$$

Thus, the product $\left[\frac{\partial S}{\partial m}\right][g]\,\Delta t$ is a column vector whose jth row is given by

$$\sum_{k=j}^{k=N} \left(\frac{\partial S}{\partial m}\right)_{jk} g_k \Delta t$$

The equation for a_i becomes, in this case,

$$a_i = \sum_j (R_m)_{ij} \sum_{k=j}^{N} \left(\frac{\partial S}{\partial m}\right)_{jk} g_k \Delta t \qquad (2.29)$$

In the limit as $N \longrightarrow \infty$, $\Delta t \longrightarrow 0$, and $i\Delta t = t$, $j\Delta t = \lambda$, $k\Delta t = \mu$, one finds that

$$a(t) = \int_0^T R_m(t, \lambda) \left[\int_\lambda^T \frac{\partial S(t, \int m)}{\partial \int m} \Big|_{\int m = \int a(\mu)} g(\mu)\, d\mu \right] d\lambda \qquad (2.30)$$

to be used in conjuction with Eq. (2.27). Interestingly enough, this is not the form obtained by Lawton (1.3) and therefore it will be called the second form of the ML equation for FM. The first form of the equation can be obtained by interchanging the order of the integrations over μ and λ. If the region of integration in the (μ, λ) plane as shown in Fig. 2.1 is examined, one sees that the first integration is with respect to μ at constant λ, and the second integration is with respect to λ. If, instead, one integrates with respect to λ first, with the limits 0 to μ, and then integrates with respect to μ from 0 to T, one obtains the 1st form of the ML equation for FM:

$$a(t) = \int_0^T \left[\int_0^\mu R(t, \lambda) d\lambda \right] \frac{\partial S(\mu, \int m)}{\partial \int m} \Big|_{\int m = \int a(\mu)} g(\mu)\, d\mu \qquad (2.31)$$

For the case of white noise, i.e.,

$$R_n(\tau) = N_o\, \delta(\tau)$$

Eq. (2.27) is readily solved:

$$v(t) - S(t, a(t)) = N_o \int_0^T \delta(t-\lambda)\, g(\lambda) d\lambda = N_o\, g(t)$$

For the case of an FM signal given by

$$S(t, m) = A \cos (\omega_c t + \int m)$$

the ML equation for FM (1st Form) becomes

$$a(t) = \frac{1}{N_o} \int_0^T \left[\int_0^\mu R(t, \lambda) d\lambda \right] [-A \sin(\omega_c \mu + \int a)] [A \cos(\omega_c \mu + \int m) + n - A \cos(\omega_c \mu + \int a)] d\mu \tag{2.32}$$

or (2nd Form)

$$a(t) = \frac{1}{N_o} \int_0^T R(t, \lambda) \left[\int_\lambda^T [-A \sin(\omega_c \mu + \int a)[A \cos(\omega_c \mu + \int m) + n - A \cos(\omega_c \mu + \int a)]] d\mu \right] d\lambda \tag{2.33}$$

White noise is selected in this analysis for three reasons:

1. White gaussian noise is the most common type of interference encountered in practice.
2. The ML estimate is simplified to a single equation.
3. If filtered noise is used, i.e., non-white noise, the noise will be whitened by the second of the two equations for the ML estimate, Eq. (2.27).

2.1.1 Likelihood function

In addition to deriving the ML equation, the equation for f(m) (more commonly known as the likelihood function) will be reformulated in terms of time because it will be important later. The equation for f(m) is

$$f(m) = -\frac{1}{2} \left[[v-S]^T [R_n]^{-1} [v-s] + [m]^T [R_m]^{-1} [m] \right] \tag{2.11}$$

The terms $[R_n]^{-1}$ [v-S] and $[R_m]^{-1}$ [m] may be regarded as transformations of the vectors [v-S] and [m] by the operators $[R_n]^{-1}$ and $[R_m]^{-1}$ respectively. These inverse operators may be obtained using the following equation:

$$[R]^{-1}_{\text{operator}} = \frac{\Delta t}{\text{Fourier Transform}\,[R(\tau)]} + \text{endpoint terms}$$

$$= \frac{\Delta t}{H(p)} + \text{endpoint terms}, \quad p = d/dt \tag{2.34}$$

when $R(t_1, t_2) = R(t_1 - t_2) = R(\tau)$, i.e., m(t) and n(t) are stationary. In general, the endpoint terms are not zero; however, in all cases used in this thesis they are zero. For the proof, see appendix A.

Thus,

$$f(m) = -\frac{1}{2}\left[[v-S] \quad [H_n^{-1}(\tfrac{d}{dt})(v-S)]\,\Delta t + [m] \quad [H_m^{-1}(\tfrac{d}{dt}) (m)]\,\Delta t\right] \tag{2.35A}$$

$$= -\frac{1}{2}\sum\left[(v-S)_i\, H_n^{-1}(\tfrac{d}{dt})(v-S)_i + m_i\, H_m^{-1}(\tfrac{d}{dt})\, m_i\right]\Delta t \tag{2.35B}$$

In the limit as $N \to \infty$, $\Delta t \to 0$, $i\Delta t \to t$, one gets

$$f(m) = -\frac{1}{2}\int_0^T \left[(v-S)\, H_n^{-1}(\tfrac{d}{dt})(v-S) + m\, H_m^{-1}(\tfrac{d}{dt})\, m\right] dt \tag{2.36}$$

2.2 Low frequency form of the maximum likelihood equation for FM

The ML equation including the carrier frequency ω_c is, in general, not convenient for analysis. Since the characteristics of FM receivers do not depend on the carrier frequency, it should be possible to eliminate terms that contain it. From Eq. (2.32) one sees that the terms containing $\omega_c t$ are given by

$$F = -A \sin(\omega_c t + \int a)\,[A\cos(\omega_c t + \int m) + n_w(t) - A\cos(\omega_c t + \int a)] \tag{2.37}$$

Using trigonometric identities, one obtains

$$F = \frac{A^2}{2}\sin\int(m-a) - \frac{A^2}{2}\sin(2\omega_c t + \int(m+a)) - A\, n_w(t)\sin(\omega_c t + \int a) + \frac{A^2}{2}\sin(2\omega_c t + 2\int a) \tag{2.38}$$

The terms involving $2\omega_c t$ have no significant contribution at low frequencies and will be filtered out by the ML equation. Hence, they can be neglected. The noise term can be expanded into two terms:

$$-A\, n_w(t) \sin\omega_c t \cos\int a - A\, n_w(t) \cos\omega_c t \sin\int a$$

Let

$$y_w = -2\ n_w \sin\omega_c t / A$$

$$x_w = +2\ n_w \cos\omega_c t / A,$$

then

$$F = \frac{A^2}{2}\ [\sin\int(m-a) + y_w \cos\int a - x_w \sin\int a] \tag{2.39}$$

Note that x_w and y_w are uncorrelated white noises, i.e.,

$$E(x_w(t)\, y_w(t+\tau)) = -\frac{4}{A^2}\ E(n_w(t)\, n_w(t+\tau) \sin\omega_c t \cos\omega_c(t+\tau))$$

$$= -\frac{2}{A^2}\ N_o \delta(\tau)\ E(\sin\omega_c \tau + \sin\omega_c(2t+\tau))$$

$$= -\frac{2}{A^2}\ N_o \omega_c \tau\, \delta(\tau) = 0 \qquad \text{(see Ref. 2.1)}$$

The autocorrelation function of x_w is

$$R_{xw} = \frac{4}{A^2}\ E(n_w(t)\, n_w(t+\tau))\ E(\sin\omega_c(t) \sin\omega_c(t+\tau))$$

$$R_{xw} = \frac{2}{A^2}\ N_o\, \delta(\tau) \cos\omega_c \tau = \frac{2N_o}{A^2}\ \delta(\tau) \tag{2.40}$$

Using a similar calculation,

$$R_{yw} = \frac{2N_o}{A^2}\ \delta(\tau) \tag{2.41}$$

It is convenient, at this point, to rewrite F as

$$F = \frac{A^2}{2}\ [\sin\int m \cos\int a - \cos\int m \sin\int a + y_w \cos\int a - x_w \sin\int a]$$

$$F = \frac{A^2}{2}\ [(\sin\int m + y_w) \cos\int a - (\cos\int m + x_w) \sin\int a]$$

$$F = \frac{A^2}{2}\ [s \cos\int a - c \sin\int a] \tag{2.42}$$

where $s(t) = \sin\int m + y_w$ (2.43A)

$c(t) = \cos\int m + x_w$ (2.43B)

Thus, s(t) and c(t) may be regarded as the basic data from which an estimate of m must be made. The ML equation can now be written as

$$a = \frac{A^2}{2N_o} \int_0^T \left[\int_0^\mu R_m(t-\lambda)d\lambda \right] (s\cos\int a - c\sin\int a)\, d\mu \qquad (2.44)$$

2.3 SNR for the maximum likelihood estimate for FM at high CNR and infinite observation interval (T)

In order to calculate the SNR for the ML equation, it is convenient to use the second form of the equation (Eq. (2.33) and Eq. (2.39) combined):

$$a = \frac{A^2}{2N_o} \int_0^T R_m(t-\lambda) \left[\int_\lambda^T (\sin\int(m-a) + y_w \cos\int a - x_w \sin\int a)\, d\mu \right] d\lambda$$

At high CNR, the term $\sin\int(m-a)$ can be replaced by $\int(m-a)$ (linearized model). The noise term, $y_w \cos\int a - x_w \sin\int a$ can be replaced by a white noise n_w whose autocorrelation function is given by

$$E(y_w(t_1)\, y_w(t_2) \cos\int a_1 \cos\int a_2 + x_w(t_1)\, x_w(t_2) \sin\int a_1 \sin\int a_2)$$

$$= R_{yw}(\tau)\, R_{\cos\int a}(\tau) + R_{xw}(\tau)\, R_{\sin\int a}(\tau)$$

$$= \frac{2N_o}{A^2}\, \delta(\tau) \left[R_{\cos\int a}(o) + R_{\sin\int a}(o) \right]$$

Since all values of a are equiprobable,

$$R_{\cos\int a}(o) = E(\cos\int a)^2 = \frac{1}{2}$$

$$R_{\sin\int a}(o) = E(\sin\int a)^2 = \frac{1}{2}$$

Therefore, $$R_{nw} = \frac{2N_o}{A^2}\,\delta(\tau) \qquad (2.45)$$

Since the SNR for values of t well inside the interval 0 to T (where T = ∞) is required, the end point conditions on a are not significant. Therefore, for purposes of simplification, one can change the λ limits to $-\infty$ to $+\infty$.

Hence, the linearized ML equation becomes

$$a = \frac{A^2}{2N_o}\int_{-\infty}^{+\infty} R_m(t-\lambda)\left[\int_{\lambda}^{\infty}(\int(m-a) + n_w)\,d\mu\right]d\lambda \qquad (2.46)$$

The operator form of this equation is

$$a = -\frac{A^2}{2N_o}\cdot\frac{H(p)}{p}\left[\frac{m-a}{p} + n_w\right] \quad \text{where } H(p) = \text{F. T. of } R_m(\tau), \quad p = d/dt \qquad (2.47)$$

Solving for the output noise, a-m, in terms of m and n_w, one gets

$$a-m = \frac{p^2 m}{\frac{A^2H(p)}{2N_o} - p^2} + \frac{\frac{A^2H(p)}{2N_o}\,p\,n_w}{\frac{A^2H(p)}{2N_o} - p^2} \qquad (2.48)$$

The output noise power is given by

$$E(a-m)^2 = \frac{1}{\pi}\int_0^{\infty}\left[\left|\frac{\omega^4}{\frac{A^2H(j\omega)}{2N_o} + \omega^2}\right|^2 S_m(\omega) + \left|\frac{\frac{A^4|H(j\omega)|^2}{4N_o^2}\,\omega^2}{\frac{A^2H(j\omega)}{2N_o} + \omega^2}\right|^2 S_n(\omega)\right]d\omega \qquad (2.49A)$$

$$E(a-m)^2 = \frac{1}{\pi} \int_0^\infty \frac{\omega^4 H(j\omega) + \frac{A^4}{4N_o^2} H^2(j\omega)\,\omega^2 \frac{2N_o}{A^2}}{\left[\frac{A^2 H(j\omega)}{2N_o} + \omega^2\right]^2} d\omega \qquad (2.49B)$$

$$E(a-m)^2 = \frac{1}{\pi} \int_0^\infty \frac{\omega^2 H(j\omega)}{\frac{A^2}{2N_o} H(j\omega) + \omega^2} d\omega \qquad (2.49C)$$

Thus, the SNR at high CNR can be written as

$$SNR = \frac{E(m)^2}{E(a-m)^2} = \frac{\sigma^2 \pi}{\int_0^\infty \frac{\omega^2 H(j\omega)\, d\omega}{\frac{A^2}{2N_o} H(j\omega) + \omega^2}} \qquad (2.50)$$

or

$$SNR = \frac{\sigma^2 \pi}{\int_0^\infty \frac{\omega^2 H(j\omega)\, d\omega}{\frac{2\omega_n CNR}{\pi} H(j\omega) + \omega^2}} \qquad (2.51)$$

using Eq. (1.5).

For the case $R_m(\tau) = \sigma^2 e^{-\omega_m |\tau|}$

$$H(j\omega) = \frac{2\omega_m \sigma^2}{\omega^2 + \omega_m^2}$$

the SNR is given by

$$SNR = \frac{\sigma^2 \pi}{\int_0^\infty \frac{2\omega_m \sigma^2 \omega^2 d\omega}{4\omega_m \sigma^2 \omega_n \frac{CNR}{\pi} + \omega^2 \omega_m^2 + \omega^4}} \qquad (2.52A)$$

$$SNR = \frac{\pi}{2\omega_m \int_0^{\infty} \frac{\omega^2 d\omega}{\omega^4 + \omega_m^2 \omega^2 + 4\omega_m \sigma^2 \omega_n \frac{CNR}{\pi}}} \qquad (2.52B)$$

$$SNR = \frac{\pi}{2\omega_m \frac{\pi}{2\sqrt{\omega_m^2 + 2\sqrt{4\omega_m \sigma^2 \omega_n \frac{CNR}{\pi}}}}} \qquad (2.52C)$$

$$SNR = \frac{\pi}{1 + 4\sqrt{\frac{\sigma^2 \omega_n}{\omega_m^3} \frac{CNR}{\pi}}} \qquad (2.52D)$$

$$SNR = \sqrt{1 + 4\sqrt{\frac{\beta^3 CNR}{2\pi}}} \approx \left[\frac{8\beta^3 CNR}{\pi}\right]^{1/4} \qquad (2.52E)$$

where $\beta = \omega_n/\omega_m$, $\sigma^2 = \omega_n^2/2$.

For the case $R_m(\tau) = \sigma^2 \frac{\sin\omega_m\tau}{\omega_m\tau}$

$$H(j\omega) = \begin{cases} \sigma^2 \pi/\omega_m , & |\omega| < \omega_m \\ 0 , & |\omega| > \omega_m \end{cases}$$

the SNR is calculated as follows:

$$SNR = \frac{\sigma^2 \pi}{\int_0^{\omega_m} \frac{\frac{\sigma^2 \pi}{\omega_m} \omega^2 d\omega}{2\frac{\omega_n \sigma^2}{\omega_m} CNR + \omega^2}} = \frac{\omega_m}{\int_0^{\omega_m} \frac{\omega^2 d\omega}{2\frac{\omega_n \sigma^2}{\omega_m} CNR + \omega^2}} \qquad (2.53A)$$

$$SNR = \frac{\omega_m}{\omega_m - \sqrt{2\frac{\omega_n \sigma^2}{\omega_m} CNR}\ \tan^{-1}\left[\frac{\omega_m}{\sqrt{2\frac{\omega_n \sigma^2}{\omega_m} CNR}}\right]} \qquad (2.53B)$$

$$SNR = \frac{1}{1 - \sqrt{\beta^3 CNR}\ \tan^{-1}\left[\frac{1}{\sqrt{\beta^3 CNR}}\right]} \qquad (2.53C)$$

$$SNR = \frac{1}{\frac{1}{3\beta^3 CNR} - \frac{1}{5(\beta^3 CNR)^2} + \frac{1}{7(\beta^3 CNR)^3} - \text{etc.}} \qquad (2.53D)$$

$$SNR \approx 3\beta^3 CNR \qquad \text{for} \qquad 3\beta^3 CNR >> 1.8 \qquad (2.53E)$$

Thus, for rectangular modulation spectra, the usual FM improvement formula is obtained. This result justifies the assumption made in section 2.1 that the ML estimator requires no prefiltering because it is an optimum estimator.

Note that for low order Butterworth modulation spectra, the full FM improvement is not obtained. The spectrum of the output noise for this situation is given by the integrand of Eq. (2.49C) and it is shown in Fig. 2.2. Note that the noise spectrum in the region $|\omega| < \omega_m$ has the characteristic parabolic shape for an FM receiver. However, the output also contains noise power from the region $|\omega| > \omega_m$, which we ordinarily filter out in the rectangular modulation spectrum case. But this type of filter is not optimum for the low order Butterworth spectrum case; an optimum Weiner must be used to get the best results. From

Papoulis (2.2), we find that the optimum Weiner filter is given by

$$H_o(\omega) = \frac{S_m(\omega)}{S_m(\omega) + S_{nl}(\omega)} \tag{2.54}$$

where $S_{nl}(\omega)$ = spectrum of the unfiltered output noise of an FM at high CNR

$$\doteq \begin{cases} \frac{2N_o}{A^2}\,\omega^2 & , \quad |\omega| < \omega_n \\ 0 & , \quad |\omega| > \omega_n \end{cases} \tag{2.55}$$

Hence,

$$H_o(\omega) \doteq \frac{S_m(\omega)}{S_m(\omega) + \frac{2N_o}{A^2}\,\omega^2} \quad , \quad |\omega| < \omega_n \tag{2.56}$$

The spectral density of the output noise is

$$\frac{S_{nl}(\omega)\,S_m(\omega)}{S_m(\omega) + S_{nl}(\omega)} = \frac{\omega^2 S_m(\omega)}{\frac{A^2}{2N_o} S_m(\omega) + \omega^2} \quad , \quad |\omega| < \omega_n \tag{2.57}$$

which agrees with the integrand of Eq. (2.49C). Thus, at high CNR, the ML receiver operates like an FM discriminator with a Weiner Filter. Furthermore the SNR-CNR equation for low order Butterworth modulation spectra does not contradict the usual FM receiver formula

$$\text{SNR} = 3\beta^3\,\text{CNR},$$

but merely indicates that this type of modulation is more difficult to separate from the noise. A general formula for the SNR for a kth order Butterworth modulation spectrum is derived in Appendix B. The result is

$$SNR = \frac{K+1}{K} \quad \frac{\sin \frac{3\pi}{2K+2}}{\sin \frac{\pi}{2K}} \quad \left[\frac{2K \sin \frac{\pi}{2K}}{\pi} \quad \beta^3 \, CNR \right]^{(2K-1)/(2K+2)} \tag{2.58}$$

which is valid for β^3 CNR >> 1

2.4 Solution of the maximum likelihood equation for FM

The basic technique to be used on the computer will be to evaluate the function $a_R(t)$, given by

$$a_R(t) = \frac{A^2}{2N_o} \int_0^T R_m(|t-\lambda|) \int_\lambda^T [s \cos \int a_i - c \sin \int a_i] \, d\mu \tag{2.59}$$

$$= \text{result of substituting } a_i \text{ in the ML equation}$$

$$= a_R(a_i)$$

for a succession of $a_i(t)$ (estimates of the solution) in some systematic manner so that

$$\int_0^T |a_R(\gamma) - a_i(\gamma)| \, d\gamma = \text{Total solution error (TSE)} \tag{2.60}$$

becomes arbitrarily small. Clearly, when $a_R(t) = a_i(t)$ the total solution error is zero and the equation is solved.

Since the number of times $a_R(t)$ must be evaluated is likely to be large, the first step in preparing the program is to choose a set of equations which will evaluate $a_R(t)$ with a minimum of computer operations. Two possible methods are evident:

1. Direct integration of the equation for $a_R(t)$ using a stored table of $R_m(\tau)$.
2. The formation of a set of differential equations, with appropriate initial conditions, whose solution is $a_R(t)$.

If N is the number of sample points involved, method 1 requires $\sim N^2$ multiplications to obtain the N samples of $a_R(t)$, while method 2 requires $\sim KN$ multiplications where K depends on the order of the differential equations and $K << N$. Hence, the 2nd method is preferable. For convenience, choose $R_m(\tau)$ so that its Fourier Transform, $S_m(\omega)$, is a Kth order Butterworth function (2.3). Then

$$S_m(\omega) = \sigma^2 \omega_m^{2K-1} \cdot \frac{2K \sin \frac{\pi}{2K}}{\omega_m^{2K} + \omega^{2K}} \tag{2.61}$$

and

$$S_m(p) = \sigma^2 \omega_m^{2K-1} \cdot \frac{2K \sin \frac{\pi}{2K}}{\omega_m^{2K} + (-1)^K p^{2K}} \tag{2.62}$$

To obtain the corresponding $R_m(\tau)$, $S_m(p)$ must be separated into two functions of p, one with all the left hand p-plane poles of $S_m(p)$ and the other with all the right hand p-plane roles of $S_m(p)$. Consequently, let

$$\frac{2K \omega_m^{2K-1} \sin \frac{\pi}{2K}}{\omega_m^{2K} + (-1)^K p^{2K}} = H(p) + H(-p) \tag{2.63}$$

where

H(p) contains only poles in the rh p plane

and

H(-p) contains only poles in the lh p plane.

Then, according to the theory of the double-sided Laplace transform,

$$R_m(t) = \begin{cases} \sigma^2 \mathcal{L}T^{-1}[H(p)] & , \ t \geq 0 \\ R_m(-t) & , \ t \leq 0 \end{cases} \tag{2.64}$$

The operator form of the ML equation with $S_m(p)$ given by Eq. (2.62) becomes

$$a_R(t) = \frac{A^2 \sigma^2}{2N_o} \omega_m^{2K-1} \frac{2K \sin \frac{\pi}{2K}}{\omega_m^{2K} + (-1)^K p^{2K}} b_1(t) \quad , \quad p = d/dt \tag{2.65}$$

where

$$b_1(t) = \int_t^T (s \cos\int a_i - c \sin\int a_i) \, d\mu \tag{2.66}$$

The differential equation for $a_R(t)$ is readily obtained from the equation above; however, the initial conditions on $a_R(t)$ and its derivatives are not easily obtained. To avoid this difficulty, ones defines four new functions, $b_2(t)$, $b_3(t)$, $b_4(t)$ and $b_5(t)$ with the equations

$$D(p) \cdot b_2(t) = b_1(t) \tag{2.67A}$$

$$b_3(t) = N(p) \cdot b_2(t) \tag{2.67B}$$

$$D(-p) \cdot b_4(t) = b_1(t) \tag{2.67C}$$

$$b_5(t) = N(-p) \cdot b_4(t) \tag{2.67D}$$

where

$$H(p) = \frac{N(p)}{D(p)} \quad , \quad H(-p) = \frac{N(-p)}{D(-p)} \quad , \quad p = d/dt$$

so that

$$a_R(t) = \frac{A^2 \sigma^2}{2N_o} \left[b_3(t) + b_5(t) \right] \tag{2.68}$$

With this set of equations defining $a_R(t)$, the initial condition problem is eliminated because $b_2(t)$ has zero initial conditions at $t=0$ and $b_4(t)$ has zero initial conditions at $t=T$. To prove this theorem, let

$$R(t) = LT^{-1} \frac{1}{D(p)} \qquad t \geq 0$$

$$= 0 \qquad t < 0 \tag{2.69}$$

Then

$$b_2(t) = \int_0^t R(t-\lambda)\ b_1(\lambda)\, d\lambda \qquad (2.70)$$

is Eq. (2.67A) written in the time domain. By inspection, $b_2(0) = 0$. The first derivative of $b_2(t)$, obtained by differentiating Eq. (2.70), is

$$\dot{b}_2(t) = \int_0^t \dot{R}(t-\lambda)\ b_1(\lambda)\, d\lambda + R(0)\ b_1(t) \qquad (2.71)$$

which is zero at t=0 because R(0) = 0. Repeated differentiation with respect to t will show that

$$b^{(i)}(0) = 0 \quad , \quad i = 0,\ 1,\ 2,\ \ldots\ K-1 \qquad (2.72)$$

because

$$R^{(j)}(0) = 0 \quad , \quad j = 0,\ 1,\ 2,\ \ldots\ K-2 \qquad (2.73)$$

The latter equation is demonstrated to be correct by applying the initial value theorem of the Laplace Transform to $1/D(p)$ where D(p) is a polynominal of degree K. A similar proof holds for the initial conditions at $t=T$ in Eq. (2.67C) for $b_4(t)$.

Although Eqs. (2.67B) and (2.67D) are also differential equations, they present no problem because they define $b_3(t)$ and $b_4(t)$ simply as linear sums of $b_2(t)$ and $b_4(t)$ and their derivatives.

2.4.1 Iterative methods

The second step in preparing the program is to choose a systematic method of varying $a_i(t)$ so that it will approach $a_R(t)$. Various methods have been suggested in the literature, the most common being the iterative method. This method corresponds to Newton's iteration technique for solving for the root of an equation extended to N-dimensional (vector) space.

Newton's method in one dimension for finding the root of $g(z) = 0$ is

$$z_{new} = z_{old} - \left.\frac{g(z)}{\frac{\partial g}{\partial z}}\right|_{z = z_{old}} \tag{2.74}$$

For the N-dimensional case (where z is a vector),

z_{new}, z_{old}, $g(z)$ = column vectors

$\frac{\partial g}{\partial z}$ = N * N matrix

Thus, in terms of matrices, Newton's method becomes

$$[z]_{new} = [z]_{old} - \left.\left(\left[\frac{\partial g}{\partial z}\right]^{-1} [g(z)]\right)\right|_{[z] = [z]_{old}} \tag{2.75}$$

In our case, one finds that

$$[g(z)] \rightarrow [a] - [R_m] \left[\frac{\partial S}{\partial m}\right] [R_n]^{-1} [v-S]$$

$$\left[\frac{\partial g}{\partial z}\right] \rightarrow \left[\frac{\partial}{\partial a}\right] [a]^T - \left[\frac{\partial}{\partial m}\right] \left[[R_m] \left[\frac{\partial S}{\partial m}\right] [R_n]^{-1} [v-S]\right]^T$$

$$= [1] - \left[\frac{\partial}{\partial m}\right] [v-S]^T [R_n]^{-1} \left[\frac{\partial S}{\partial m}\right]^T [R_m]$$

so that

$$[a]_{new} = [a]_{old} - \left[[1] - \left[\frac{\partial}{\partial m}\right] [v-S]^T [R_n]^{-1} \left[\frac{\partial S}{\partial m}\right]^T [R_m]\right]^{-1} \cdot \left.\left[[a] - [R_m] \left[\frac{\partial S}{\partial m}\right] [R_n]^{-1} [v-S]\right]\right|_{[a] = [a]_{old}} \tag{2.76}$$

When the CNR is very low, the term

$$- \left[\frac{\partial}{\partial m}\right] [v-S]^T [R_n]^{-1} \left[\frac{\partial S}{\partial m}\right]^T [R_m]$$

may be neglected in comparison with the unit matrix [1] because the elements of the matrix $A^2[R_n]^{-1}$ will be very small. Thus, we obtain the technique proposed by Van Trees (1.5), i.e.,

$$[a]_{new} = [a]_{old} - [a]_{old} + [R_m] \left[\frac{\partial S}{\partial m}\right] [R_n]^{-1} [v-S] \Big|_{[a] = [a]_{old}} \tag{2.77A}$$

$$[a]_{new} = [R_m] \left[\frac{\partial S}{\partial m}\right] [R_n]^{-1} [v-S] \Big|_{[a] = [a]_{old}} \tag{2.77B}$$

which corresponds to repeated resubstitution in the ML equation. However, the technique is limited to low CNR and may not pick out the maximum likelihood solution since the likelihood function is not evaluated in the process. Thus, when it does converge, it has a high probability of leading to a solution with a relative maximum likelihood but not to the correct solution (if one assumes that it is equally likely to converge to any one of the solutions of the ML equation).

An extension of this procedure to try to obtain convergence at higher CNR would be to approximate

$$- \left[\frac{\partial}{\partial m}\right] [v-S]^T [R_n]^{-1} \left[\frac{\partial S}{\partial m}\right]^T [R_m]$$

by an appropriate constant, α, so that the iteration equation becomes

$$[a]_{new} = [a]_{old} - \frac{1}{1+\alpha} \left[[R_m] \left[\frac{\partial S}{\partial m}\right] [R_n]^{-1} [v-S] - [a] \right] \Big|_{[a]=[a]_{old}} \tag{2.78}$$

However, convergence proofs for this method exist only for linear integral equations (2.4, 2.5, 2.6) and a few nonlinear integral equations with

non-periodic kernels. Many tests using this method were attempted but failed to converge, i.e., the limit of a_i, as $i \rightarrow \infty$, did not appear to exist. Furthermore, the effective gain, G, of the ML equation,

$$G = \frac{\int_0^T |a_R(a_i)| \, d\lambda}{\int_0^T |a_i| \, d\lambda} \tag{2.79}$$

is very large, particularly at high CNR, forcing the use of very small values of ϵ. As a result, even if the method would lead to a solution, the number of iterations required would be too large for the method to be practical.

The most natural method for this problem, we concluded, is to select $a_i(t)$ so as to maximize the likelihood function $f(a_i)$ at each level of iteration. We used the following steps:

1. Let $a_o(t) = 0$
2. Let $a_1(t) = \epsilon_1 a_R(a_o)$
3. Vary ϵ_1 until

   $f(a_1)$ = a maximum

   The $a_1(t)$ obtained is called a_{im}
4. Let $a_2(t) = a_{im} + \epsilon_2 (a_R(a_{im}) - a_{im})$
5. Vary ϵ_2 until

   $f(a_2)$ = a maximum
6. Continue the process until TSE (a_i) (Eq. (2.60)) is arbitrarily small.

In step 3, in general, more than one maximum will be found, indicating that more than one solution is possible. Since the absolute maximum likelihood estimate of m (Eq. (2.1B) is being sought, and since

$f(a_i)$ is a measure of the likelihood of a_i, the best a_i to choose among the available set of a_i appears to be the a_i corresponding to an absolute maximum of $f(a_i)$. It should be pointed out, however, that this does not guarantee that the final result has an absolute maximum likelihood. As far as is known, such a guarantee can only be obtained through a test of all possible vectors in the vector space, which is clearly impractical if not impossible.

An alternate procedure is to choose a_i so that the total solution error is a minimum. Since the maxima of the likelihood function and the minima of the total solution error do not coincide, the best one can do is to choose the minima of the solution error closest to the absolute maximum of the likelihood function. A test of this procedure indicated that it does not converge to the solution as fast as the first method.

2.4.2 Evaluation of the likelihood function

The evaluation of f(a) proceeds as follows: Let

$$H_m(p) = S_m(p) = \sigma^2 \omega_m^{2K-1} \frac{2K \sin \frac{\pi}{2K}}{\omega_m^{2K} + (-1)^K p^{2K}} \tag{2.62}$$

$$H_n(p) = S_n(p) = N_o$$

so that Eq.(2.36) for f(a) becomes

$$f(a) = -\frac{1}{2} \int_0^T \left[\frac{1}{N_o} [v-S]^2 + a \underbrace{\left[\frac{\omega_m^{2K} + (-1)^K p^{2K}}{2K \sigma^2 \omega_m^{2K-1} \sin \frac{\pi}{2K}} \right]}_{\text{operator}} a \right] dt \tag{2.80}$$

(2.81A)

where

$$[v-S]^2 = [A \cos(\omega_c t + \int m) + Ay \sin \omega_c t + Ax \sin \omega_c t - A \cos(\omega_c t + \int a)]^2$$

$$= \left[A \cos \omega_c t \left[\cos \int m + x - \cos \int a\right]\right. \tag{2.81B}$$
$$\left. - A \sin \omega_c t \left[\sin \int m + y - \sin \int a\right]\right]^2$$

$$= \frac{A^2}{2} \left[(s-\sin \int a)^2 + (c-\cos \int a)^2\right] - \frac{A^2}{2} (\cos 2\omega_c t)$$
$$\left[(s-\sin \int a)^2 - (c-\cos \int a)^2\right] - A^2 \sin 2\omega_c t \, (s-\sin \int a)\,(c-\cos \int a) \tag{2.81C}$$

The terms multiplied by $\sin 2\omega_c t$ and $\cos 2\omega_c t$ have a negligible contribution to the integral for $\omega_c T >> 1$. Hence, they will be neglected. Thus,

$$f(a) = \frac{-A^2}{4N_o} \int_0^T \left[(s-\sin \int a)^2 + (c-\cos \int a)^2 + \frac{N_o}{A^2 \sigma^2 K \omega_m^{2K-1} \sin \frac{\pi}{2K}}\right. \tag{2.82}$$
$$\left. a\,(\omega_m^{2K} a + (-1)^K a^{(2K)})\right] dt$$

Unfortunately, it turns out that this quantity has only minute variations near its maximum points because the fixed contribution, given by

$$- \frac{A^2}{4 N_o} \int_0^T (s^2 + c^2 + 1)\, dt$$

far exceeds the variable contribution given by

$$+ \frac{A^2}{2N_o} \int_0^T \left[s \sin \int a + c \cos \int a - \frac{N_o\, a\,(\omega_m^{2K} a + (-1)^K a^{(2K)})}{2A^2 \sigma^2 K \omega_m^{2K-1} \sin \frac{\pi}{2K}}\right] dt$$

Hence, a better quantity to examine is L defined by

$$L = \frac{1}{T} \int_0^T \left[s \sin \int a + c \cos \int a - \frac{\pi\, a\,(\omega_m^{2K} a + (-1)^K a^{(2K)})}{4 K \beta^3 CNR \sin \frac{\pi}{2K}\ \omega_m^{2K+2}}\right] dt \tag{2.83}$$

which is the normalized variable portion of f(a). Note that by subtracting the term

$$\frac{A^2}{4N_o} \int_0^T (s^2 + c^2 + 1)\, dt$$

from f(a) and using the remainder to form L, we have not changed the locations of the extrema of f(a). The a-values of the maxima of f(a) correspond exactly to the a-values of the maxima of L because the subtracted term is not a function of a. Using the above definition (Eq.(2.83), L is an absolute maximum when p(a|v) is an absolute maximum.

2.4.3 Expected value of the likelihood function

The expected value of the likelihood function defined by Eq. (2.83) will be determined based on the linear model for K=1 and K=∞. For convenience, L can be separated into two parts, namely

$$L_1 = \frac{1}{T} \int_0^T [s \sin\int a + c \cos\int a]\, dt$$

$$L_2 = \frac{1}{T} \int_0^T \frac{\pi\, a\, (\omega_m^{2K}\, a + (-1)^K\, a^{(2K)})}{4K\, \beta^3\, CNR \sin\frac{\pi}{2K}\, \omega_m^{2K+2}}\, dt$$

so that

$$L = L_1 - L_2$$

By inspection, it can be seen that the expected value of each component is simply the expected value of the corresponding integrand. In order to determine the expected value of L_2, one can define

$$L_2(\tau) = \frac{\pi}{4\beta^3\, CNR\, \omega_m^4}\, E\,(a(t+\tau)\,[\omega_m^2\, a(t) - \ddot{a}(t)]\,) \qquad (2.84A)$$

$$= \frac{\pi}{4\,\beta^3\,CNR\,\omega_m^4}\,E\left(a(t+\tau)\int_{-\infty}^{+\infty} 2\omega\,\sigma^2\,R_m^{-1}\,(t-\lambda)\,a(\lambda)\,d\lambda\right) \tag{2.84B}$$

$$= \frac{N_o}{A^2}\int_{-\infty}^{+\infty} R_m^{-1}\,(t-\lambda)\,E\,(a(t+\tau)\,a(\lambda))\,d\lambda \tag{2.84C}$$

$$= \frac{N_o}{A^2}\int_{-\infty}^{+\infty} R_m^{-1}\,(t-\lambda)\,R_a\,(t-\lambda+\tau)\,d\lambda \tag{2.84D}$$

at K=1. It can be shown that Eq. (2.84D) is valid for any K. Then at $\tau=0$, $L_2(0)$ is the required expected value. The integral in Eq. (2.84D) is a convolution in the time domain which can be replaced by a multiplication in the ω domain. Hence,

$$L_2(0) = \frac{N_o}{A^2\pi}\int_0^{\infty} \frac{S_a(\omega)}{H_m(\omega)}\,d\omega \tag{2.85}$$

By solving Eq. (2.48) (linear Model) for a, one gets

$$a = \frac{H_m(p)\,(m+pn)}{H_m(p) - \frac{2N_o}{A^2}\,p^2}\,, \text{ where } p = \frac{d}{dt}$$

Hence,

$$S_a(\omega) = \frac{H_m^{\,3}(\omega)}{\left[H_m(\omega) + \frac{2N_o}{A^2}\,\omega^2\right]^2} + \frac{H_m^{\,2}(\omega)\,\frac{2N_o}{A^2}\,\omega^2}{\left[H_m(\omega) + \frac{2N_o}{A^2}\,\omega^2\right]^2} \tag{2.86A}$$

$$S_a(\omega) = \frac{H_m^{\,2}(\omega)}{H_m(\omega) + \frac{2N_o}{A^2}\,\omega^2} \tag{2.86B}$$

Therefore, $L_2(0)$ reduces to

$$L_2(0) = \frac{N_o}{A^2\pi}\int_0^{\infty} \frac{H_m(\omega)\,d\omega}{H_m(\omega) + \frac{2N_o}{A^2}\,\omega^2} \tag{2.87}$$

where $H_m(\omega) = \dfrac{2\omega_m \sigma^2}{\omega_m^2 + \omega^2}$

Substituting the above equation for $H_m(\omega)$ in the equation for $L_2(0)$ gives the result

$$L_2(0) = \frac{\omega_m \sigma^2}{\pi} \int_0^\infty \frac{d\omega}{\omega^4 + \omega_m^2 \omega^2 + \dfrac{A^2 \omega_m \sigma^2}{N_o}} \tag{2.88A}$$

$$= \frac{\sigma^2}{2\omega_m^2 \sqrt{\dfrac{A^2\sigma^2}{N_o \omega_m^3}} \sqrt{1 + 2\sqrt{\dfrac{A^2\sigma^2}{N_o \omega_m^3}}}} \tag{2.88B}$$

$$= \frac{\beta^2}{8\sqrt{\dfrac{\beta^3 CNR}{2\pi}} \sqrt{1 + 4\sqrt{\dfrac{\beta^3 CNR}{2\pi}}}} \approx \frac{1}{16\, \beta^{\frac{1}{4}} \left(\dfrac{CNR}{2\pi}\right)^{\frac{3}{4}}} \tag{2.88C}$$

for $\dfrac{\beta^3 CNR}{2\pi} \gg \dfrac{1}{4}$

For the case in which

$$H_m(\omega) = \begin{cases} \sigma^2 \pi / \omega_m & |\omega| < \omega_m \\ 0 & |\omega| > \omega_m \end{cases}$$

the equation for $L_2(0)$ becomes

$$L_2(0) = \frac{N_o}{A^2 \pi} \int_0^{\omega_m} \frac{\dfrac{\sigma^2 \pi}{\omega_m}\, d\omega}{\dfrac{\sigma^2 \pi}{\omega_m} + \dfrac{2N_o}{A^2} \omega^2} \tag{2.89A}$$

$$L_2(0) = \frac{\sigma^2}{2\omega_m} \int_0^{\omega_m} \frac{d\omega}{\omega^2 + \frac{A^2 \pi \sigma^2}{2N_o \omega_m}} \tag{2.89B}$$

Upon performing the integration, one gets the result

$$L_2(0) = \frac{\sigma^2}{2\omega_m^2} \frac{1}{\sqrt{\frac{A^2 \pi \sigma^2}{2N_o \omega_m^3}}} \tan^{-1} \frac{1}{\sqrt{\frac{A^2 \pi \sigma^2}{2N_o \omega_m^3}}} \tag{2.90A}$$

$$= \frac{\beta^2}{4} \frac{1}{\sqrt{\beta^3 \, CNR}} \tan^{-1} \frac{1}{\sqrt{\beta^3 \, CNR}} \tag{2.90B}$$

$$= \frac{\beta^2}{4} \left[\frac{1}{\beta^3 \, CNR} - \frac{1}{3 (\beta^3 \, CNR)^2} + \frac{1}{5 (\beta^3 \, CNR)^4} - \text{etc} \right] \tag{2.90C}$$

$$\approx \frac{1}{4 \beta \, CNR} \quad \text{for} \quad \beta^3 \, CNR \gg \frac{1}{3} \tag{2.90D}$$

The expected value of the first part of L, namely

$$L_1 = \frac{1}{T} \int_0^T (s \sin\int a + c \cos\int a) \, dt \tag{2.91}$$

is given by

$$E(s \sin\int a + c \cos\int a)$$

$$= E(\cos\int(m-a) + y_w \sin\int a + x_w \cos\int a) \tag{2.92A}$$

$$= E(\cos\int(m-a)) + E(y_w \sin\int a + x_w \cos\int a) \tag{2.92B}$$

The noise term, $y_w \sin\int a + x_w \cos\int a$, has an expected value of zero. The term $\cos\int(m-a)$ can be evaluated if a is gaussian as in the linear model (m is given as gaussian) as follows:

Let $\theta = \int(m-a)$

Then $$E(\theta)^2 = E(\int(m-a))^2 = \sigma_\theta{}^2 \tag{2.93}$$

and $$E(\cos\theta) = \int_{-\infty}^{+\infty} \cos\theta \; p(\theta)\, d\theta \tag{2.94A}$$

$$E(\cos\theta) = \int_{-\infty}^{+\infty} \cos\theta \; \frac{e^{-\theta^2/2\sigma_\theta{}^2}}{\sqrt{2\pi\,\sigma_\theta{}^2}} \; d\theta = e^{-\sigma_\theta{}^2/2} \tag{2.94B}$$

The expected value of θ^2 is readily obtained from Eq. (2.48). The result is

$$E(\theta)^2 = \frac{1}{\pi} \int_0^\infty \frac{H(j\omega)}{\frac{A^2}{2N_o}\, H(j\omega) + \omega^2} \; d\omega \tag{2.95}$$

which is the same as Eq. (2.87). Hence

$$E(\theta)^2 = 2L_2(\theta) \tag{2.96}$$

so that

$$E(\theta)^2 \approx \begin{cases} \dfrac{1}{8\,\beta^{\frac{1}{4}}\,(\frac{CNR}{2\pi})^{\frac{3}{4}}} & \text{for } R_m(\tau) = \sigma^2\, e^{-\omega_m |\tau|} \qquad (2.97A) \\ \dfrac{1}{2\,\beta\,CNR} & \text{for } R_m(\tau) = \dfrac{\sigma^2 \sin \omega_m \tau}{\omega_m \tau} \qquad (2.97B) \end{cases}$$

[rectangular modulation spectrum]

Thus, the expected value of L approximately given by

$$E(L) \doteq 1 - \sigma_\theta{}^2 \tag{2.98A}$$

$$\doteq \begin{cases} 1 - \dfrac{1}{8\,\beta^{\frac{1}{4}}\,(\frac{CNR}{2\pi})^{\frac{3}{4}}} & \text{for } R_m(\tau) = \sigma^2\, e^{-\omega_m |\tau|} \qquad (2.98B) \\ 1 - \dfrac{1}{2\,\beta\,CNR} & \text{for } R_m(\tau) = \dfrac{\sigma^2 \sin \omega_m \tau}{\omega_m \tau} \qquad (2.98C) \end{cases}$$

The essential result, then, is that if no spikes are present, the expected value of L is approximately 1 for reasonably large values of β and CNR.

2.5 Computer simulation of the maximum likelihood estimator

In order to demonstrate that the procedure presented in section 2.4.1 leads to the solution of the ML equation, the procedure was employed to solve the equation on a digital computer. The equation was simulated on the IBM 7040 with the Fortran IV program given in Appendix F using the following conditions:

$$R_m(\tau) = \sigma^2 e^{-\omega_m |\tau|}$$

$$R_n(\tau) = N_o \delta(\tau)$$

$$\text{CNR} = 3\text{db} \qquad \omega_m = \frac{\pi}{25} \qquad \omega_n = \frac{\pi}{25}$$

$$\beta = 5 \qquad \sigma^2 = \frac{\pi^2}{50}$$

Δt = time between samples = .1 sec

N = number of samples = 250

$m(t) = \sigma$, $0 \leq t \leq T$ (FM pulse)

n(t) = gaussian random numbers with bandwidth $\pi / \Delta t = 10\pi$ [see Appendix E]

= widest possible bandwidth in this computer simulation

Fig. 2.2 shows a graph of the likelihood function, $L(\epsilon_1)$ obtained in accordance with step 3 of the procedure. Figs. 2.3 and 2.4 show the corresponding variations in the total solution error, $TSE(\epsilon_1)$ and the signal—to - noise ratio, $SNR(\epsilon_1)$. Note that the $L(\epsilon_1)$ curve has several peaks, anyone of which could lead to a solution. However, it has only one absolute maximum. In addition, it is clear that this peak is a good

choice because the SNR (ϵ_1) curve also indicates a peak in the vicinity of this peak. The significance of the fact that the peaks in the SNR (ϵ_1) and L (ϵ_1) coincide is very great; this is the first indication that demodulation is taking place, i.e., that the correct signal is being extracted from the noise. (Of course, the SNR (ϵ_1) curve is only possible when the modulation is known beforehand. In a realistic demodulation problem, this curve would not be available). The curves of L(ϵ_i), TSE(ϵ_i) and SNR(ϵ_i) are similar to those of L(ϵ_1), TSE(ϵ_1) and SNR(ϵ_1) respectively and will not be given.

Figs. 2.6 and 2.7 show the plots of SNR, TSE, L and ϵ as a function of the iteration number. Note that the likelihood function L is a continuously increasing function (approaching some asymptotic value). This must be so since at any iteration the choice $\epsilon = 0$, which keeps L constant, is available. However, if the best choice of ϵ for maximum L is $\epsilon = 0$, the iteration process would stop because all the values attained by the various functions at $\epsilon = 0$ would be repeated at all future iterations. Fortunately, in the many programs that were tried, this situation never occurred. If it did, we would have used a constant for a_R in the next iteration and then returned to the normal routine.

Fig. 2.8 shows the approximate solution of the ML equation for the conditions stated earlier after 10 iterations of the procedure developed in section 2.4.1.

The large size of the TSE should not be regarded as an indication that the approximate solution is far from the true solution. For example, consider the equation

$$x = 1000 \sin (x-1) \qquad (2.99)$$

for which

$$TSE = |1000 \sin (x-1) - x| \tag{2.100}$$

The correct solution is approximately $x = 1.001$; however, if $x = 1.1$ (which represents a 10% error) is substituted in Eq. (2.100), the TSE is 99.9, which is quite large. Thus, the TSE should be compared to the maximum value it can attain, which is approximately 1000; then the TSE of 99.9 indicates a relatively good solution. The approximate maximum value of the TSE for the ML equation is derived in appendix D for the case $K = 1$. The result is

$$TSE_{max} \approx \frac{\beta^3 \, CNR}{\pi} (\omega_m T) (\omega_m T - 1) \tag{2.101}$$

$$\approx 535$$

for the conditions given at the beginning of this section. The total solution error should be compared to this value for purposes of estimating how far away the approximate solution is from the true solution.

In addition to programming the ML equation for a Butterworth modulation spectrum of order $K = 1$, the case $K = 3$ was programmed. The SNR values for the ML estimate after 10 iterations for both $K = 1$ and $K = 3$ obtained with various noise samples are shown in Fig. 2.9 along with the asymptotic SNR-CNR lines for $K = 1$, 3 and ∞. An attempt was made to determine the threshold of the ML estimate; however, the number of points needed for a reasonable estimate (based on $500 \cdot 2\pi/\omega_n$ seconds of noise) would be about 200 at each CNR. Unfortunately, this would require an unreasonable amount of computer time since the computer time for each point is about 7 minutes. In addition, 10 iterations at each point is probably a little low. Judging from the results, about 20 iterations would be needed for dependable results. Furthermore, it appears that a

truer test of the ML equation for SNR purposes should involve a longer interval T since at the start of each interval, the estimator is given the correct initial phase angle. If a longer time interval T were used, the estimator would be given less noiseless information.

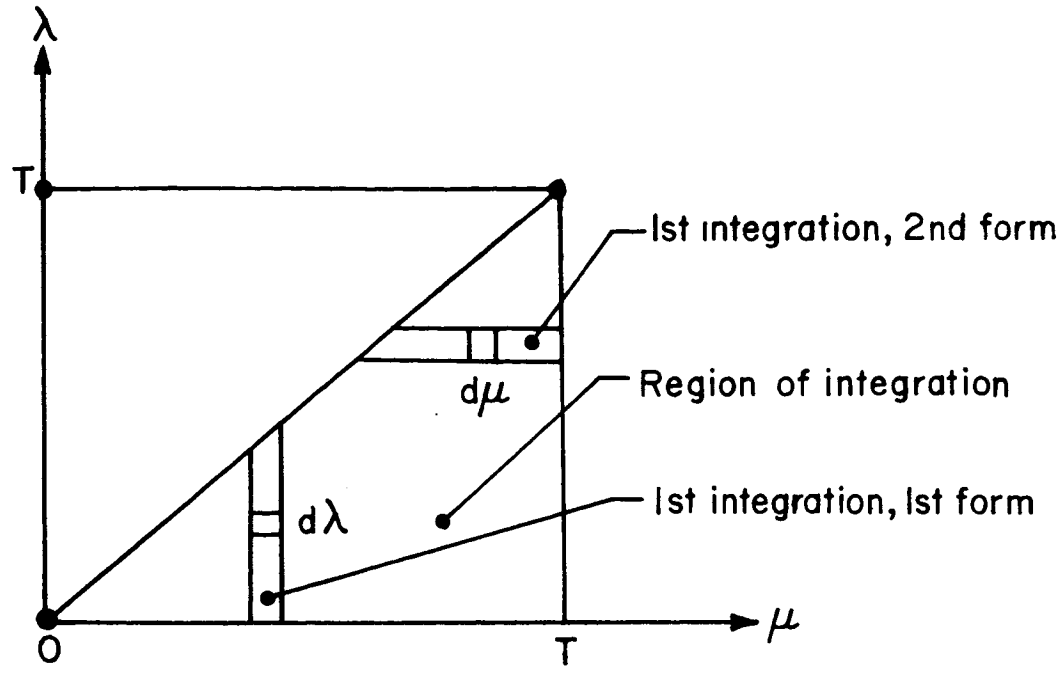

Fig. 2.1 Region of integration for the ML equation

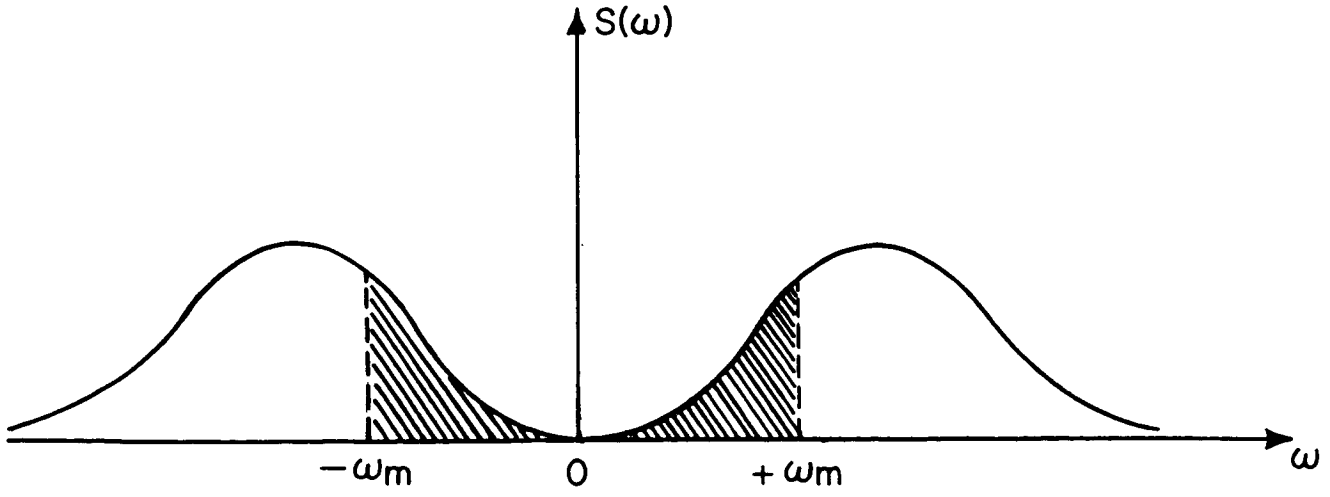

Fig. 2.2 Spectrum of the output noise for the ML estimate at high CNR and Butterworth modulation spectrum of order K=1

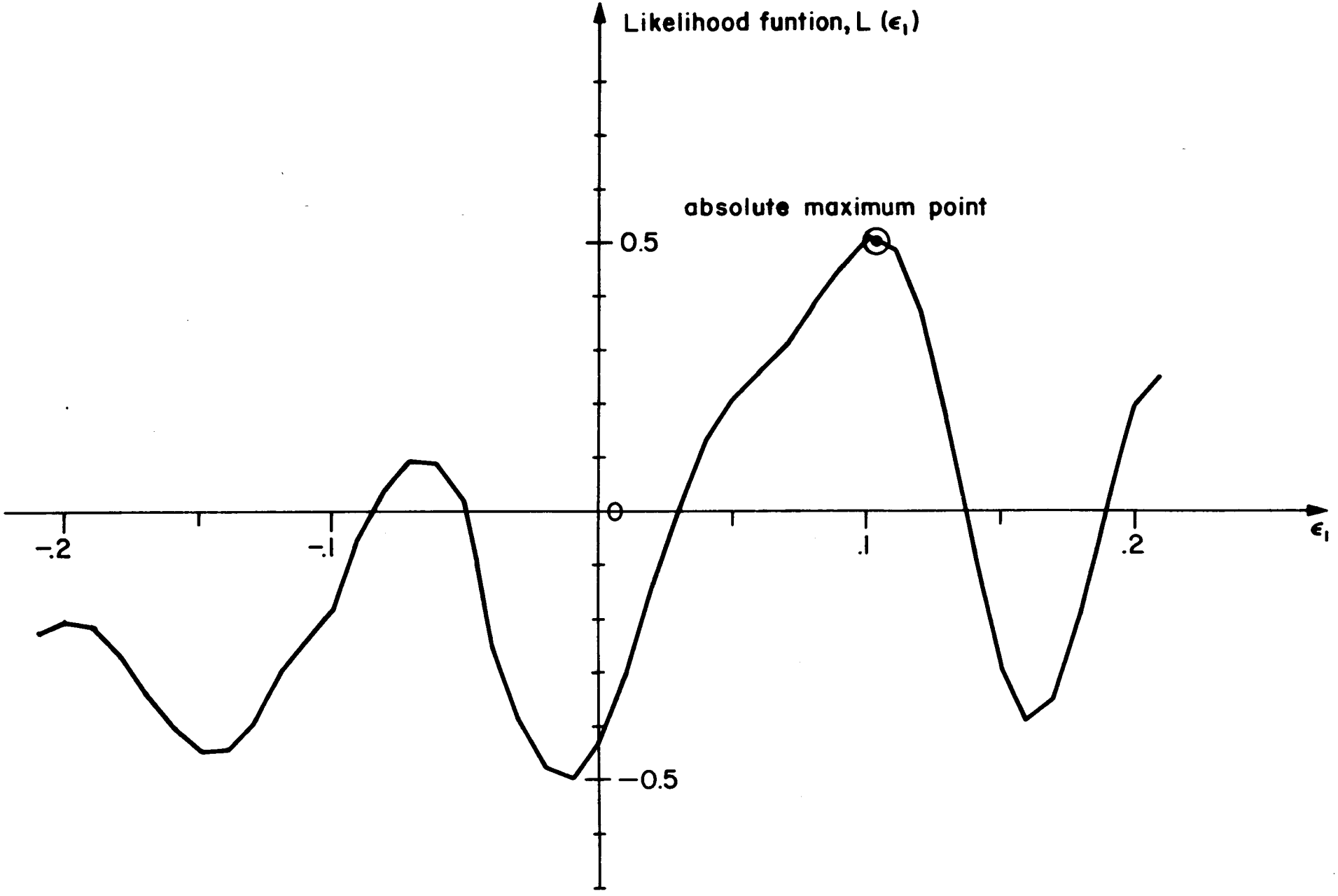

Fig. 2.3 Graph of the likelihood function versus ϵ_1

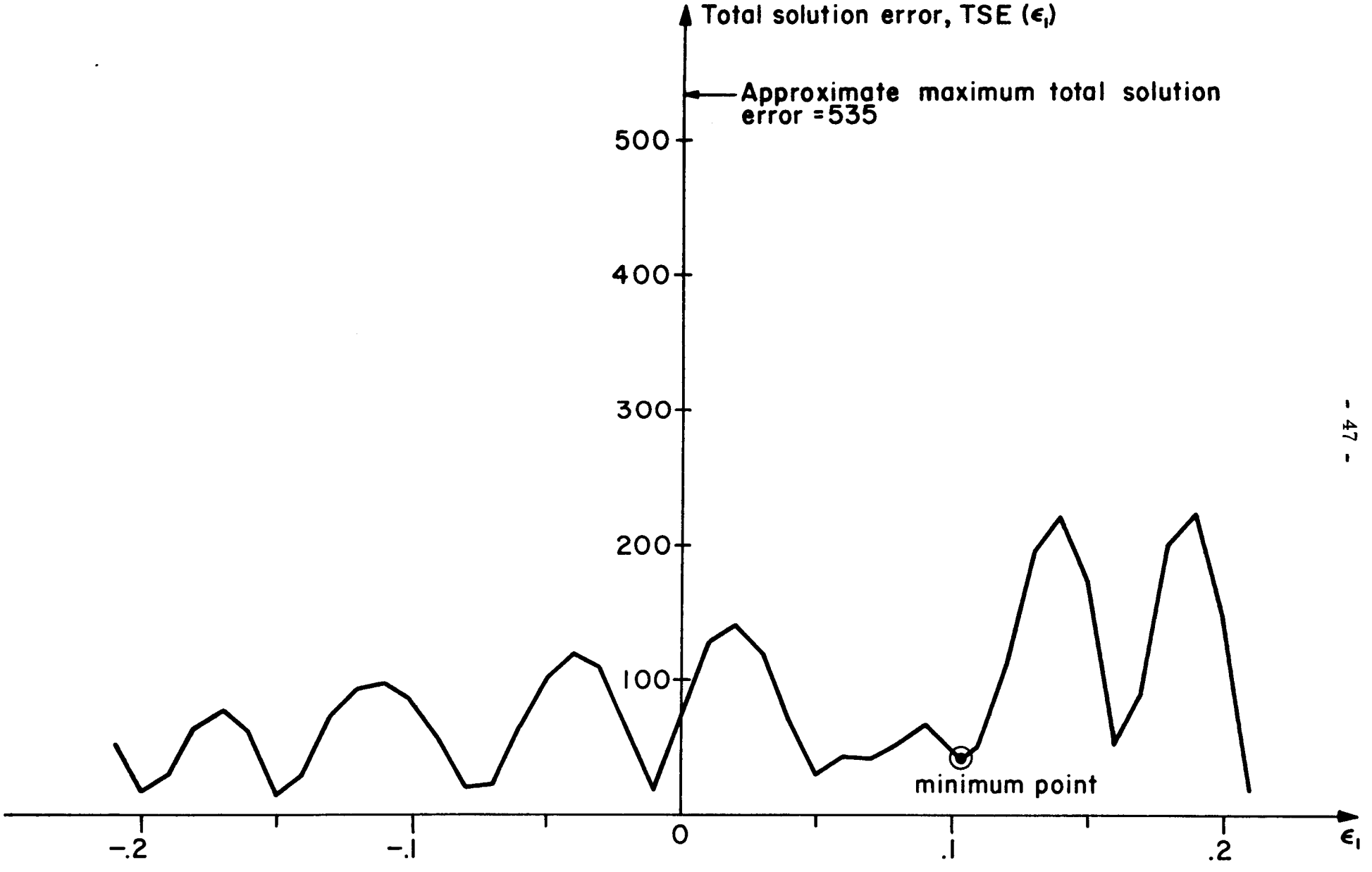

Fig. 2.4 Graph of the total solution error versus ϵ_1

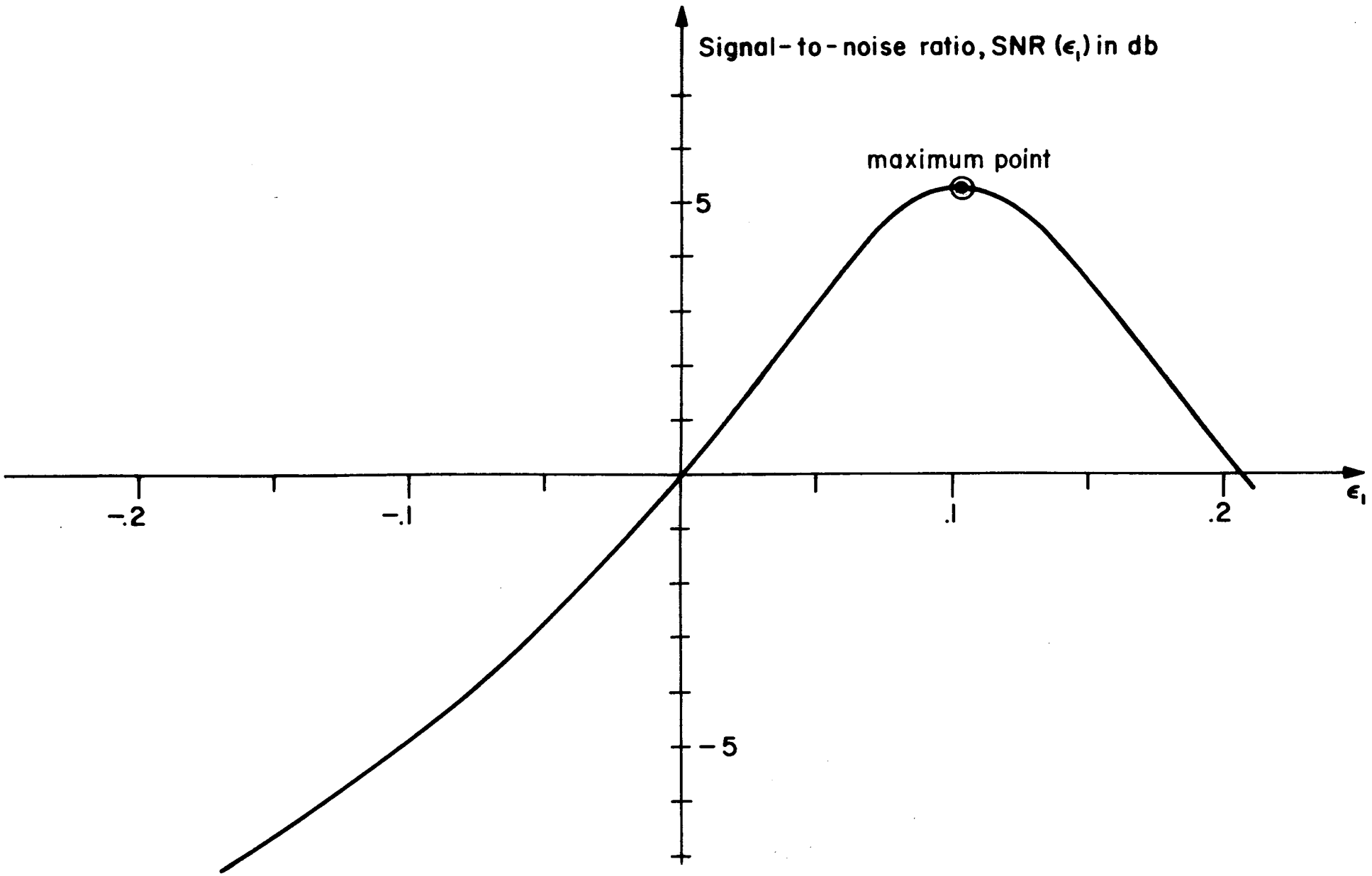

Fig. 2.5 Graph of the signal-to-noise ratio versus ϵ_1

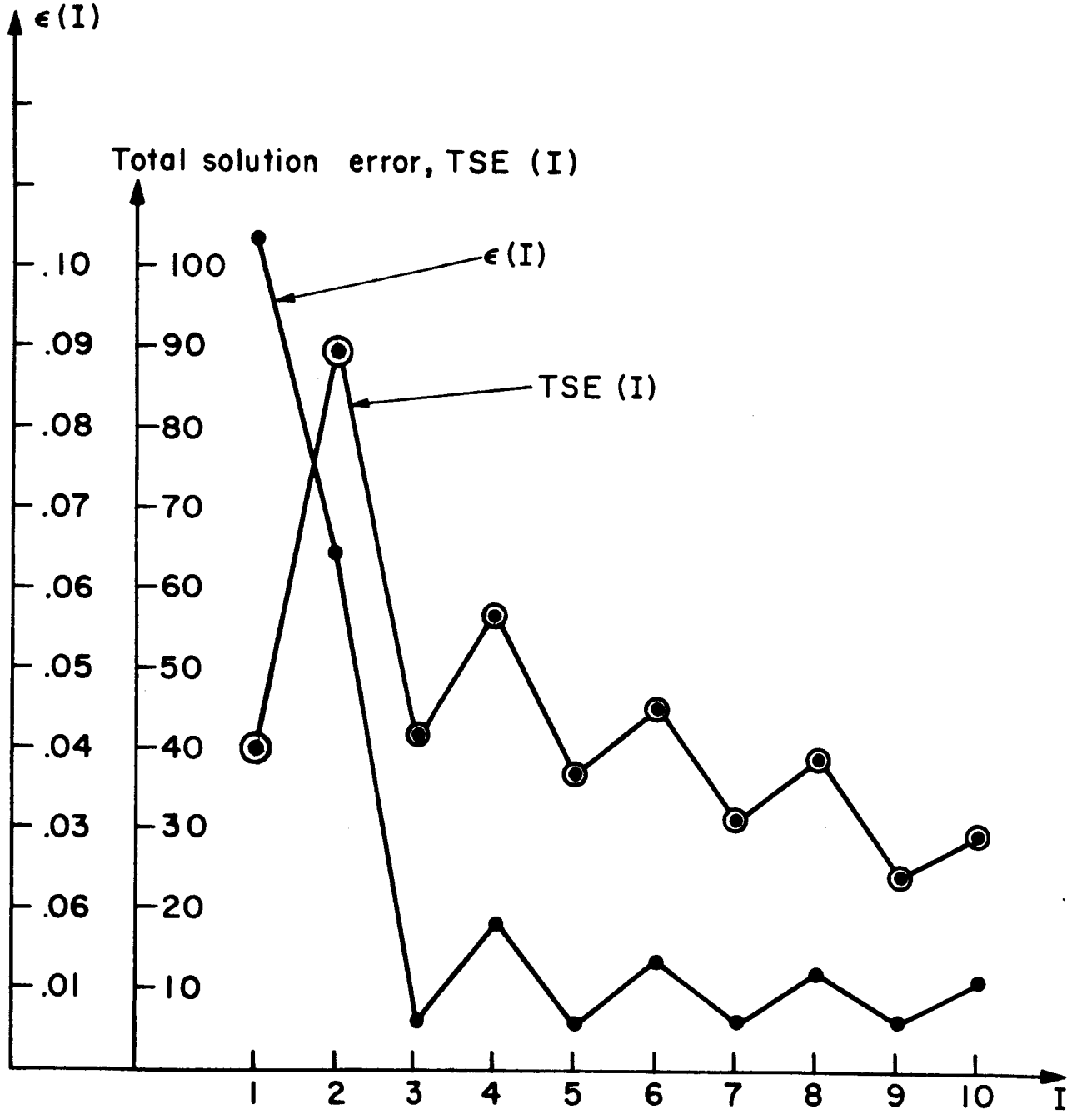

Fig. 2.6 Graph of ϵ and the total solution error versus the iteration number

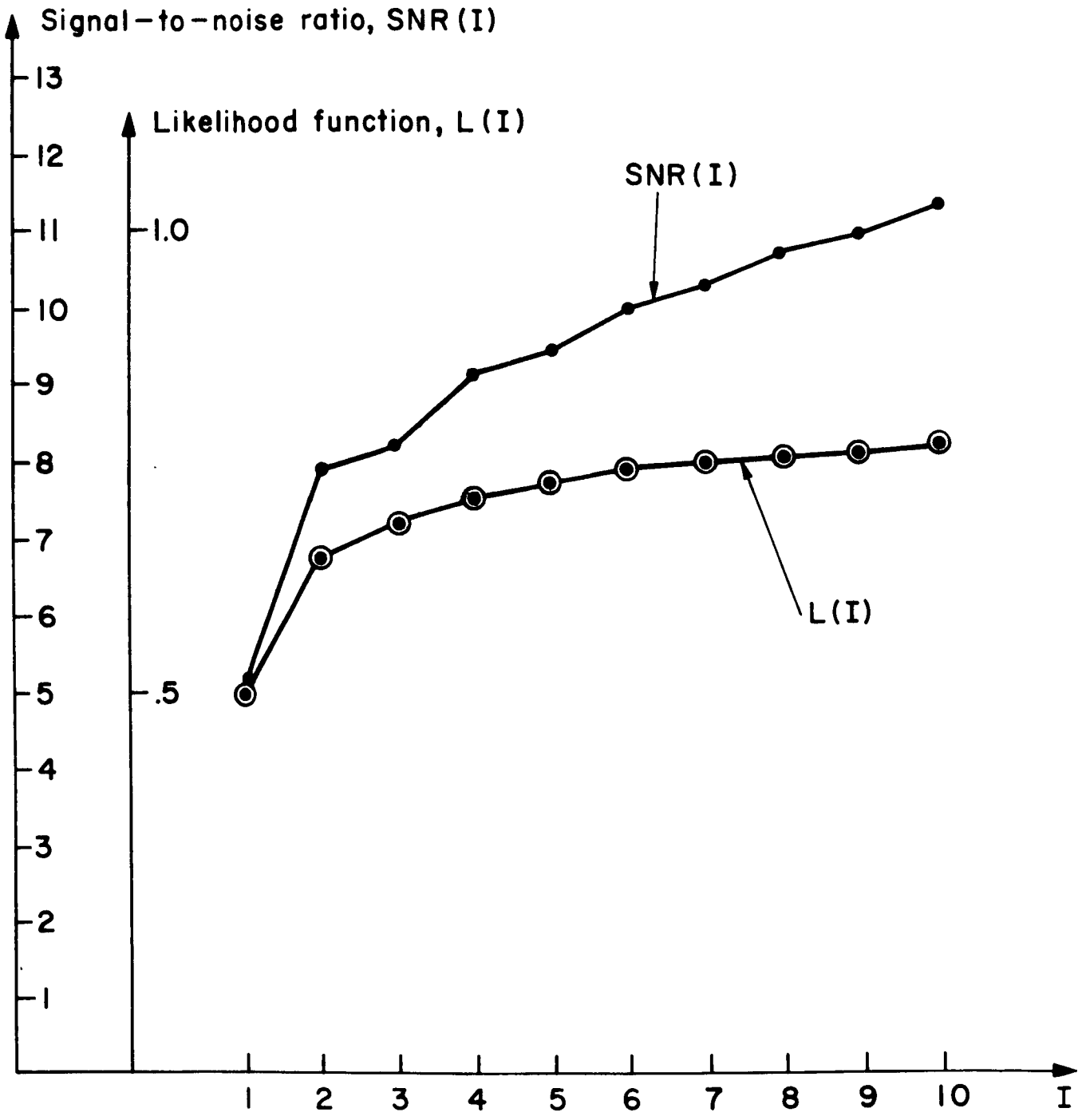

Fig. 2.7 Graph of the signal-to-noise ratio and the likelihood function versus the iteration number

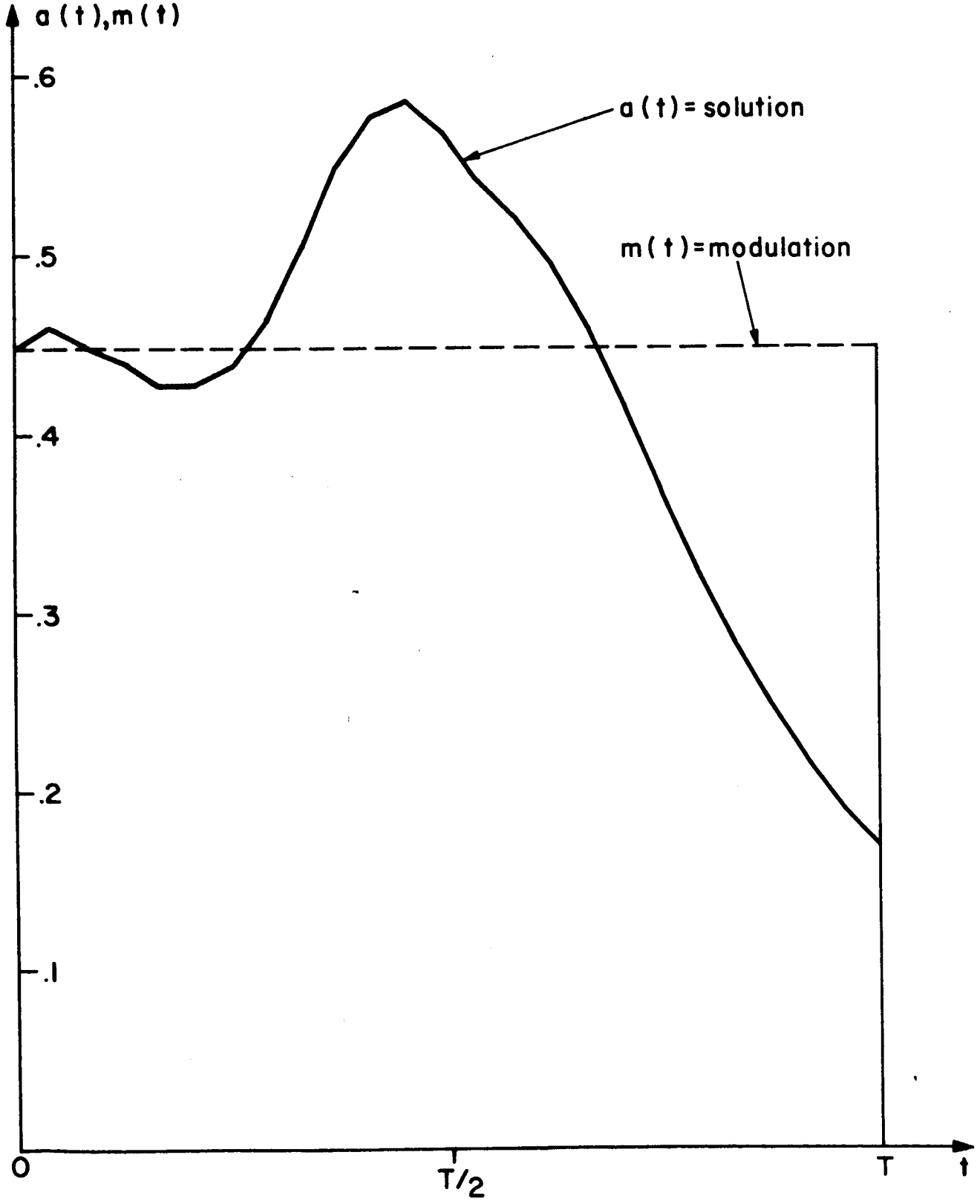

Fig. 2.8 Graph of the solution of the ML equation after 10 iterations

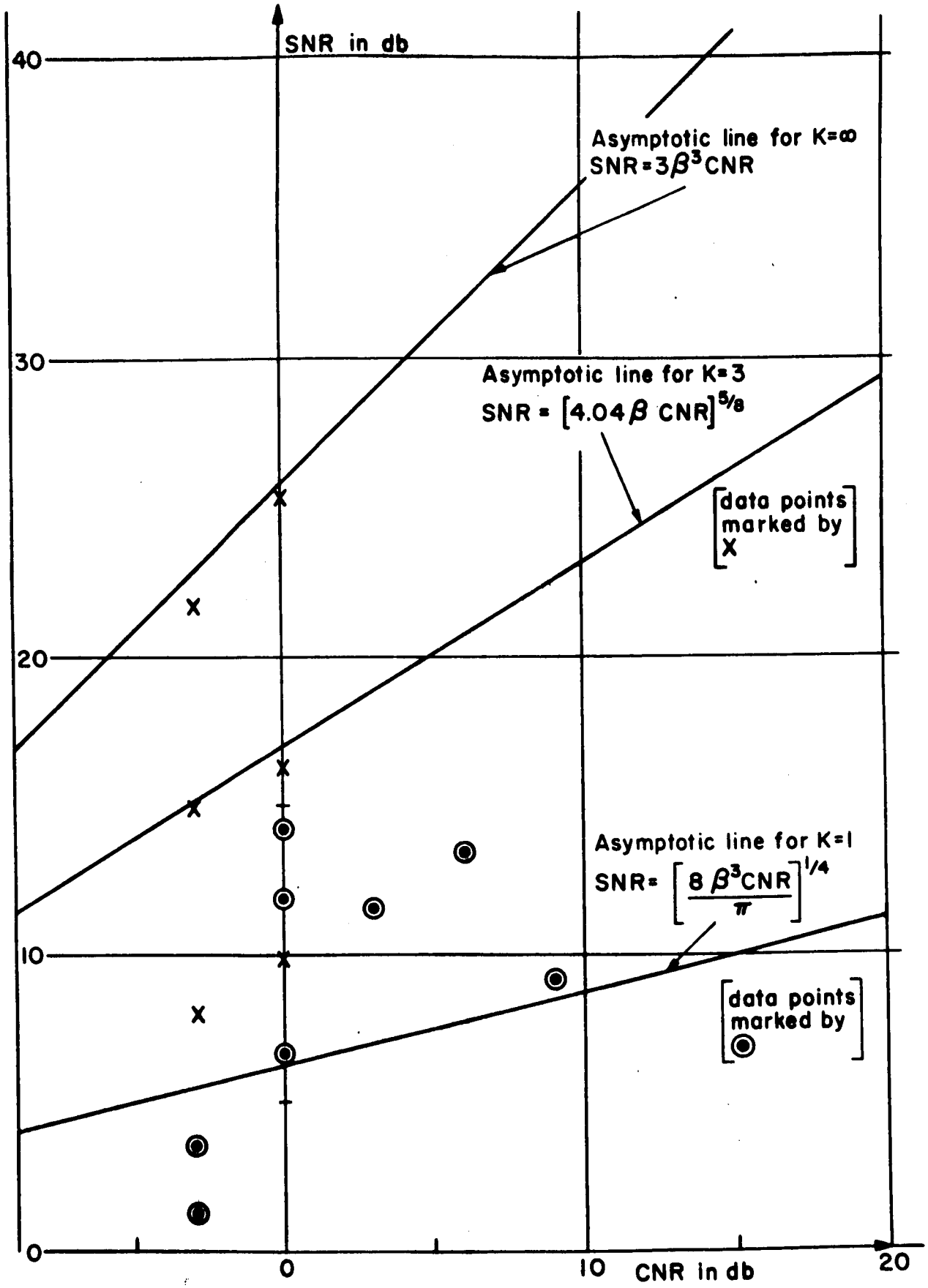

Fig. 2.9 Plot of SNR-CNR points from the ML equation simulation

Chapter 3

SPIKE DETECTION

3.1 FM discriminator

Theoretically, spike detection can be applied to any one of the three well known FM receivers, namely the phase-locked loop (PLL), FM with feedback (FMFB) or the FM discriminator. For purposes of simplification, we will apply it to the FM discriminator.

Before considering how to build an acceptable spike detector, it will be worthwhile to review the principles of operation of the discriminator type of FM receiver. Fig. 3.1 shows the block diagram of the complete receiver. In effect, the FM discriminator receiver measures the rate of the change with respect to time, of the angle θ associated with the signal plus noise vector [(R, θ) in polar coordinates, (s, c) in rectangular coordinates] as shown in Fig. 3.2. The equations for the basic voltages in the FM discriminator are given below (see Fig. 3.1):

1. Input to the receiver

$$v = A \cos (\omega_c t + \int m) + n_w(t) \tag{3.1}$$

2. Input to the limiter

$$e_1 = A\, c \cos \omega_c t - A\, s \sin \omega_c t \tag{3.2}$$

where $s = \sin \int m + y$ (3.3)

$$c = \cos \int m + x \tag{3.4}$$

$$x, y = \text{noise with bandwidth } \omega_n \tag{3.5}$$

3. Input to the discriminator

$$e_2 = \frac{c \cos \omega_c t - s \sin \omega_c t}{\sqrt{s^2 + c^2}} \tag{3.6}$$

4. Input to the low pass filter

$$e_3 = \frac{d}{dt} (\tan^{-1} \frac{s}{c}) = \frac{\dot{s}c - \dot{c}s}{s^2 + c^2} \tag{3.7A}$$

$$= \frac{d}{dt} (\theta) = \dot{\theta} \tag{3.7B}$$

Fig. 3.3 shows typical input and output waveforms for an FM discriminator at high and low β with the noise bandwidth (ω_n) and the carrier-to noise ratio (CNR) fixed. In addition, the modulation shown is sinusoidal,

i.e. $m = \beta\omega_m \cos \omega_m t$ (3.8)

Studies of these waveforms (which are readily observed on an oscilloscope) have led various investigators such as Rice (1.7) and Cohn (3.1) to describe the output of the FM discriminator as consisting of the following components:

1. Modulation
2. Gaussian Noise
3. Doublets (with area zero)
4. Spikes (with area 2π)

The first component is the transmitted information. The last three components are the three types of noise which can occur with various signal vector-noise vector configurations. Fig. 3.4 shows the type of situation which produces gaussian noise in θ and $\dot{\theta}$, i.e., when the amplitude of the noise vector is much less than the amplitude of the signal vector (fixed at unity amplitude). For simplicity, the modulation has been set to zero. When the noise vector is large and comes close to the origin (0), but does not circle the origin as in Fig. 3.5, the discriminator output contains a doublet. Note that the net change in θ, $\theta_2-\theta_1$, is $<< 2\pi$. When the noise vector is large and does circle the origin, we have a spike. This condition is shown in Fig. 3.6. Note that in this case the net change in θ is approximately 2π.

The approximate spectrums of each of the four components at the output of the discriminator are shown in Figs. 3.7 A, B, C and D. The spectrum of the modulation is chosen as rectangular for simplicity. The

spectrum of the gaussian noise is obtained by noting that the gaussian noise is approximately (see appendix D)

$$n_g = \frac{d}{dt}(y \cos \int m - x \sin \int m) \tag{3.9}$$

at the output of the discriminator. Evaluating the autocorrelation function of y cos $\int m$ - x sin $\int m$, we find that

$$E[(y_1 \cos \int m_1 - x_1 \sin \int m_1)(y_2 \cos \int m_2 - x_2 \sin \int m_2)] \tag{3.10A}$$

$$= E(y_1 y_2)\, E(\cos \int m_1 \cos \int m_2) + E(x_1 x_2)\, E(\sin \int m_1 \sin \int m_2)$$

$$- E(x_1 y_2)\, E(\cos \int m_1 \sin \int m_2) - E(x_2 y_1)\, E(\sin \int m_1 \cos \int m_2)$$

$$= 2R_x(\tau)\, R_{\cos \int m}(\tau) \tag{3.10B}$$

$$= R_g(\tau) \tag{3.10C}$$

since $$E(x_1 x_2) = E(y_1 y_2) = R_x(\tau) \tag{3.11}$$

$$E(x_1 y_2) = E(x_2 y_1) = 0 \tag{3.12}$$

$$E(\cos \int m_1 \cos \int m_2) = E(\sin \int m_1 \sin \int m_2) = R_{\cos \int m}(\tau) \tag{3.13}$$

For simplicity, one can assume that

$$S_x(\omega) = \begin{cases} \frac{2No}{A^2} & |\omega| < \omega_n \\ 0 & |\omega| > \omega_n \end{cases} \tag{3.14}$$

(see Fig. 1.2) and that

$$S_{\cos \int m}(\omega) = \begin{cases} \frac{\pi}{2\omega_n} & |\omega| < \omega_n \\ 0 & |\omega| > \omega_n \end{cases} \tag{3.15}$$

The latter assumption is based on the fact that

$$E(\cos \int m)^2 = 1/2 \tag{3.16}$$

and that the bandwidth of the modulated carrier is the same as the bandwidth of the noise: Thus,

$$S_g(\omega) = 2\omega^2 S_x(\omega) * S_{\cos \int m}(\omega) \tag{3.17}$$

where the ω^2 factor is introduced by the $d/_{dt}$ operator in Eq. (3.9). Evaluating the convolution in Eq. (3.17), one finds that

$$S_g(\omega) = \begin{cases} \frac{2No}{A^2}\omega^2\left[1-\frac{|\omega|}{2\omega_n}\right] & , \ |\omega| < 2\omega_n \\ 0 & , \ |\omega| > 2\omega_n \end{cases} \qquad (3.18)$$

The spectra of the spike noise and the doublet noise are not known exactly. The best one can do is approximate them by assuming that the spikes and doublets have typical shapes like those shown in Fig. 3.8. [However, wide variations from these shapes occur.] The doublet waveform indicates that the spectrum is bandlimited and has a parabolic shape at the origin. The spike waveform indicates that the spectrum is also bandlimited but is flat at the origin. It is assumed in both cases that the sequences of doublets and spikes at the output of the discriminator occur randomly and have a finite probability of occurrence. Hence, their occurrence follows a poisson distribution.

3.2 Spike detection in a digital FM system

The first work on spike detection was performed by Schilling (1.6). He built a spike detector for a synchronous FSK system in which positive and negative FM pulses are the transmitted modulation. The receiver is an FM discriminator followed by a low pass filter and a sampler. The sampler measures the sign of the pulse at a particular sampling instant t_2 and decides that a <u>one</u> has been transmitted if the sign is positive and a <u>zero</u> if the sign is negative. The effect of a spike on a pulse after the low pass filter is to decrease the amplitude of the pulse or even reverse the sign of the pulse and cause an error. [Rice (1.7) has shown that the probability of a positive spike with positive modulation and a negative spike with negative modulation is negligible; hence spikes practically always tend to cancel modulation area.] To detect the presence of a spike, a simple

threshold scheme was set up; if the magnitude of the voltage e_3 (see Fig. 3.1) exceeded a threshold level e_{TH}, a spike was presumed to have occurred and the time of occurence, t_1, was noted.

Suppose the situation shown in Fig. 3.9 occurs, i.e., the output of the discriminator consists of a positive modulation pulse plus a negative spike [for simplicity, the spike is shown as an impulse $-2\pi\,\delta(t-t_1)$]. Then the output of a low pass filter H_1 with bandwidth $>>\omega_n$ consists of the sum of the two waveforms shown in Fig. 3.10. [$h_1(t)$ is the impulse response of the low pass filter H_1.] Note that in this case, no error occurs because the sign of the sum of two waveforms at the sampling instant t_2 is still positive. However, there is an interval of time which can be exactly determined, during which the occurrence of a spike will definitely cause an error, i.e., the sign of the modulation pulse at the sampling instant is reversed. If a spike occurred whose time of occurrence fell into this interval, the decision on the sign of the modulation pulse was reversed. Using this technique, a large portion of the errors due to spikes were corrected.

Note that doublets are not taken into account in the analysis, i.e., no attempt was made to distinguish between the two types of disturbances. Certainly, doublets could also have exceeded the threshold level e_{TH} and although they do not cause errors directly, they could lead to errors if the modulation is reversed when it should not be. The best explanation that can be presented at this time is that most large doublets occur when the modulation is near a zero crossing. Hence, they would be rejected by the above error correction scheme because they occur too far from the sampling instant.

3.3 Spike detection in an analog FM system

As a first approach to the problem, a spike detector was designed using the following basic properties of a spike:

a. The amplitude of the signal plus noise vector, R(t), at the input to the discriminator is a minimum at the time of occurrence of a spike.

b. The area under a spike is equal to 2π. The first property is used to decide the time at which a spike decision (yes or no) has to be made. The second property is used to make the spike decision. Fig. 3.3 shows the block diagram of the proposed spike detector. The filter impulse responses are as follows:

$$h_1(t) = \begin{cases} 1/1-k & , \quad 0 < t < T_1 = \frac{\pi}{\omega_n} \\ 0 & , \quad \text{elsewhere} \end{cases} \tag{3.19}$$

$$h_2(t) = \begin{cases} k/1-k & , \quad 0 < t < T_2 = \frac{\pi}{\omega_m} \\ 0 & , \quad \text{elsewhere} \end{cases} \tag{3.20}$$

where $k = \sin \frac{\pi T_1}{2 T_2} = \sin \frac{\pi \omega_m}{2\omega_n} = \sin \frac{\pi}{2\beta}$. (3.21)

k is so chosen that the modulation ($\sin \omega_m t$) cancels out at the output of the subtractor. [The two filter combination has the effect of a bandpass filter with a zero at $p = j\omega_m$. For the case of modulation with a rectangular spectrum, this two filter combination will eliminate most of the modulation but not all of it. A more complicated filter design would be required for this case to remove all of the modulation.] Thus, the output of the subtractor is the discriminator output noise put through a filter with the impulse response $h_{12}(t)$ as shown in Fig. 3.12. It has the effect of measuring the area under the input if $k/1-k \ll 1$ or if $T_1 \ll T_2$. If spikes are sufficiently infrequent that the interval from 0 to T_2 contains at most one spike, then it can still operate satisfactorily if the R(t) measurement is also used in the decision box.

Fig. 3.13 A, B, C shows the various waveforms and thresholds that enter the decision box. $R^2(t)$ is the output of a square-law amplitude

detector for the signal plus noise vectors. $\triangle\theta$ (t) is the output of the two filter combination which estimates the spike area. The decision box output is a pulse indicating the detection of a spike when $R^2 < R_o^2$ and $|\triangle\theta| > \triangle\theta_o$. The center of the pulse is the estimated time of occurrence of the spike and the direction of the pulse is the direction of the spike. Note that if $\triangle\theta(t)$ exceeds the $\triangle\theta_o$ threshold due to the area measuring properties of the negative portion of the $h_{12}(t)$ filter shown in Fig. 3.12, this will not be recorded as a spike as long as $R^2(t)$ is greater than R_o^2.

This spike detection scheme was simulated on a digital computer using the following parameters:

Noise Bandwidth = $\omega_n = \pi/5$ rad/sec

Modulation Bandwidth = $\omega_m = \pi/25$ rad/sec

Modulation index = $\beta = 5$ (modulation = $\beta\omega_m \cos \omega_m t$)

Carrier-to-noise ratio = CNR = 3db

Carrier Amplitude = A = 1.0

k = .628

Spike Area Threshold = $\triangle\theta_o = 3.14$

Signal + Noise Modulus Threshold = $R_o = .5$

Number of actual spikes present = 42

(Calculated number of spikes based on Rice's paper (1.7) = 45)

The results were as follows:

Total number of spikes detected = 69

Total number of true spikes detected = 36

Total number of false spikes detected = 33

Net improvement = +3

These results are not satisfactory because too many errors were made, i.e., too many doublets were identified as spikes.

From Fig. 3.5, it appears that in the no modulation case, doublets can have positive and negative areas up to π; a study of the situations

that could occur with modulation present indicated that this result is also true for that case. [In both instances one assumes that the path of the tip of the noise vector is a smooth curve approximately elliptical in shape with no ripples, i.e., tangents to the curve do not intersect the curve.] However, the presence of spikes during the interval t to $t+T_2$ and fractions of doublets at the end points of this interval can shift the output of filter no. 2 sufficiently to produce estimates of doublet areas which exceed π when filter no. 1 includes the positive or negative area of the doublet but not both areas. Thus, a stronger test is needed to distinguish between spikes and doublets.

In the second approach to the problem, the first property, (a), was retained but two different properties were substituted for (b) to try to reduce doublet errors. These properties are:

b. The energy of a spike is spread over a wide frequency range, much wider than the modulation bandwidth and wider than the input noise bandwidth.

c. The direction of a spike is opposite to the direction of the modulation while the reverse is true for doublets.

Again, property (a) is used to decide the time at which a spike decision must be made. The second property, used in conjunction with some threshold setting identifies a disturbance as a spike if the disturbance has sufficient energy in a wide bandwidth ($>>\omega_n$). The third property is used to distinguish spikes from doublets.

Fig. 3.11 can also be used to describe this spike detection system if the third (dashed) input to the decision box is used. Fig. 3.13 A, B, C again applies to the operation of the decision box with the following additional feature:

If property (c) is not met during the entire spike interval (indicated by the width of pulse at the spike detector output in Fig. 3.13C), the spike is rejected and a doublet is assumed to have occurred.

The second scheme was tested with the following new parameters:

$T_1 = \pi / 50\omega_n$ (max. possible for this program)

$k = \sin \frac{\pi}{100\beta} = .00628$

$\Delta \theta_o = 5\omega_n T_1$

In effect, a spike was recorded if the short term average of the discriminator output (with the modulation removed) exceeded the long term average by an amount equal to 10 times the input noise bandwidth, ω_n, assuming the proper spike and modulation directions are observed. Fig. 3.14 shows the essential features of the threshold system. Using this system, the following results were obtained:

Total number of true spikes present = 42

Total number of spikes detected = 19

Total number of true spikes detected 18

Total number of false spikes detected = 1

Net improvement = +17

In trying to optimize this system, three parameters can be varied, namely $\Delta\theta_o$, R_o and T_1.

The first few tests showed that the best threshold setting for R_o was $R_o = \infty$. Hence, R_o was ignored as a parameter. $\Delta\theta_o$ and T_1 were varied and the results, in terms of the net number of spikes detected (N_{SD}), are plotted in Fig. 3.15. The best setting for T_1 was .5 seconds or $\pi/10\omega_n$. The best setting for $\Delta\theta_o$ was .7 radians.

At these two threshold settings, it was possible to add an additional 3 spikes (not shown in Fig. 3.15) to the total of 21 by assuming that property (c) could be dropped if a $|\Delta\theta| = 3$ radians threshold was exceeded.

In other words, if the net area under the disturbance is large enough and occurs in a very small interval of time, the assumption that the disturbance is a spike is a good one regardless of the sign of the modulation. Thus, a final improvement of 24 spikes was obtained by spike detection or 24/42 = 57% of the total number of spikes. In the process, a total of 4 false spikes were also detected.

A study of data obtained in attempting to detect spikes using the second approach indicates that most errors are due to the occurrence of spikes and doublets at low values of modulation. Near m = 0, the estimate of the sign of the modulation at the output of filter no. 2 is often incorrect due to the presence of spikes and doublets within the range of the filter's impulse response as noted in the previous error analysis. Thus, errors are often made in this region in deciding whether or not a sharp disturbance is a spike or a doublet when property c is the deciding factor. Consequently, it would appear that a reliable technique for estimating the sign of modulation near m = 0 is required. It is possible that a nonlinear device between the output of the discriminator and the input of filter no. 2, which reduces the value of the discriminator output when R(t) is small and a spike or a doublet is occurring, may improve the estimate of the sign of the modulation and, thus, improve the spike detection results. A second possibility is the use of a threshold on $|m|$ such that no spike decision would be made unless $|m|$ exceeded some level m_o.

3.4. Spike elimination

The method employed for eliminating the effects of spikes was that of adding a reverse pulse at the time of occurrence of the detected spike. In order to do this, the discriminator output is delayed by an amount equal to the spike detection time plus 1/2 the width of the spike to be added.

The results of a computer simulation indicated that the method was satisfactory and that the width and shape of the pulse added was not significant as long as the pulse had area 2π and had a duration much less than $2\pi/\omega_m$. A rectangular pulse of length $2\pi/\omega_n$ and height ω_n was found to be satisfactory. The spectrum of the original spike plus the added pulse is that of a doublet with neglible area in region $-\omega_m$ to $+\omega_m$ in the spectral density domain. Hence, the effect of the spike is completely removed.

3.5. SNR improvement with spike detection

The amount of the improvement on SNR obtained by spike detection can be calculated with the aid of Eq. (D.11) derived in appendix D:

$$SNR = \frac{3\beta^3 CNR}{1 + 12\ CNR \frac{\beta Ns}{f_m}} \qquad (D.11)$$

where Ns = number of spikes/second present in the discriminator (function of β, CNR, ω_n)

If N_{s1} = number of spikes/second after spike detection and elimination then the SNR improvement is

$$SNRI = \frac{1 + 12\ CNR \frac{\beta N_s}{f_m}}{1 + 12\ CNR \frac{\beta Ns1}{f_m}} \qquad (3.22)$$

In our case

$$CNR = 2$$

$$\beta = 5$$

$$f_m = \pi/25$$

$$N_s = 42/5076$$

$$N_{s1} = (42-24)/5076 = 18/5076$$

Hence, the SNRI is readily found to be 2.03 or about 3db.

A determination of the threshold improvement, however, is a much more difficult task. In order to do this, one would have to run

the spike detection program for a very long period so that a sufficient number of spikes would be included to permit a reasonable amount of confidence in the final result. At a CNR of 6db, the computer program has about 1 spike per minute of computer time. Thus, about 42 minutes of computer time would be needed to obtain results comparable to the results obtained at a CNR of 3db. In addition, if the result is not good, additional computer time may be needed to make adjustments in the parameters T_1 and $\Delta\theta_o$. This adjustment appears to be likely since the statistics of the noise must change if more than 57% of the spikes are to be eliminated.

Another approach to the determination of threshold for spike detection is to assume that the SNR improvement will be approximately 3db for CNR's higher than 3db. Using this assumption, the location of the 1db threshold is determined by placing a line 4db below and parallel to the SNR = $3\beta^3$CNR line which is the zero spikes/second line. The intersection of the 4db line with the SNR-CNR curve for the discriminator with sinusoidal modulation as shown in Fig. 4.4, gives a threshold of 8.3db. Since the discriminator threshold is 9.5db, the threshold improvement is 1.2db.

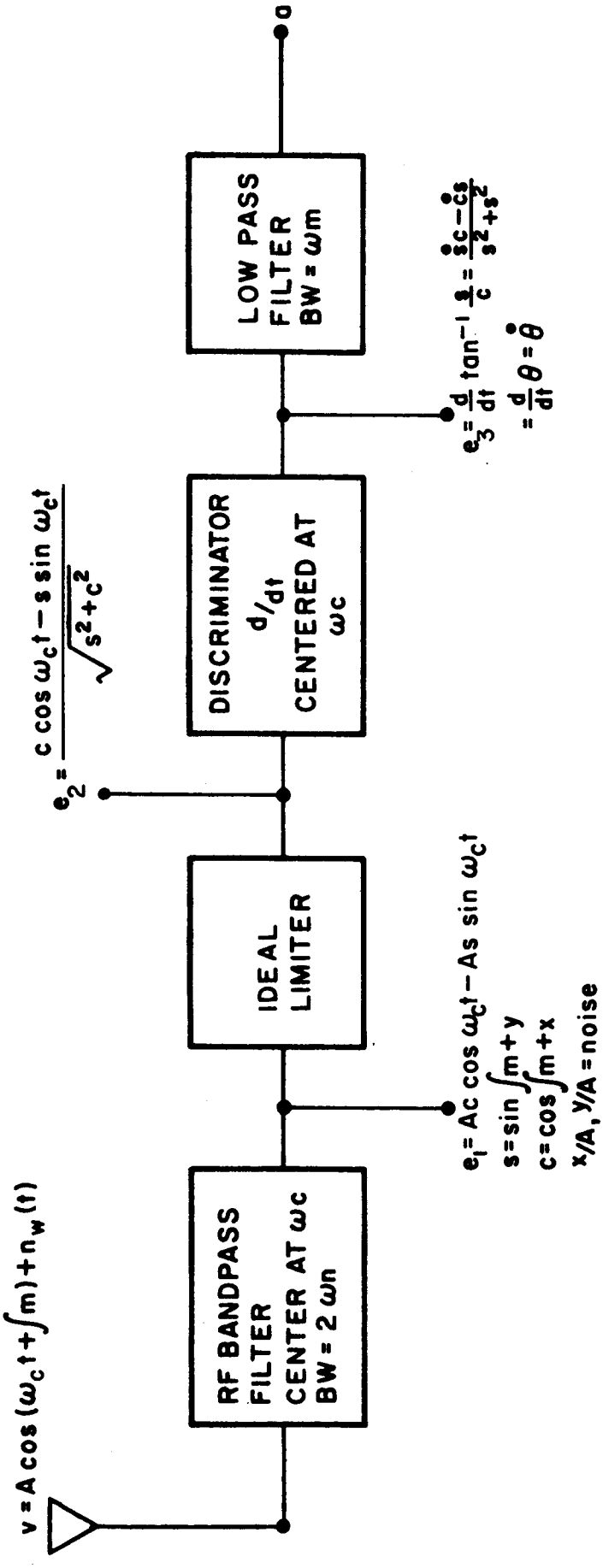

Fig. 3.1 Block diagram of the FM discriminator

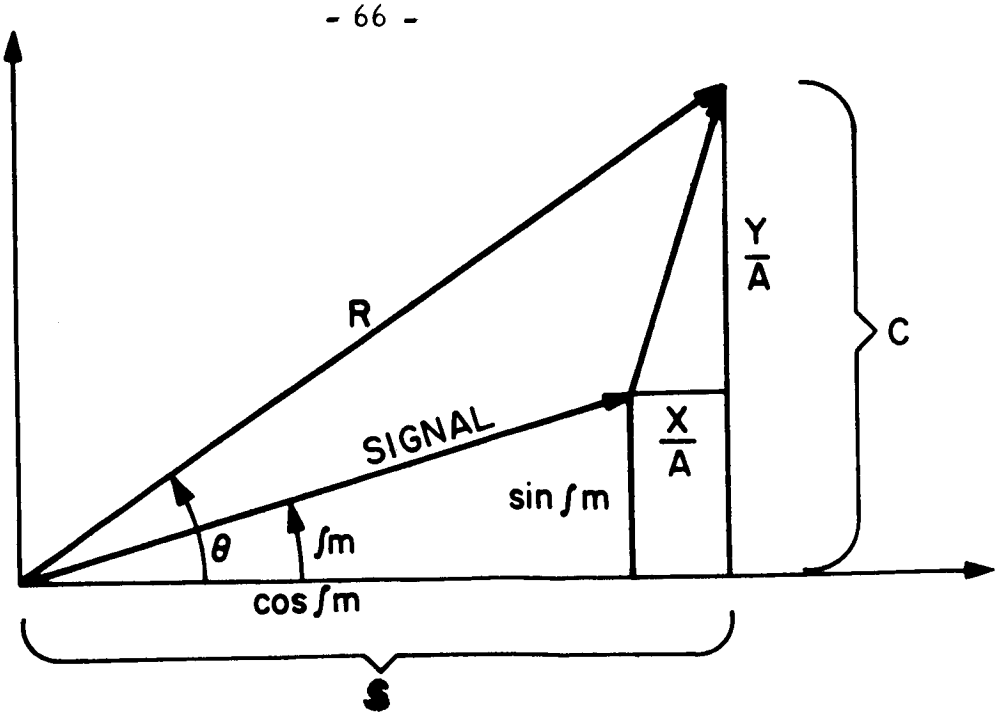

Fig. 3.2 Signal and noise vectors in the FM discriminator

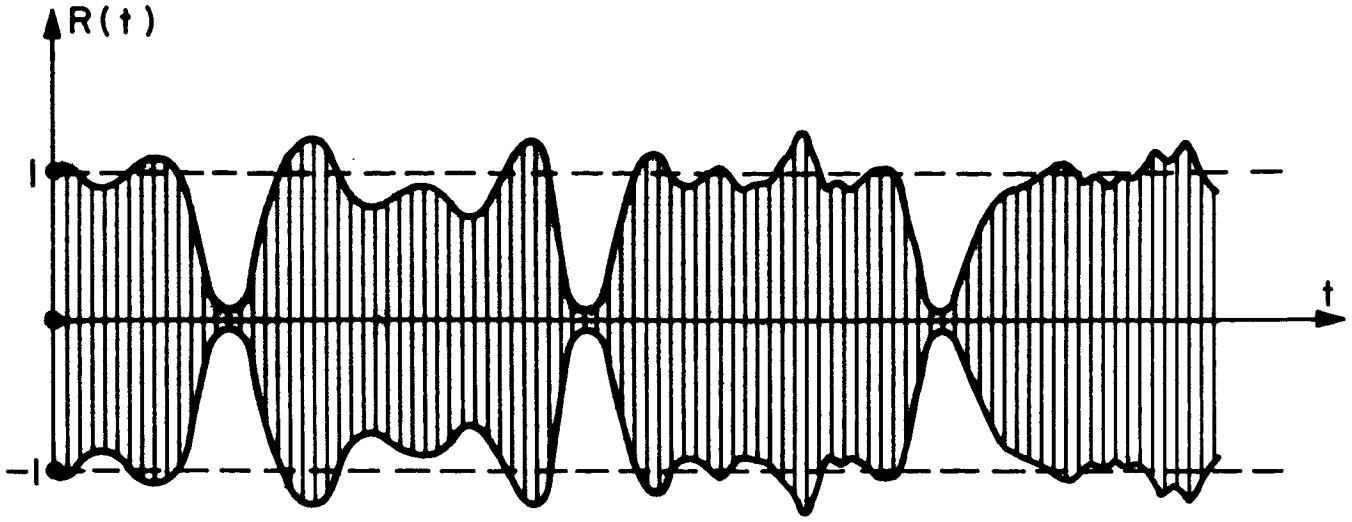

Fig. 3.3a Typical graph of the amplitude of the signal plus noise vector versus time

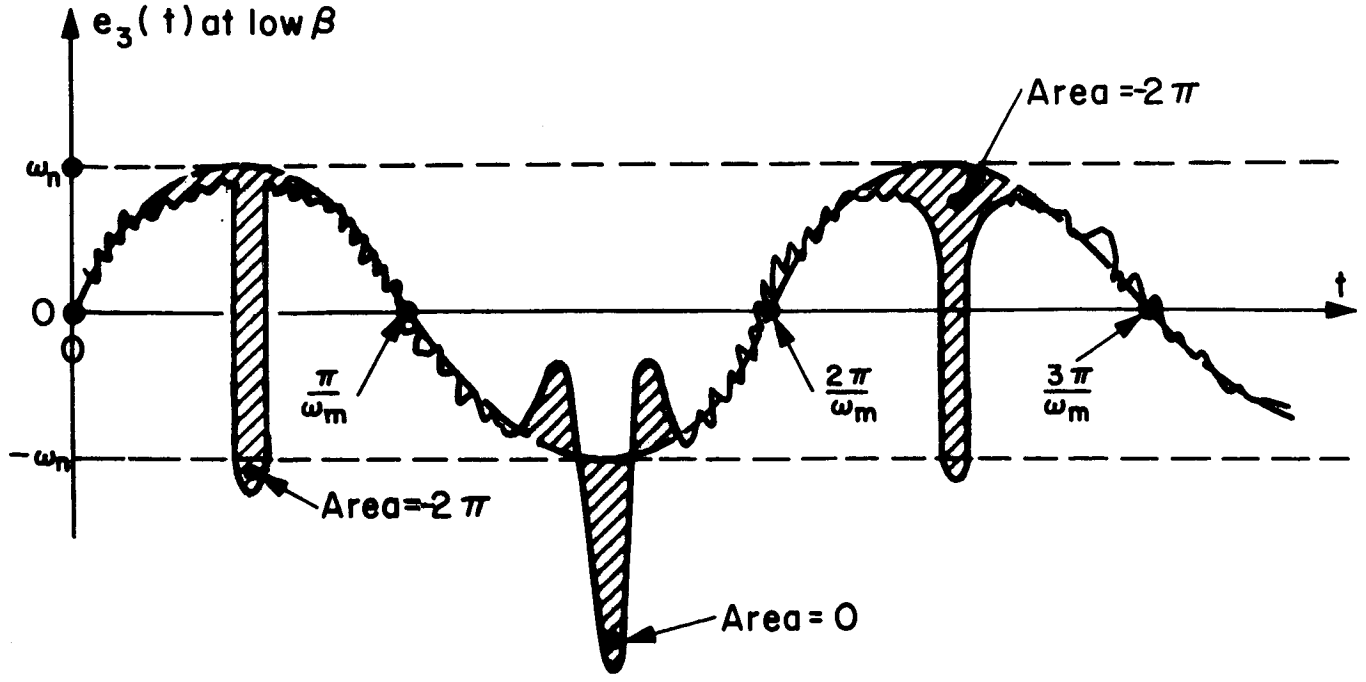

Fig. 3.3b Typical graph of the discriminator output versus time at low β

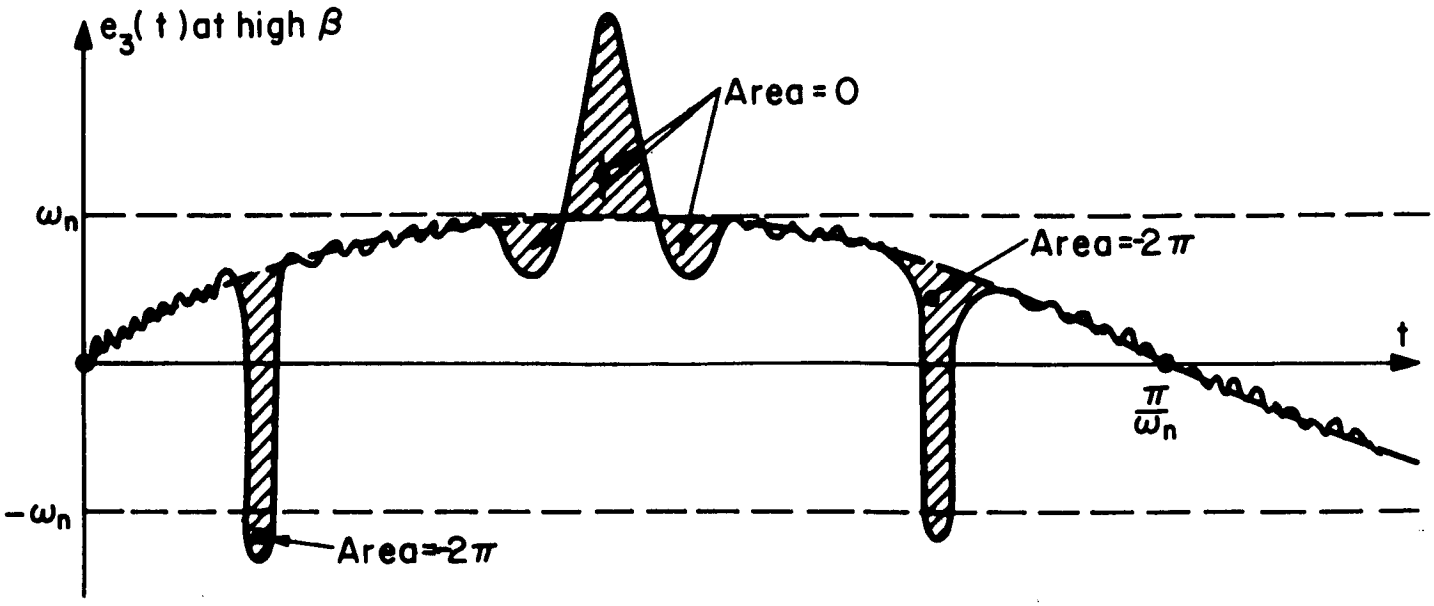

Fig. 3.3 c Typical graph of the discriminator output

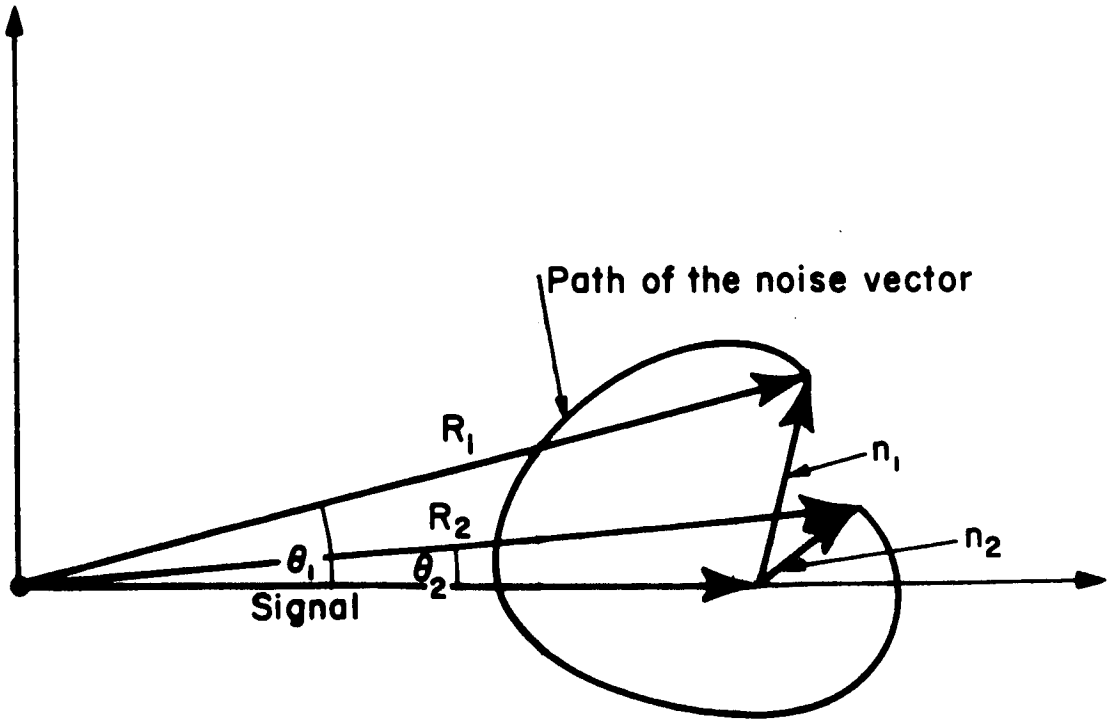

Fig. 3.4 Noise vector path for gaussian noise

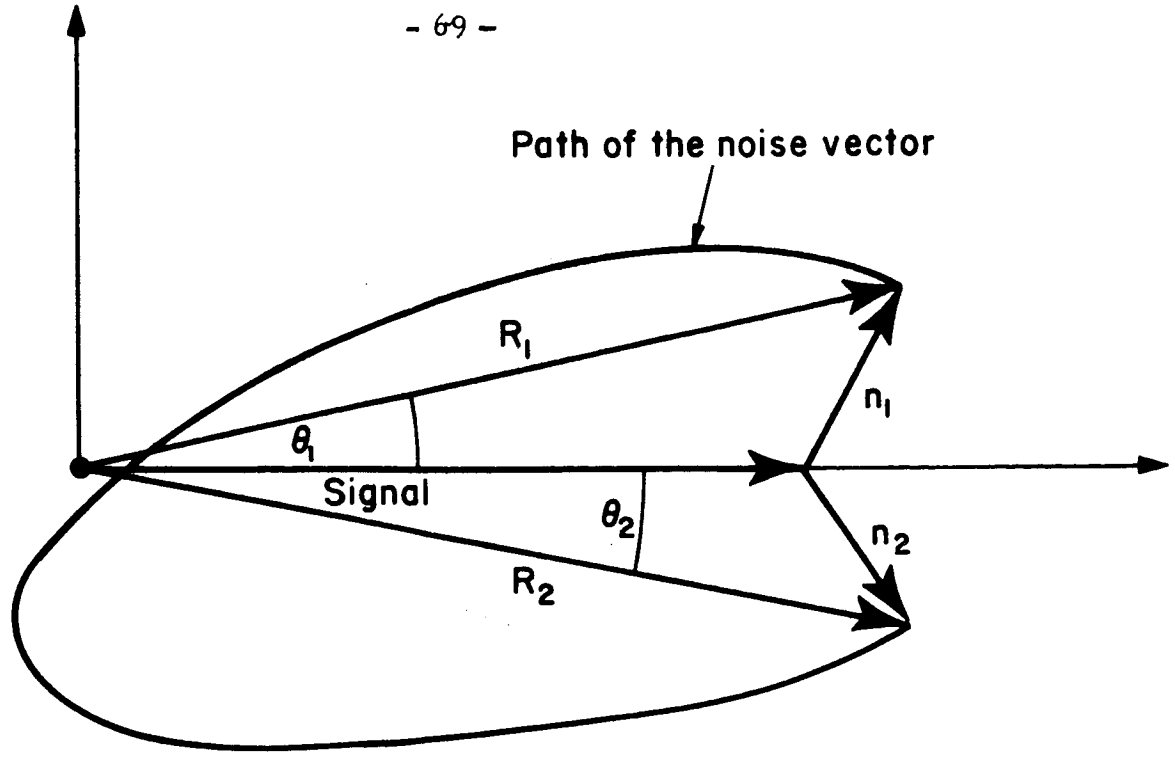

Fig. 3.5 Noise vector path for a doublet

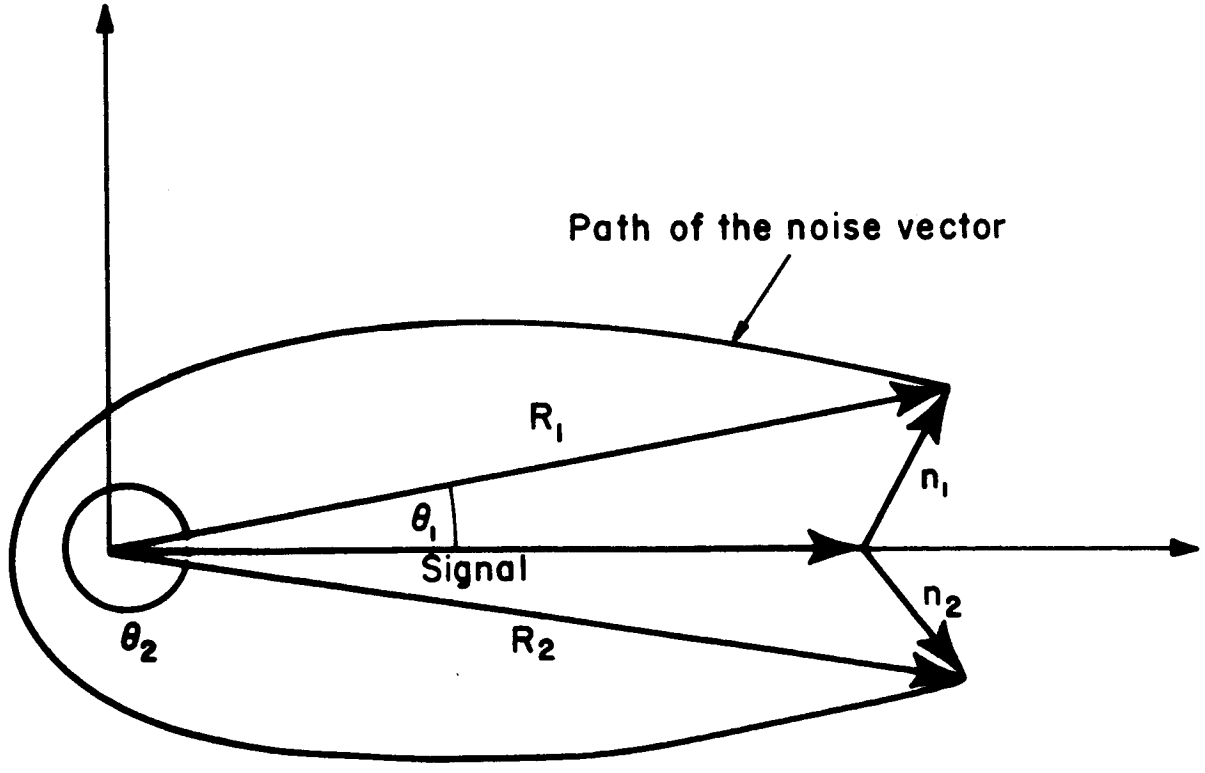

Fig. 3.6 Noise vector path for a spike

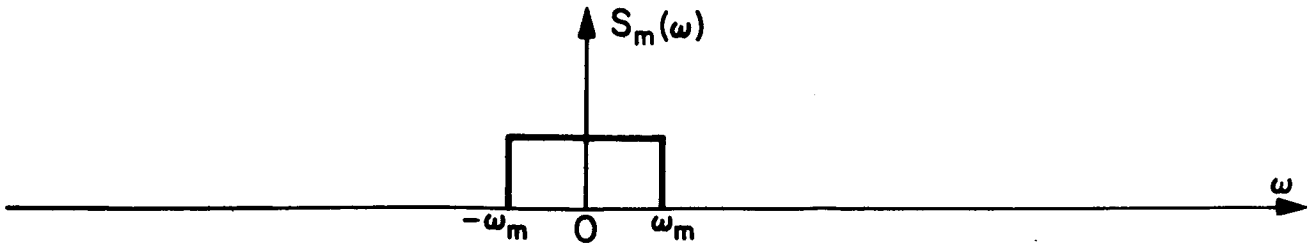

Fig. 3.7a Spectrum of the modulation

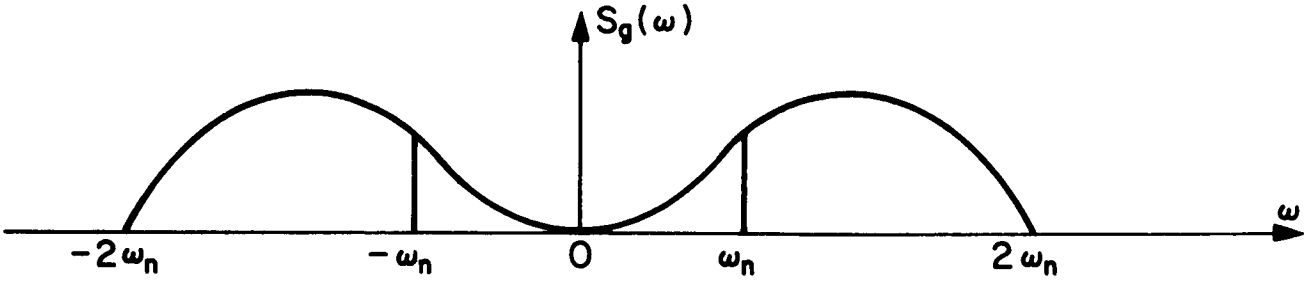

Fig. 3.76 Spectrum of the gaussian noise

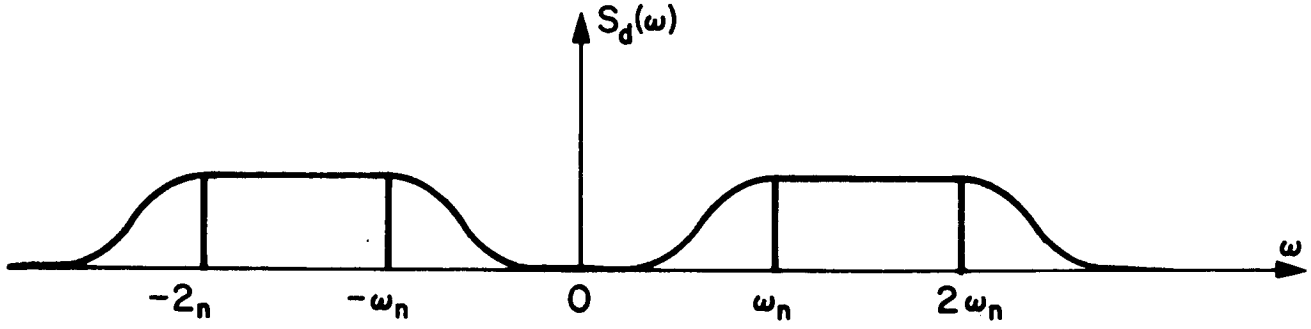

Fig. 3.7c Spectrum of the doublet noise

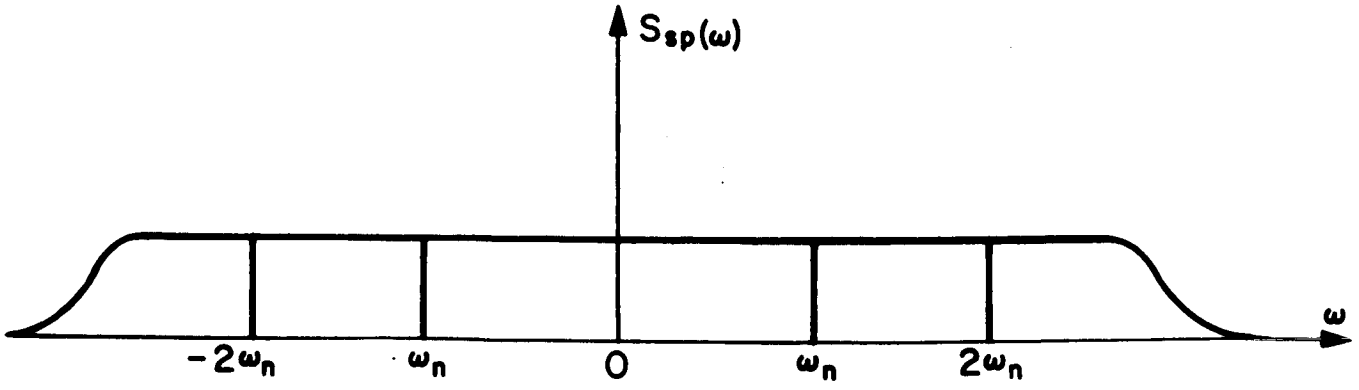

Fig. 3.7d Spectrum of the spike noise

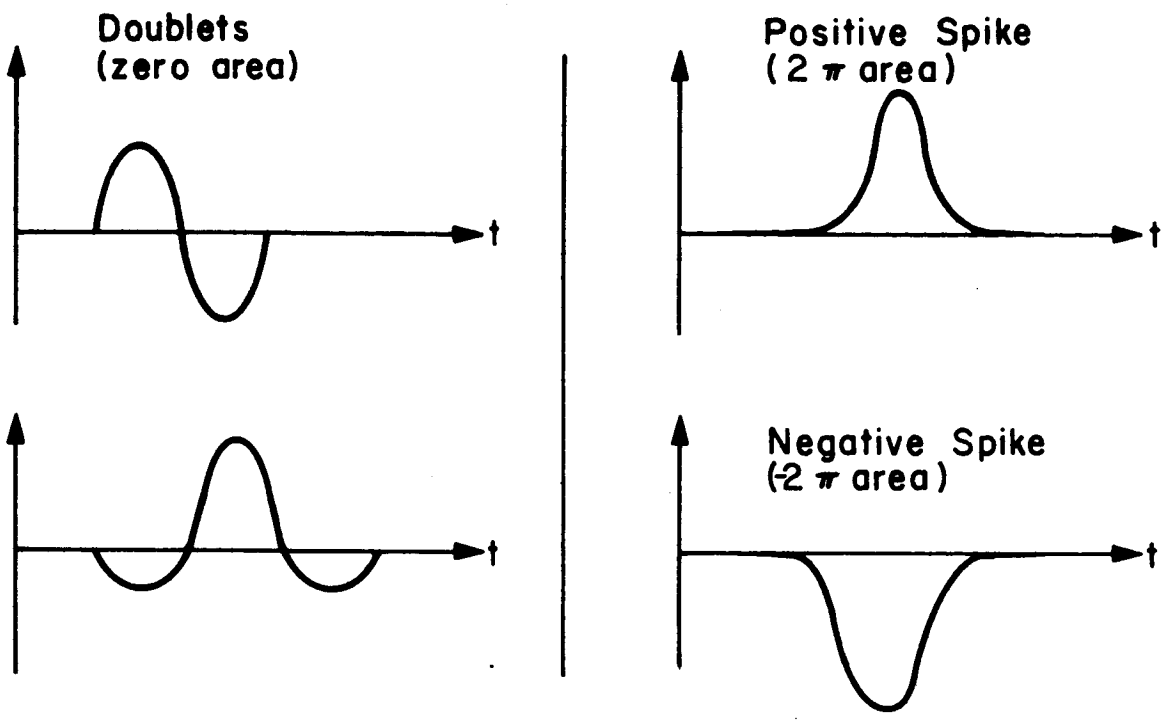

Fig. 3.8 Typical shapes of spikes and doublets

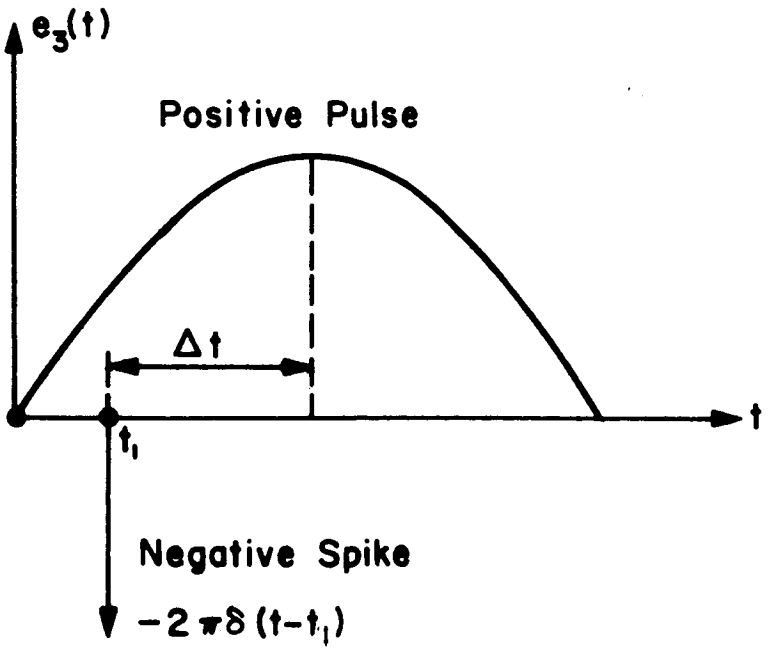

Fig. 3.9 Positive pulse and negative spike in an FSK system using a discriminator demodulator

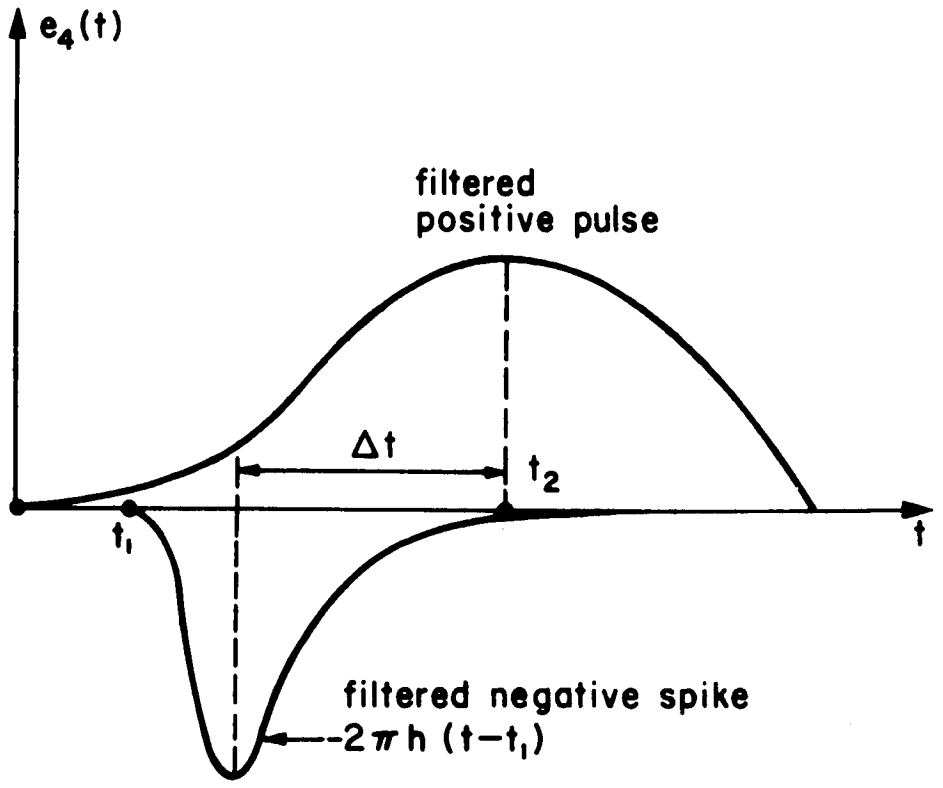

Fig. 3.10 Filtered positive pulse and negative spike in an FSK system using a discriminator

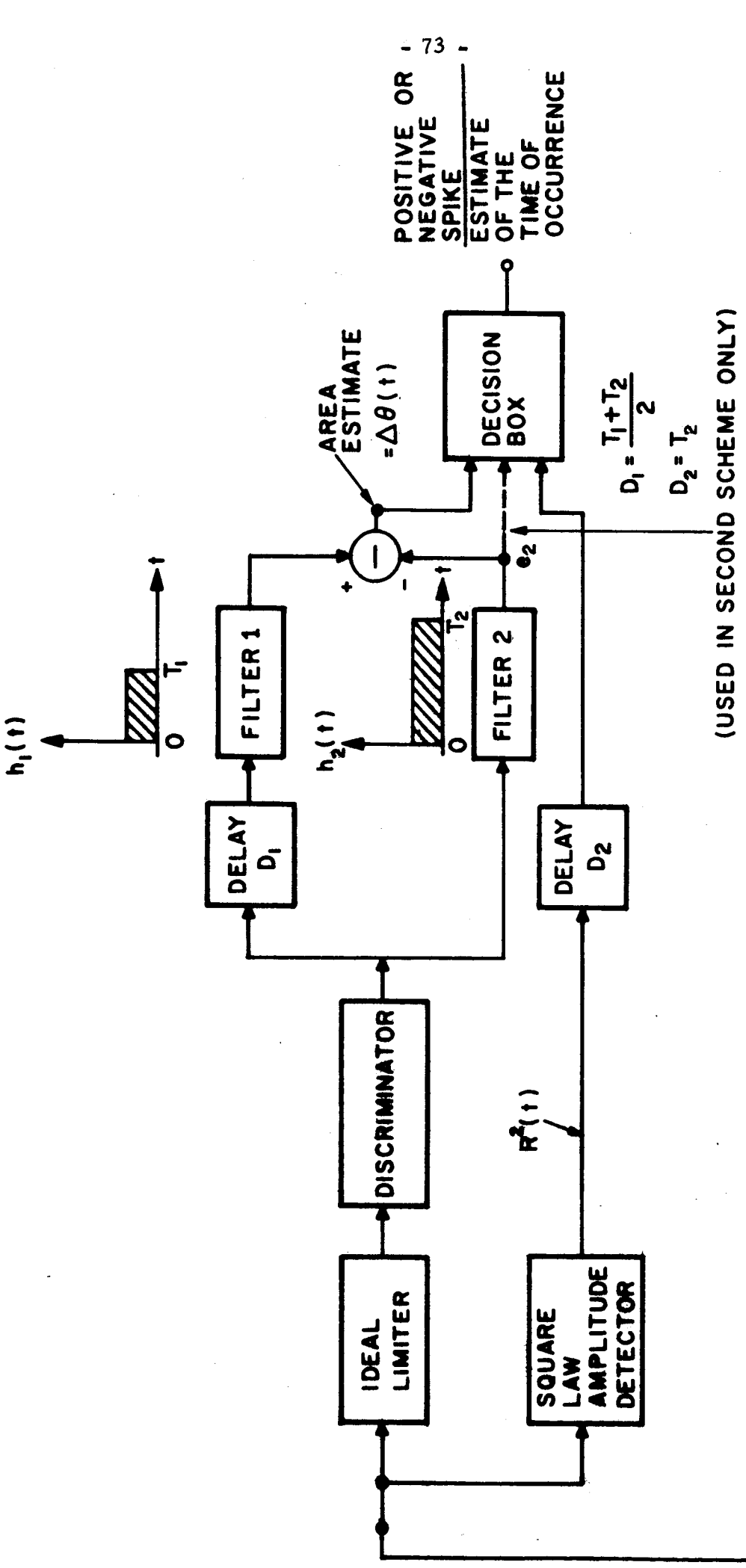

Fig. 3.11 Block diagram of the spike detection system

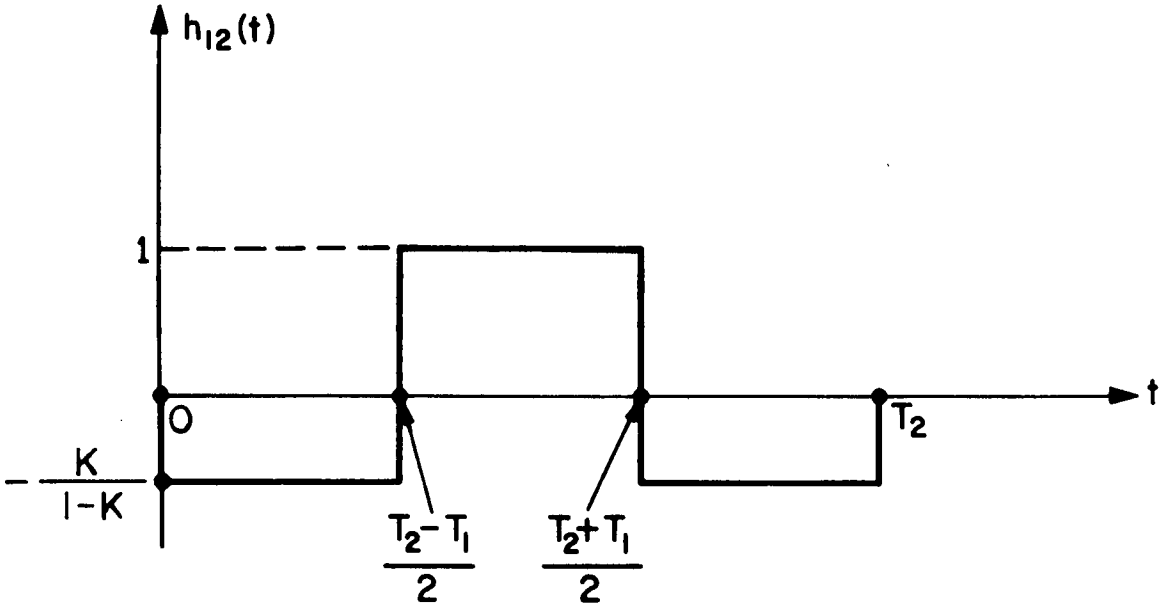

Fig. 3.12 Impulse response of the two filter combination

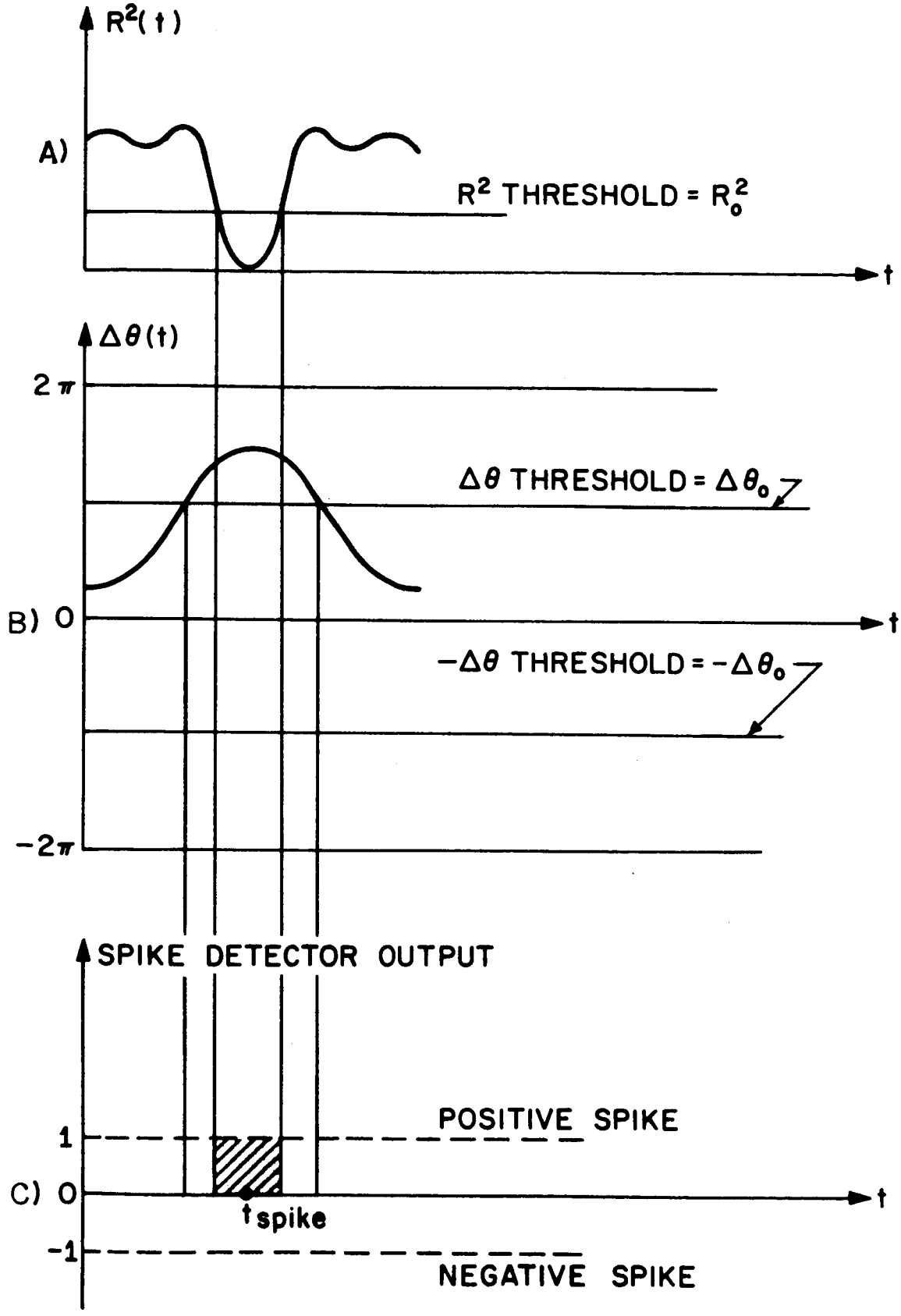

Fig. 3.13 Threshold levels in the decision box

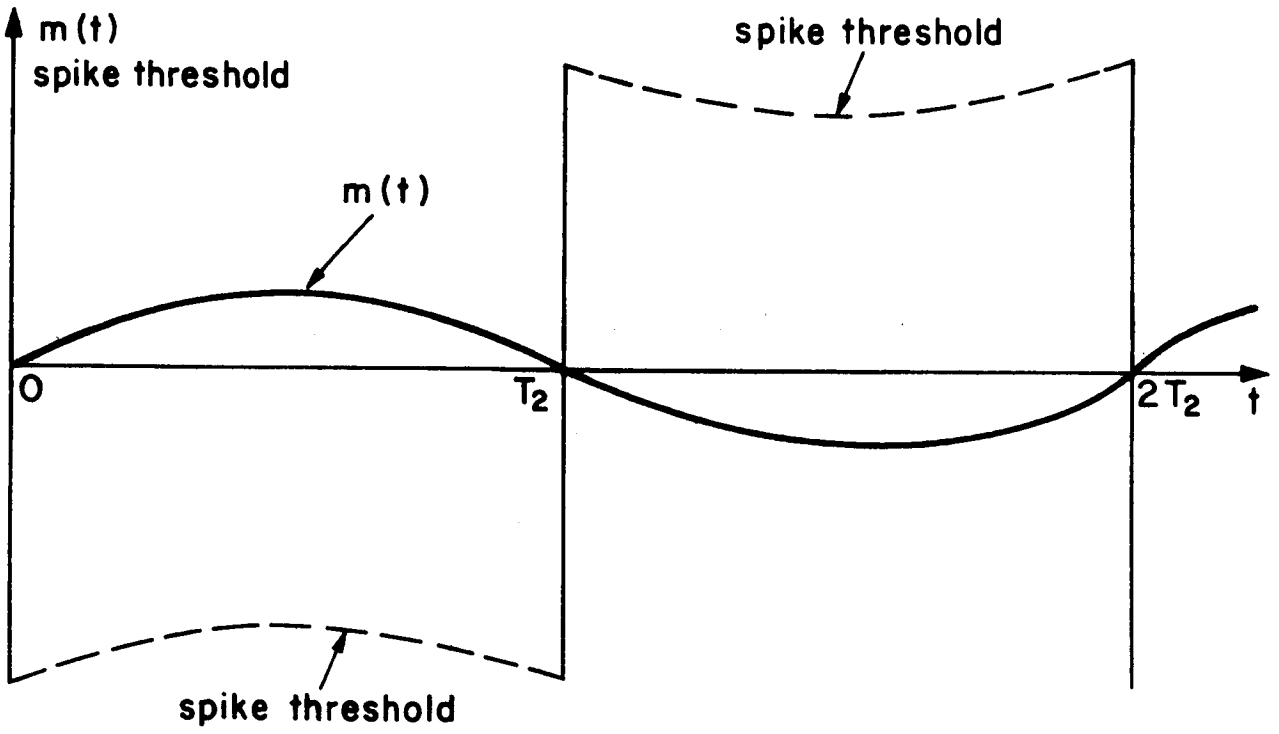

Fig. 3.14 Variation of the spike threshold with time

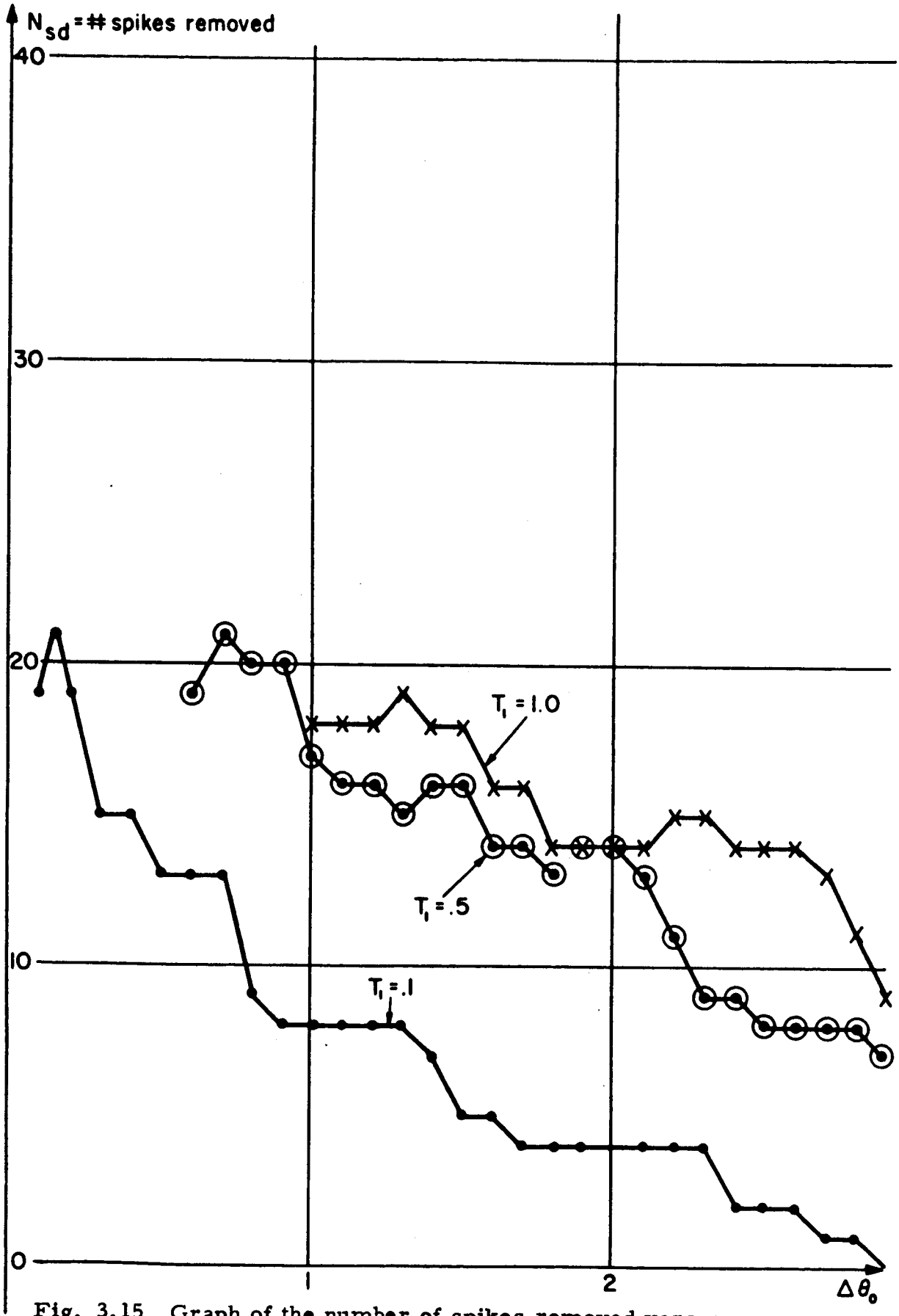

Fig. 3.15 Graph of the number of spikes removed versus $\Delta\theta_o$ and T_1

Chapter 4

SIMPLE FM RECEIVERS

There are other FM receivers which are not optimum, but are worthy of investigation because they can be completely analyzed. Two such receivers are defined as follows:

$$1.\quad a(t) = \frac{1}{\sigma^2}\int_{-\infty}^{+\infty} R_m(t-\lambda)[\underline{\dot{s}}\underline{c}-\underline{\dot{c}}\underline{s}]\,d\lambda \tag{4.1}$$

and

$$2.\quad a(t) = \frac{1}{\sigma^2}\int_{-\infty}^{+\infty} R_m(t-\lambda)[\underline{\dot{s}}\underline{c}-\underline{\dot{c}}\underline{s}]\underbrace{[B+1-(\underline{s}^2+\underline{c}^2)]}_{D}\,d\lambda \tag{4.2}$$

where $\underline{s} = \sin\int m + y$ $\qquad$ B, D = functions of the CNR chosen to

$\underline{c} = \cos\int m + x$ $\qquad$ maximize the SNR

To show that they are FM receivers, consider the case when the noise is zero. We get

$$1.\quad a(t) = \frac{1}{\sigma^2}\int_{-\infty}^{+\infty} R_m(t-\lambda)\,m(\lambda)\,d\lambda \tag{4.3}$$

$$2.\quad a(t) = \frac{1}{\sigma^2}\int_{-\infty}^{+\infty} R_m(t-\lambda)\,m(\lambda)\underbrace{[B/D]}_{=1 \text{ at CNR}=\infty}\,d\lambda \tag{4.4}$$

indicating that a(t) is a filtered version of the original modulation.

4.1. Analysis of FM receiver no. 1

In order to perform the analysis of receiver no. 1, certain simple approximations will be made to find the various spectrums required.

1. Noise: x, y

Bandwidth = ω_n

Power = $2N_o\omega_n/\pi A^2$

$$S_x(\omega) = S_y(\omega) = \begin{cases} 2N_o/A^2, & |\omega| < \omega_n \\ 0, & |\omega| > \omega_n \end{cases}$$

$S_{xy}(\omega) = 0$

2. Signal: $\cos \int m$, $\sin \int m$

Bandwidth = ω_n

Power = 1/2

$$S_c(\omega) = S_s(\omega) = \begin{cases} \pi/2\omega_n & , |\omega| < \omega_n \\ 0 & , |\omega| > \omega_n \end{cases}$$

$S_{sc}(\omega) = 0$

3. Modulation : m

Bandwidth = ω_m

Power = σ^2

$$S_m(\omega) = \begin{cases} \sigma^2 \pi/\omega_m & , |\omega| < \omega_m \\ 0 & , |\omega| > \omega_m \end{cases}$$

From these spectrums, we can derive four other spectrums that will be needed.

1. $$S_{x\dot{x}}(\omega) = S_{y\dot{y}}(\omega) = \begin{cases} 2j\omega N_o/A^2 & , |\omega| < \omega_n \\ 0 & , |\omega| > \omega_n \end{cases}$$

2. $$S_{\dot{x}}(\omega) = S_{\dot{y}}(\omega) = \begin{cases} 2\omega^2 N_o/A^2 & , |\omega| < \omega_n \\ 0 & , |\omega| > \omega_n \end{cases}$$

3. $$S_{c\dot{c}}(\omega) = S_{s\dot{s}}(\omega) = \begin{cases} j\omega\pi/2\omega_n & , |\omega| < \omega_n \\ 0 & , |\omega| > \omega_n \end{cases}$$

4. $$S_{\dot{c}}(\omega) = S_{\dot{s}}(\omega) = \begin{cases} \omega^2 \pi/2\omega_n & , |\omega| < \omega_n \\ 0 & , |\omega| > \omega_n \end{cases}$$

Prior to the low pass filter (indicated by $\frac{1}{\sigma^2} \int_{-\infty}^{\infty} R(t-\lambda) \ldots d\lambda$) the output of the FM receiver is $\underline{\dot{s}c} - \underline{c\dot{s}}$ which can be expanded as follows:

$$\underline{\dot{s}c} - \underline{\dot{c}s} = m + [y(\cos \int m) + x(\sin \int m) - \dot{y} \cos \int m - \dot{x} \sin \int m] + [y\dot{x} - x\dot{y}] \quad (4.5)$$

It is interesting to note that the terms in the first set of brackets may be regarded as the high CNR gain terms because they will determine

SNR at high CNR. The terms in the second set of brackets are the threshold terms since they will produce the bending of the SNR curve at low CNR.

In order to find the output noise, one first notes that the modulation term m is uncorrelated with any of the other terms. Therefore, the spectrum of the noise is the spectrum of the remaining 6 terms. If we multiply the 6 terms by themselves shifted in time, we will get 36 terms, of which 12 of them will have non-zero expected values. These 12 terms are listed in Fig. 4.1.

Upon examining the 12 terms in Fig. 4.1 we see that their evaluation, which depends upon convolving the appropriate spectrums, can be reduced to two general convolutions shown in Fig. 4.2 and Fig. 4.3. The convolutions are readily performed and we get

$$1.\quad S_1(\omega) * S_2(\omega) = \begin{cases} \frac{\omega_n^3}{6\pi}\left[2 - 3\frac{\omega}{\omega_n} + 3\frac{\omega^2}{\omega_n^2} - \frac{\omega^3}{\omega_n^3}\right], & |\omega| < 2\omega_n \\ 0, & |\omega| > 2\omega_n \end{cases} \tag{4.6}$$

$$2.\quad S_3(\omega) * S_3(\omega) = \begin{cases} \frac{\omega_n^3}{12\pi}\left[4 - 6\frac{\omega}{\omega_n} + \frac{\omega^3}{\omega_n^3}\right], & |\omega| < 2\omega_n \\ 0, & |\omega| > 2\omega_n \end{cases} \tag{4.7}$$

Each noise term must then pass thru a rectangular low pass filter of bandwidth ω_m.

The corresponding output power is given by

$$R_1(0) = \frac{1}{\pi}\int_0^{\omega_m} S_1(\omega) * S_2(\omega)\, d\omega \tag{4.8}$$

for the first type of convolution and by

$$R_2(0) = \frac{1}{\pi}\int_0^{\omega_m} S_3(\omega) * S_3(\omega)\, d\omega \tag{4.9}$$

for the second type of convolution.

Evaluating these integrals we get

$$R_1(0) = \begin{cases} \frac{\omega_m^4}{24\pi^2}\left[8\beta^3 - 6\beta^2 + 4\beta - 1\right], & \beta \geq 1/2 \\ \frac{\omega_n^4}{3\pi^2}, & \beta \leq 1/2 \end{cases} \tag{4.10}$$

and

$$R_2(0) = \begin{cases} \frac{\omega_m^4}{48\pi^2}\left[16\beta^3 - 12\beta^2 + 1\right], & \beta \geq 1/2 \\ 0, & \beta \leq 1/2 \end{cases} \tag{4.11}$$

Using the appropriate convolution types and convolution coefficients from Fig. 4.1, we find that the net output noise power is

$$P_{noise} = \frac{4N_o\pi}{A^2\omega_n}\left[R_1(0) + R_2(0)\right] + \frac{8N_o^2}{A^4}\left[R_1(0) + R_2(0)\right] \tag{4.12A}$$

$$= \begin{cases} \left[\frac{4N_o\pi}{A^2\omega_n} + \frac{8N_o^2}{A^4}\right]\left[\frac{\omega_m^4}{48\pi^2}\right]\left[32\beta^3 - 24\beta^2 + 8\beta - 1\right] & \text{for } \beta \geq 1/2 \\ \left[\frac{4N_o\pi}{A^2\omega_n} + \frac{8N_o^2}{A^4}\right]\left[\frac{\omega_n^4}{3\pi^2}\right] & \text{for } \beta \leq 1/2 \end{cases} \tag{4.12B}$$

The output SNR can now be obtained using Eq. (1.6):

$$SNR = \begin{cases} \frac{24\beta^4 CNR}{\left[32\beta^3 - 24\beta^2 + 8\beta - 1\right]\left[1 + \frac{1}{2CNR}\right]}, & \beta \geq 1/2 \\ \frac{1.5CNR}{1 + \frac{1}{2CNR}}, & \beta \leq 1/2 \end{cases} \tag{4.13}$$

Fig. 4.4 shows a plot of Eq. (4.13) for $\beta = 5$ and a plot of Rice's results for the FM discriminator at $\beta = 5$. We see that this simple FM receiver has an improvement factor of approximately β instead of the $3\beta^3$ improvement factor usually associated with FM receivers at high CNR.

Hence, it can be called a spread spectrum receiver because the improvement is proportional to the amount of spectrum spreading produced by the modulator. The 1db threshold of this receiver is determined by setting

$$\frac{1}{2CNR} = \frac{1}{4} \tag{4.14}$$

Therefore, its threshold is fixed at CNR = 3db.

4.2 Analysis of FM receiver no. 2

As in receiver no. 1, the various power spectral densities and autocorrelation functions are specially chosen to simplify the calculations. In this case, where many autocorrelation functions must be multiplied, the simplest possible choice is to make all of the density functions gaussian shaped. Fig. 4.5 lists the spectrums and auto correlation functions to be used.

If

$$\underline{s} = \sin \int m + y \tag{4.15}$$

$$\underline{c} = \cos \int m + x \tag{4.16}$$

is substituted in the function

$$[\dot{\underline{s}}\,\underline{c} - \dot{\underline{c}}\,\underline{s}]\,[B + 1 - \underline{s}^2 - \underline{c}^2] \tag{4.17}$$

a total of 30 terms are obtained which are listed in Fig. 4.6. In column 4 all correlated terms are listed which are below a given term on the list. Thus a total of 86 correlation functions must be calculated using the tables in Figs. 4.5 and 4.6. The details of the calculation are excessively complicated and will not be given here. The results are summarized in Fig. 4.7.

The output signal power for this receiver is contained in term 1 of Fig. 4.7, i.e.

$$R_m\,[(B-2/\rho)^2 + 16\,R_x^2].$$

$\frac{\omega_n^2}{2}(B-2/\rho)^2$ is the modulation power while $16\ R_m\ R_x^2$ can be lumped with all the rest of the noise terms. Knowing the modulation power out, we can identify the variable D in Eq. (4.2) as

$$D = B-2/\rho \tag{4.18}$$

The calculation of the output noise thru a low pass filter of bandwidth ω_m is again a tedious problem. The spectral density of all of the output noise terms in Fig. 4.7 were expanded and summed to form the following Taylor series:

$$S(\omega) \doteq S(0) + \frac{\omega^2}{2}\ \ddot{S}(0) \tag{4.19}$$

$\doteq$ spectral density of the unfiltered output noise. The filtered output noise power was then calculated using the formula

$$\text{Noise power out} \doteq \frac{\omega_m}{\pi}\ S(0) + \frac{\omega_m}{6\pi}\ \ddot{S}(0) \tag{4.20}$$

Using this technique, the SNR was evaluated giving the following result:

$$\text{SNR} = \frac{6\sqrt{2\pi}\,\rho^2\beta^3}{(2\rho+1)(6\beta^2-1)} \cdot \frac{B^2-4B/\rho+4/\rho^2}{B^2-2B(\rho+2)/\rho+(\rho+2)^2/\rho^2 +} \tag{4.21}$$

$$\frac{2(6\sqrt{3\rho}-1)}{3\sqrt{3}(2\rho+1)(6\beta^2-1)} +$$

$$\frac{8\beta^3(6\beta^2+5)}{(2\rho+1)(6\beta^2-1)(1+\beta^2)^{3/2}} +$$

$$\frac{16\beta^2}{\sqrt{3}(2\rho+1)(6\beta^2-1)} +$$

$$\frac{(4\rho+1)(12\beta^2-1)}{\sqrt{2\rho^2}(2\rho+1)(6\beta^2-1)}$$

B must be chosen so that SNR is a maximum. Upon examining Eq. (4.21) it is seen that the maximation problem can be reduced to finding the maximum value of

$$Z = \frac{B^2 + c_o B + c_1}{B^2 + c_2 B + c_3} \tag{4.22}$$

The result, obtained by setting dZ/dB equal to zero, is

$$Z_{max} = \frac{c_o c_2 - 2(c_1 - c_3) - 2\sqrt{(c_1 - c_3)^2 + (c_2 - c_0)(c_1 c_2 - c_0 c_3)}}{c_2^2 - 4c_3} \tag{4.23}$$

at

$$B = \frac{(c_1 - c_3) - \sqrt{(c_1 - c_3)^2 + (c_2 - c_0)(c_1 c_2 - c_0 c_3)}}{(c_2 - c_0)} \tag{4.24}$$

where

$$c_0 = -\frac{4}{\rho} \tag{4.25A}$$

$$c_1 = +\frac{4}{\rho^2} \tag{4.25B}$$

$$c_2 = -2 - \frac{4}{\rho} \tag{4.25C}$$

$$c_3 \doteq 1 + \frac{4}{\rho} + \frac{4}{\rho^2} + \frac{1}{3\beta^2} \quad (\text{for } \rho,\ \beta >> 1) \tag{4.25D}$$

With these substitutions, one finds that

$$Z_{max} \doteq \frac{3\beta^2 + 2}{2}, \tag{4.26}$$

$$B \doteq 1 + \frac{2}{\rho} + \frac{1}{3\beta^2} \tag{4.27}$$

$$SNR \doteq \frac{3\sqrt{2\pi}}{4}\beta^3 \rho \tag{4.28}$$

$$\doteq 1.88\beta^3\rho$$

for $\rho,\ \beta >> 1$

A plot of SNR versus CNR for $\beta = 5$ using a more accurate formula for c_3 (obtained by comparing Eqs. (4.21) and (4.22)) is shown in Fig. 4.1. The graph shows that this receiver represents and improvement over the previous FM receiver; however, the SNR is still less than that of the discriminator and the threshold is much poorer than the discriminator threshold.

No.	Term	Convolution Type	Convolution Coefficient
1	$y_1 y_2 (\cos \int m_1)(\cos \int m_2)$	1	$N_o \pi / A^2 \omega_n$
2	$x_1 x_2 (\sin \int m_1)(\sin \int m_2)$	1	"
3	$\dot{y}_1 \dot{y}_2 (\cos \int m_1)(\cos \int m_2)$	1	"
4	$\dot{x}_1 \dot{x}_2 (\sin \int m_1)(\sin \int m_2)$	1	"
5	$-y_1 \dot{y}_2 (\cos \int m_1)(\cos \int m_2)$	2	"
6	$-x_1 \dot{x}_2 (\sin \int m_1)(\sin \int m_2)$	2	"
7	$-\dot{y}_1 y_2 (\cos \int m_1)(\cos \int m_2)$	2	"
8	$-\dot{x}_1 x_2 (\sin \int m_1)(\sin \int m_2)$	2	"
9	$y_1 y_2 \dot{x}_1 \dot{x}_2$	1	$4N_o^2 / A^4$
10	$\dot{y}_1 \dot{y}_2 x_1 x_2$	1	"
11	$-\dot{y}_1 y_2 \dot{x}_1 x_2$	2	"
12	$-y_1 \dot{y}_2 x_1 \dot{x}_2$	2	"

Fig. 4.1 Table of noise terms for FM receiver no. 1

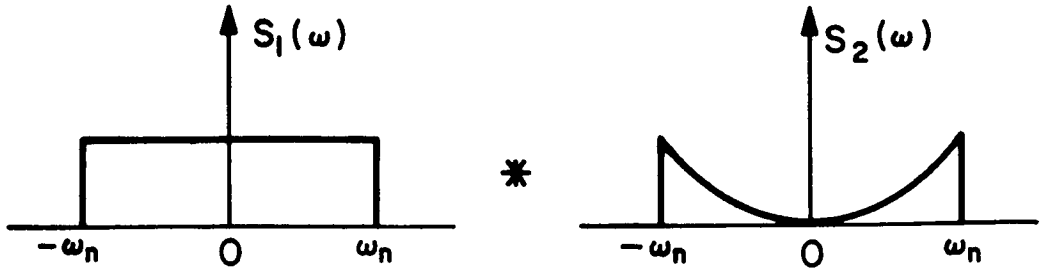

Fig. 4.2 Type 1 convolution

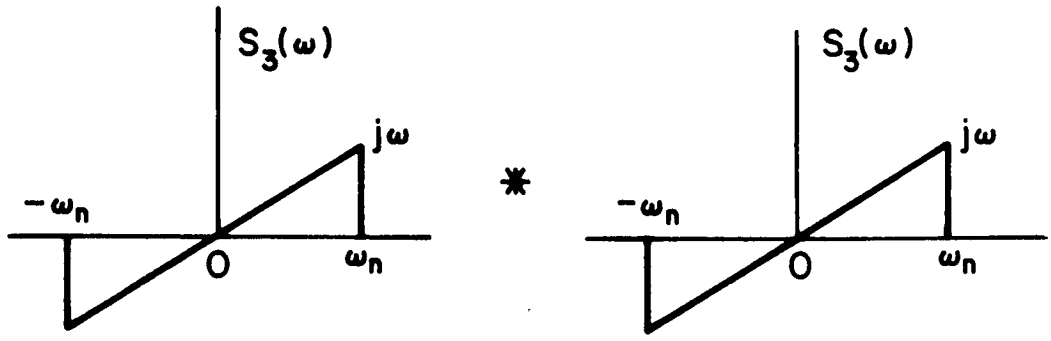

Fig. 4.3 Type 2 convolution

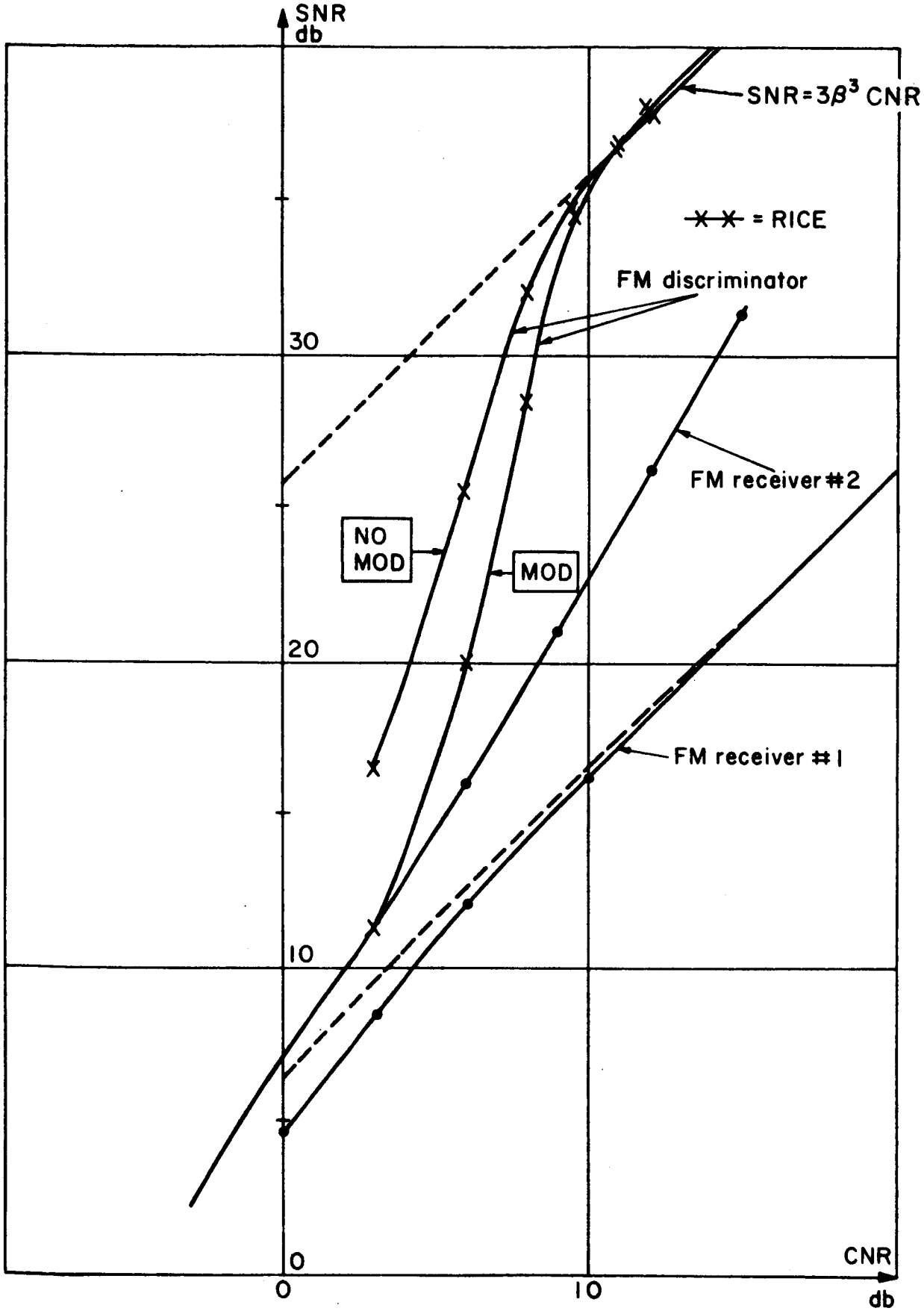

Fig. 4.4 SNR versus CNR for FM receivers no. 1 and no. 2

Time function	Symbol	Autocorrelation function	Spectral Density
modulation	$E(m_1 m_2)$	$R_m = \frac{\omega_n^2}{2} e^{-\omega_m^2 \tau^2/4}$	$S_m = \frac{\omega_n^2}{2}\sqrt{\frac{4\pi}{\omega_m^2}}\, e^{-\omega^2/\omega_m^2}$
* signal	$E(s_1 s_2)$ $E(c_1 c_2)$	$R_{ss} = R_{cc} = \frac{1}{2} e^{-\omega_n^2 \tau^2/4}$	$S_{ss} = S_{cc} = \frac{1}{2}\sqrt{\frac{4\pi}{\omega_n^2}}\, e^{-\omega^2/\omega_n^2}$
noise	$E(x_1 x_2)$ $E(y_1 y_2)$	$R_x = R_y = \frac{1}{2CNR} e^{-\omega_n^2 \tau^2/4}$	$S_{xx} = S_{yy} = \frac{1}{2CNR}\sqrt{\frac{4\pi}{\omega_n^2}}\, e^{-\omega^2/\omega_n^2}$

Additional derived autocorrelation functions and spectral densities

noise	$E(\dot{x}_1 \dot{x}_2)$ $E(\dot{y}_1 \dot{y}_2)$	$R_{\dot{x}} = R_{\dot{y}} = \frac{\omega_n^2(2-\omega_n^2\tau^2)}{8CNR} e^{-\omega_n^2 \tau^2/4}$	$S_{\dot{x}\dot{x}} = S_{\dot{y}\dot{y}} = \frac{\omega^2}{2CNR}\sqrt{\frac{4\pi}{\omega_n^2}}\, e^{-\omega^2/\omega_n^2}$
noise	$E(x_1 \dot{x}_2)$ $E(y_1 \dot{y}_2)$	$R_{x\dot{x}} = R_{y\dot{y}} = \frac{\omega_n^2 \tau}{4CNR} e^{-\omega_n^2 \tau^2/4}$	$S_{x\dot{x}} = S_{y\dot{y}} = \frac{-j\omega}{2CNR}\sqrt{\frac{4\pi}{\omega_n^2}}\, e^{-\omega^2/\omega_n^2}$
* signal	$E(\dot{s}_1 \dot{s}_2)$ $E(\dot{c}_1 \dot{c}_2)$	$R_{\dot{s}} = R_{\dot{c}} = \frac{\omega_n^2(2-\omega_n^2\tau^2)}{8} e^{-\omega_n^2 \tau^2/4}$	$S_{\dot{s}\dot{s}} = S_{\dot{c}\dot{c}} = \frac{\omega^2}{2}\sqrt{\frac{4\pi}{\omega_n^2}}\, e^{-\omega^2/\omega_n^2}$
* signal	$E(s_1 \dot{s}_2)$ $E(c_1 \dot{c}_2)$	$R_{s\dot{s}} = R_{c\dot{c}} = \frac{\omega_n^2 \tau}{4} e^{-\omega_n^2 \tau^2/4}$	$S_{s\dot{s}} = S_{c\dot{c}} = \frac{-j\omega}{2}\sqrt{\frac{4\pi}{\omega_n^2}}\, e^{-\omega^2/\omega_n^2}$

Fig. 4.5 Table of signal and noise spectrums and autocorrelation functions for FM receiver no. 2

* In this section, $s = \sin \int m$, $c = \cos \int m$.

Double Frequency Signal	$E(s2_1 s2_2)$	$R_{s2} = \frac{1}{2} e^{-\omega_n^2 \tau^2}$	$S_{s2} = \frac{1}{2}\sqrt{\frac{\pi}{\omega_n^2}}\, e^{-\omega^2/4\omega_n^2}$
Double Frequency Signal	$E(s2_1 \dot{s}2_2)$	$R_{s2\dot{s}2} = \omega_n^2 \tau e^{-\omega_n^2 \tau^2}$	$S_{s2\dot{s}2} = \frac{-j\omega}{2}\sqrt{\frac{\pi}{\omega_n^2}}\, e^{-\omega^2/4\omega_n^2}$
Double Frequency Signal	$E(\dot{s}2_1 \dot{s}2_2)$	$R_{\dot{s}2} = \omega_n^2 (1-2\omega_n^2 \tau^2) e^{-\omega_n^2 \tau^2}$	$S_{\dot{s}2\dot{s}2} = \frac{\omega^2}{2}\sqrt{\frac{\pi}{\omega_n^2}}\, e^{-\omega^2/4\omega_n^2}$

Figure 4.5 Continued

* $s2 = \sin 2\int m$

	term	coefficient	correlated terms
1	m	B	1, 6, 7
2	$y(\cos \dot{\int} m)$	(2-B)	2, 5, 15, 17, 19, 22
3	$x(\sin \dot{\int} m)$	-(2-B)	3, 4, 16, 18, 20, 21
4	$\dot{x}(\sin \int m)$	-B	4, 16, 18, 20, 21
5	$\dot{y}(\cos \int m)$	B	5, 15, 17, 19, 22
6	my^2	-2	6, 7
7	mx^2	-z	7
8	$y^2(\sin \dot{2} \int m)$	+1/2	8, 10, 13
9	$xy(\cos \dot{2} \int m)$	+1	9, 11
10	$x^2(\sin \dot{2} \int m)$	-1/2	10, 12
11	$y\dot{x}(\cos 2 \int m)$	- 1	11, 14
12	$x\dot{x}(\sin 2 \int m)$	+1	12
13	$yy(\sin 2 \int m)$	- 1	13
14	$x\dot{y}(\cos 2 \int m)$	-1	14
15	$y^3(\cos \dot{\int} m)$	+1	15, 17, 19, 22
16	$xy^2(\sin \dot{\int} m)$	- 1	16, 20, 21, 24
17	$x^2y\ (\cos \dot{\int} m)$	+1	17, 19, 22, 23
18	$x^3\ (\sin \dot{\int} m)$	- 1	18, 20, 21
19	$y^2\dot{y}(\cos \int m)$	- 1	19, 22
20	$x^2\dot{x}(\sin \int m)$	+1	20, 21
21	$y^2\dot{x}(\sin \int m)$	+ 3	21, 24
22	$x^2\dot{y}(\cos \int m)$	- 3	22, 23
23	$yx\dot{x}(\cos \int m)$	+ 2	23
24	$y\dot{y}x(\sin \int m)$	- 2	24
25	$y^3\ \dot{x}$	+1	25, 26, 27, 28, 29, 30
26	$x^3\ \dot{y}$	- 1	26, 27, 28, 29, 30
27	$yx^2\dot{x}$	+1	27, 28, 29, 30
28	$xy^2\dot{y}$	- 1	28, 29, 30
29	$y\dot{x}$	(1-B)	29, 30
30	$x\dot{y}$	-(1-B)	30

Fig. 4.6 Table of output terms for FM receiver no. 2

Term Type	Common Factor	Correlation Terms	Term
mod* mod	R_m	$R_m \left[(B-2/\rho)^2 + 16\, R_x^2 \right]$	1
signal*	R_s	$2R_s \left[(B-2/\rho)^2\, R_x + 24 R_x \dot{R}_x^2 + 16 R_x \dot{R}_{xx}^2 \right]$	2
noise* signal* noise	$\dot{R}_s$	$2\dot{R}_s \left[(B-2-2/\rho)^2\, R_x + 8\, R_x^3 \right]$	3
	R_{ss}	$4R_{ss} \left[(B-2/\rho)(B-2-z/\rho) + 8R_x^2 \right] \dot{R}_{xx}$	4
	R_{sz}	$4R_{sz} \left[R_x \dot{R}_x - \dot{R}_{xx}^2 \right]$	5
	$\dot{R}_{sz}$	$2\dot{R}_{sz}\, R_x^2$	6
	$R_{sz\dot{s}z}$	$8R_{sz\dot{s}z}\, R_x\, \dot{R}_{xx}$	7
noise* noise	R_x	$2\left[(B-1-2/\rho)^2 + 8\, R_x^2 \right] \left[R_x \dot{R}_x + \dot{R}_{xx}^2 \right]$	8

ρ = CNR (for simplicity)

Fig. 4.7 Table of output correlation functions for FM receiver no. 2

Chapter 5

CONCLUSIONS

While the ML equation is solvable with the method presented in section 2.4.1, the procedure is much too lengthy to be of practical value at present. In order to reduce the complexity of the process, a way should be sought to maximize the likelihood function $L(\epsilon)$ without evaluating it for a large sequence of values of ϵ. If this is not possible, then the possibility of simplifying the modulation must be considered. The use of transformed modulation consisting of uncorrelated rectangular pulses representing the original bandlimited modulation sampled at the Nyquist rate may lead to significant simplifications. (The original signal can be reconstructed from the ML estimate of the samples at the receiver by employing the sampling theorem).

Additional reduction of computer time can be obtained if a phase-locked loop or some other FM receiver can be designed to supply the initial approximate solution for the procedure for solving the ML equation. This will be a necessary step if the equation is to be solved for large values of T. Otherwise, considerable computer time will be wasted seeking a coarse approximation to the solution. The device that produces approximate solutions with the highest likelihood would probably be best.

The problem of solving the ML equation for the case of a rectangular spectrum is not handled satisfactorily by using a Butterworth function of very high order. It may be possible to construct a differential equation for the solution by using the fact that the autocorrelation function for this case,

$$R_m(\tau) = \frac{\sigma^2 \sin\omega_m \tau}{\omega_m \tau}$$

is a solution of the time varying differential equation

$$\tau \ddot{R}_m + 2 \dot{R}_m + \omega_m^2 \tau R_m = 0$$

The generality of the method developed for solving the ML equation for FM indicates that it could be used to solve the ML equation for other types of modulation as well as other similar miximization problems not particularly associated with communications. Thus, a deeper mathematical investigation of the method would be worthwhile to determine the extent of applicability as well as to determine the circumstances under which it will lead to erroneous results.

The spike detection system developed in Chapter 3 is definitely not optimum; much work remains to be done in this area. It is possible that the likelihood function developed in section 2.4.2 could be used for spike detection. However, what is really needed is a function which measures the likelihood of a spike having occurred in a particular observation interval based on the data obtained in that interval.

The two non-feedback FM receivers which were analyzed in Chapter 4 were investigated because the determination of an optimum explicit function of FM data would be of great value. Basically, the reason is that the determination of the noise paths which cause spikes and the estimation of the number of spikes per second is much easier if the FM receiver is defined by an explicit function operating on the data followed by a low pass filter. Rice's (1.7) analysis of the FM discriminator is the best example of this technique. Thus, an important step toward understanding optimum FM receivers would be the formulation of a function which includes the CNR and other pertinent constants as well as the FM data and which provides an improvement over the FM discriminator, i.e., it results in an FM receiver with an SNR greater than the SNR at the output of the FM discriminator.

The attempts to determine thresholds of FM receivers in this thesis have led us to the conclusion that the method of direct simultation is too lengthy a process for a digital computer. The amount of data that must be examined is too great; other techniques must be developed which do not require direct simulation. The approach suggested by Spilker (5.1), for example, is interesting but it would be far more significant if the results could be identified in some way with specific SNR-CNR points.

A novel approach to the problem, suggested by Rice, is presently being investigated by Schilling and Osborne. The method consists of determining the response of a given FM receiver to certain typical noise waveforms. The noise chosen is the most probable n(t) or the expected n(t) given certain noise parameters. Using this method, the expected number of spikes per second and the location of threshold can be determined.

APPENDIX A

Inverse autocorrelation matrix operator

The equation

$$[R]^{-1} = \frac{\Delta t}{F.T.(R(\tau))} + \text{end point terms}$$

$$= \frac{\Delta t}{H(jw)} + \text{end point terms} \qquad jw = \frac{d}{dt} \qquad (2.34)$$

= a continuous operator + end point terms

for $w_o \Delta t << 1$

where $R(\tau)$ = an autocorrelation function

$H(jw)$ = Fourier Transform of $R(\tau)$

$\Delta \tau = \Delta t$ = sampling interval

w_o = bandwidth of $H(jw)$ in radians / second

$[R]$ = a matrix in which

$$R_{ij} = R((i-j)\Delta\tau), \quad \left.\begin{matrix} i = \text{row} \\ j = \text{column} \end{matrix}\right\} \text{of } [R]$$

= a discontinuous or sample operator

relates a sample operator to a continuous operator. This is an extremely useful tool since the inversion of a matrix is, in general, a complicated problem.

To demonstrate that the equation is valid, a simple example will be evaluated. Let

$$R(\tau) = e^{-w_o|\tau|} = r \qquad (A.1)$$

Then the matrix $[R]$ is given by

$$[R] = \begin{bmatrix} 1 & r & r^2 & r^3 & r^4 \\ r & 1 & r & r^2 & r^3 \\ r^2 & r & 1 & r & r^2 \\ r^3 & r^2 & r & 1 & r \\ r^4 & r^3 & r^2 & r & 1 \end{bmatrix} \qquad (A.2)$$

which has an inverse

$$[R]^{-1} = \frac{1}{1-r^2} \begin{bmatrix} 1 & -r & 0 & 0 & 0 \\ -r & 1+r^2 & -r & 0 & 0 \\ 0 & -r & 1+r^2 & -r & 0 \\ 0 & 0 & -r & 1+r^2 & -r \\ 0 & 0 & 0 & -r & 1 \end{bmatrix} \qquad (A.3)$$

Suppose this matrix operates on a sampled continuous function x(t) whose matrix is the column vector

$$[x] = \begin{bmatrix} x_1 \\ x_2 \\ x_3 \\ x_4 \\ x_5 \end{bmatrix} \qquad (A.4)$$

giving the result

$$[y] = \begin{bmatrix} y_1 \\ y_2 \\ y_3 \\ y_4 \\ y_5 \end{bmatrix} = \frac{1}{1-r^2} \begin{bmatrix} x_1 - rx_2 \\ (1+r^2)x_2 - r(x_1+x_3) \\ (1+r^2)x_3 - r(x_2+x_4) \\ (1+r^2)x_4 - r(x_3+x_5) \\ x_5 - rx_4 \end{bmatrix} \qquad (A.5)$$

Consider an intermediate value of y given

$$y_i = \frac{(1+r^2)\, x_i - r(x_{i-1} + x_{i+1})}{1-r^2} \tag{A.6}$$

$$\text{Let } x_{i-1} = x_i - \dot{x}_i \Delta t + \ddot{x}_i \frac{\Delta t^2}{2} - \text{ etc.} \tag{A.7}$$

$$x_{i+1} = x_i + \dot{x}_i \Delta t + \ddot{x}_i \frac{\Delta t^2}{2} + \text{ etc.} \tag{A.8}$$

Using the approximations

$$1 - r^2 \doteq 2w_o \Delta\tau = 2w_o \Delta t \tag{A.9}$$

$$r \doteq 1 \tag{A.10}$$

$$1-r \doteq w_o \Delta\tau = w_o \Delta t \tag{A.11}$$

which are valid if $w_o \Delta t \ll 1$, one gets

$$y_i \doteq \frac{\Delta t}{2w_o} \left[w_o^2 x_i - \ddot{x}_i \right] = \frac{w_o^2 - \left(\frac{d}{dt}\right)^2}{2w_o} x_i \Delta t \tag{A.12}$$

Checking back one finds that

$$H(jw) = \frac{w_o}{w_o^2 - p^2} \quad ; \quad \frac{1}{H(jw)} = \frac{w_o^2 - p^2}{2w_o} \tag{A.13}$$

so that the equation is valid for intermediate values of i. For the initial and final y values one gets

$$y_1 = \frac{w_o x_1 - \dot{x}_1}{2w_o} + \text{ terms containing } \Delta t \text{ factors} \tag{A.14}$$

$$y_5 = \frac{w_o x_5 + \dot{x}_5}{2w_o} + \text{ terms contain } \Delta t \text{ factors} \tag{A.15}$$

These are the initial and final value corrections to Eq. (2.34).

A second derivation of this result, which can be used to verify the case in which H(jw) is a Kth order Butterworth function, is the following:

Let $[a] = [R][b]\ \Delta t$ (A.16)

where $[a], [b]$ = column vectors,

In the limit as

$\Delta t \rightarrow 0$

$N \rightarrow \infty$

and $N\Delta t \rightarrow T$

Eq. (A.16) reduces to the equation

$$a(t) = \int_0^T R(t-\lambda)\ b(\lambda)\ d\lambda \tag{A.17}$$

If $R(\tau) = e^{-w_o|\tau|}$

then $$a(t) = \int_0^T e^{-w_o|t-\lambda|}\ b(\lambda)\ d\lambda \tag{A.18}$$

$$\dot{a}(t) = w_o \int_0^T e^{-w_o|t-\lambda|}\ \text{sgn}\ (t-\lambda)\ b(\lambda)\ d\lambda \tag{A.19}$$

$$\ddot{a}(t) = w_o^2 \int_0^T e^{-w_o|t-\lambda|}\ b(\lambda)\ d\lambda - 2w_o\ b(t) \tag{A.20}$$

where $$\text{sgn}\ (t-\lambda) = \begin{cases} +1 & \text{for } t-\lambda > 0 \\ -1 & \text{for } t-\lambda < 0 \end{cases} \tag{A.21}$$

By combining Eqs. (A.18) and (A.20), one finds that

$$b(t) = \frac{w_o^2 a - \ddot{a}}{2w_o} = \frac{w_o^2 - p^2}{2w_o}\ a(t),\quad p = d/dt \tag{A.22}$$

Comparing this result with the matrix equation for [b], i.e.,

$$[b] = \frac{1}{\Delta t}[R]^{-1}[a] , \tag{A. 23}$$

one finds that

$$[R]^{-1} \doteq \frac{w_o^2 - p^2}{2w_o} \Delta t \tag{A. 24}$$

However, this equation does not completely describe the situation; Eqs. (A. 18) and (A. 19) evaluated at t = 0 and t = T may be combined to give the results

$$\begin{aligned} w_o\, a(O) + \dot{a}\,(0) &= O \\ w_o\, a(T) - \dot{a}\,(T) &= O \end{aligned} \tag{A. 25}$$

These equations must be regarded as constraints under which Eq. (A. 24) is valid. Hence, there is no conflict between Eqs. (A. 24) and (2. 34).

Note that this result automatically eliminates the endpoint terms when a(t) is the solution of the ML equation because the form of Eq. (A. 17) with respect to the variable t is identical to the ML equation (Eq. (2. 26)).

The only place where the calculation $[R]^{-1}[a]$ is called for is in the determination of the likelihood function (Eq. (2. 11)) for a particular a(t). However, a(t) will always be generated from a function b(t) by using an equation similar to Eq. (A. 17). Consequently, the result of the operation $[R]^{-1}[a]$ is simply b(t) dt and, at the same time, the endpoint terms are zero.

APPENDIX B

SNR for the ML estimate at high CNR, large T and for a Butterworth modulation spectrum of order K

The general equation for the SNR for the ML estimate at high CNR and large T is

$$SNR = \frac{\sigma^2 \pi}{\int_0^\infty \frac{w^2 H(jw)\, dw}{\frac{2w_n\, CNR}{\pi} H(jw) + w^2}} \qquad (2.51)$$

For a Butterworth modulation spectrum of order K, H (jw) is given by

$$H(jw) = \sigma \frac{2K w_m^{2K-1} \sin\frac{\pi}{2K}}{w_m^{2K} + w^{2K}} \qquad (2.61)$$

Substituting this into the integral in Eq. (2.51) one finds that

$$\int_0^\infty \frac{w^2 H(jw)\, dw}{\frac{w_n}{\pi CNR} H(jw) + w^2} = \int_0^\infty \frac{2K\sigma^2 w_m^{2K-1} \sin\frac{\pi}{2K}\, w^2\, dw}{\frac{4K\sigma^2 w_n CNR\, w_m^{2K-1} \sin\frac{\pi}{2K}}{\pi} + w_m^{2K} w^2 + w^{2K+2}} =$$

(B.1A)

$$K\sigma^2 w_m^{2K-1} \sin\frac{\pi}{2K} \int_0^\infty \frac{w^2 dw}{G + w_m^{2K} w^2 + w^{2K+2}} \qquad (B.1B)$$

where

$$G = \frac{2}{\pi} K w_n^3\, CNR\, w_m^{2K-1} \sin\frac{\pi}{2K} \qquad (B.2)$$

$$\sigma^2 = w_n^2 / 2 \qquad (1.2)$$

The integral in Eq. (B.1B) could not be found in tables and could not be evaluated by using the sum of the residues at the poles of the integrand because the roots of the equation

$$w^{2K+2} + w_m^{2K} w^2 + G = 0 \tag{B.3}$$

could not be found except for the simple case of $K = 1$. However, this problem was avoided by obtaining an approximate value of the integral for large G.

Let

$$w^{2K+2} = G\lambda^{2K+2} \tag{B.4}$$

or

$$\lambda = wG^{-1/2K+2} \tag{B.5}$$

Then we have

$$\int_o^\infty \frac{w^2\,dw}{G + w_m^{2K} w^2 + w^{2K+2}} = \int_o^\infty \frac{G^{3/2K+2}\,\lambda^2\,d\lambda}{G + w_m^{2K} G^{1/K+1}\,\lambda^2 + G\lambda^{2K+2}} \tag{B.6A}$$

$$= \frac{1}{G^{(2K-1)/(2K+2)}} \int_o^\infty \frac{\lambda^2\,d\lambda}{1 + w_m^{2K} G^{-K/K+1}\,\lambda^2 + \lambda^{2K+2}} \tag{B.6B}$$

$$= \frac{1}{G^{(2K-1)/(2K+2)}} \left[\int_o^\infty \frac{\lambda^2 d\lambda}{1+\lambda^{2K+2}} - \frac{w_m^K}{G^{K/K+1}} \int_o^\infty \frac{\lambda^4\,d\lambda}{\left[1+\lambda^{2K+2}\right]^2} + \text{etc.} \right] \tag{B.6C}$$

where the expansion

$$\frac{1}{1+a} = 1 - a + a^2 - \text{etc.} \quad , \quad |a|<1 \tag{B.7}$$

has been used. The maximum magnitude of

$$a = \frac{w_m^{2K} \lambda^2}{G^{K/K+1}\left[1+\lambda^{2K+2}\right]} \quad , \quad K \geq 1 \tag{B.8}$$

is

$$a\,\max = \frac{w_m^{2K}}{G^{K/K+1}} \frac{1}{(1+K)\,K^{(2K-1)/(2K+2)}} \tag{B.9A}$$

$$\frac{w_m^{2K}}{2G^{K/K+1}} = \frac{1}{2\left[\frac{2}{\pi} K\beta^3 \,\text{CNR}\, \sin\frac{\pi}{2K}\right]^{K/K+1}} \tag{B.9B}$$

Hence, at high values of β^3 CNR the expansion in Eq. (B.6C) is valid.

Thus, at high β^3 CNR, the SNR is given by

$$\text{SNR} = \frac{\sigma^2 \pi G^{(2K-1)/(2K+2)}}{2K\sigma^2 w_m^{2K-1} \sin\frac{\pi}{2K} \left[\int_0^\infty \frac{\lambda^2 d\lambda}{1+\lambda^{2K+2}} - \frac{w_m^k}{G^{K/K+1}} \int_0^\infty \frac{\lambda^4 d\lambda}{\left[1+\lambda^{2K+2}\right]} - +\text{etc.}\right]} \tag{B.10}$$

which reduces to

$$\text{SNR} = \frac{K+1}{K} \frac{\sin\frac{3\pi}{K+2}}{\sin\frac{\pi}{2K}} \left[\frac{2K \sin\frac{\pi}{2K}}{\pi} \beta^3 \,\text{CNR}\right]^{(2K-1)/(2K+2)} \tag{2.58}$$

for β^3 CNR >> 1

when the equality (Ref. B.1)

$$\int_0^\infty \frac{\lambda^2 \, d\lambda}{1+\lambda^{2K+2}} = \frac{\pi}{(2K+2)\sin\frac{3\pi}{2K+2}} \qquad \text{(B.11)}$$

is used and all terms after the first term in the expansion in the denominator of Eq. (B.10) are neglected. This result checks exactly with Eqs. (2.52E) and (2.53E) where $K = 1$ and $K = \infty$ respectively.

APPENDIX C

Maximum total solution error

The total solution error for the ML equation is defined as

$$TSE = \int_0^T \left| \frac{A^2}{2N_o} \int_0^T R_m(t-\lambda) \left[\int_\lambda^T (s\cos a_i - c\sin a_i)_u du \right] d\lambda - a_i(t) \right| dt \qquad (C.1)$$

where $a_i(t)$ is not the solution but an estimate of the solution which is being tested at the i^{th} iteration. An approximate maximum value for the TSE in the no-noise case can be found by letting

$$s\cos a_i - c\sin a_i = \sin (m-a_i) = 1, \qquad (C.2)$$

the maximum value of the sine function. Then we have

$$TSE_{max} \approx \frac{A^2\sigma^2}{2N_o} \int_0^T \left[\int_0^T e^{-w_m|t-\lambda|} [T-\lambda] \, d\lambda \right] dt \qquad (C.3)$$

for the case

$$R_m(\tau) = \sigma^2 e^{-w_m|\tau|}, \qquad (C.4)$$

i.e., K = 1. The term $a_i(t)$ is small in comparison with the first term in Eq. (C.1) and may be neglected. Evaluating the integrals in Eq. (C. 3), one finds that

$$TSE_{max} \approx \frac{\beta^3 CNR\, w_m T}{\pi} \left[w_m T - 1 - e^{-w_m T} \right] \qquad (C.5)$$

For a rough approximation, the equation,

$$TSE_{max} \approx \frac{\beta^3 CNR\,(w_m T)\,(w_m T - 1)}{\pi} \qquad (2.101)$$

may be used since the inequality

$$e^{-w_m T} \ll 1$$

will generally be valid Computer studies (with noise present) have shown that this maximum value is sometimes exceed by a few percent. Thus, neglecting the noise in order to derive this approximation does not introduce a significant error.

APPENDIX D

SNR in a spike detection receiver

The basic equation for spike detection is the equation relating signal-to-noise power at the output to carrier-to-noise power at the input of the FM receiver as a function of the number of spikes per second at the output of the receiver. For sine wave modulation, the receiver input is

$$S(t) + n(t) = A \cos (w_c t + \beta \sin w_m t) + Ax \cos w_c t - Ay \sin w_c t \tag{D.1A}$$

$$S(t) + n(t) = R(t) \cos \left(w_c t + \beta \sin w_m t + \tan^{-1} \left(\frac{y \cos \phi - x \sin \phi}{1 + x \cos \phi + y \sin \phi} \right) \right)$$

where $\phi = \beta \sin w_m t$,

$$R(t) = \sqrt{(1 + x \cos \phi + y \sin \phi)^2 + (y \cos \phi - x \sin \phi)^2} \tag{D.2}$$

The output is given by

$$\frac{d}{dt} \left[\beta \sin w_m t + \tan^{-1} \left(\frac{y \cos \phi - x \sin \phi}{1 + x \cos \phi + y \sin \phi} \right) \right] \tag{D.3}$$

$$\approx \beta w_m \cos w_m t + \underbrace{\frac{d}{dt} \left[y \cos \phi - x \sin \phi \right]}_{\text{gaussian noise}} + \text{spikes}$$

with the first two terms being the signal and the gaussian noise respectively. The signal power is given by

$$E (\beta w_m \cos w_m t)^2 = \frac{\beta^2 w_m^2}{2} \tag{D.4}$$

The gaussian noise power (thru a low pass filter of bandwidth w_m) is

$$\frac{1}{\pi}\int_0^{w_m} S_g(w)\,dw = \frac{2No}{A^2\pi}\,\frac{w^3 m}{3}\left[1-\frac{3}{8\beta}\right] \qquad (D.5)$$

where $S_g(w)$ is the approximate spectral density of the gaussian noise. (See the derivation of Eq. (3.18)). The spike noise power may be calculated as follows: Let the spikes be random pulses of width E, height $\pm 2\pi/\epsilon$ and rate N_s (spikes/second) as in Figure D.1. The autocorrelation function for the spikes is shown in Figure D.2. The spectral density of the spike noise power at w = O is given by:

$$S_{sp}(O) = \int_{-\infty}^{+\infty} R_{sp}(\tau)\,d\tau = \frac{4\pi}{\epsilon}\,Ns\,\epsilon \qquad (D.6)$$

$$S_{sp}(O) = 4\pi^2 Ns$$

Assuming that $S_{sp}(w) \approx S_{sp}(O)$ over the bandwidth of the low pass filter, the spike noise is given by

$$\frac{1}{\pi}\int_0^{w_m} S_{sp}(O)dw = 4\pi\, w_m N_s \qquad (D.7)$$

Thus, the signal-to-noise power ratio (SNR) is equal to

$$SNR = \frac{\frac{\beta^2 w^2 m}{2}}{\frac{N_o w^3 m\,(1-3/8\beta)}{3A^2\pi} + 4\pi\, w_m N_s} \qquad (D.8)$$

The carrier-to-noise ratio is given by Eq. (1.5):

$$CNR = \frac{A^2\pi}{4N_o w_n} \qquad (1.5)$$

Hence, the SNR can be written in terms of the CNR as follows:

$$SNR = \frac{3\beta^2\left(\frac{w_n}{w_m}\right) CNR}{1 - \frac{3}{8\beta} + \frac{12\left(\frac{w_n}{w_m}\right) CNR}{f_m} N_s} \qquad (D.9)$$

where $f_m = w_m / 2\pi$.

Since $w_n = \beta w_m$, the equation reduces to

$$SNR = \frac{3\beta^3 CNR}{1 - \frac{3}{8\beta} + \frac{12\beta CNR}{f_m} N_s} \qquad (D.10)$$

For gaussian modulation, the result is the same if the equations

$$w_n^2 = 2E(m)^2 \doteq 2\sigma \leftarrow \left[\begin{array}{l}\text{approximately valid for} \\ \text{sinewave modulation}\end{array}\right]$$
$$w_n = \beta w_m \doteq \sqrt{2\sigma}$$

are used where

m = modulation
σ^2 = modulation power

Usually, the small correction term $3/8\beta$ is neglected in comparison with the two other terms in the denominator of Eq. (D.10). Thus, the standard form is

$$SNR = \frac{3\beta^3 CNR}{1 + 12 CNR \frac{\beta N_s}{f_m}} \qquad (D.11)$$

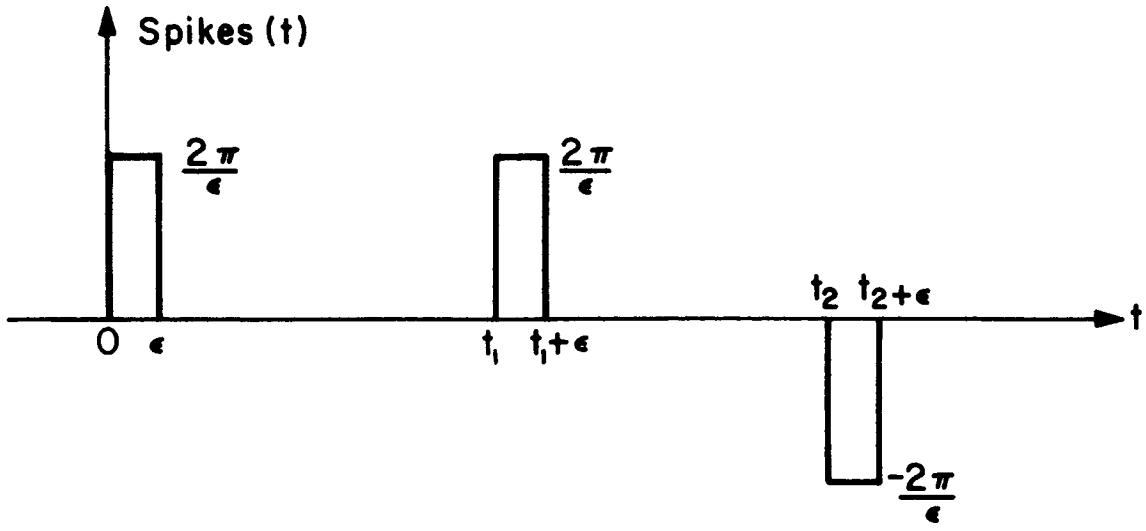

Fig. D.1 Approximation of spikes with a series of random pulses

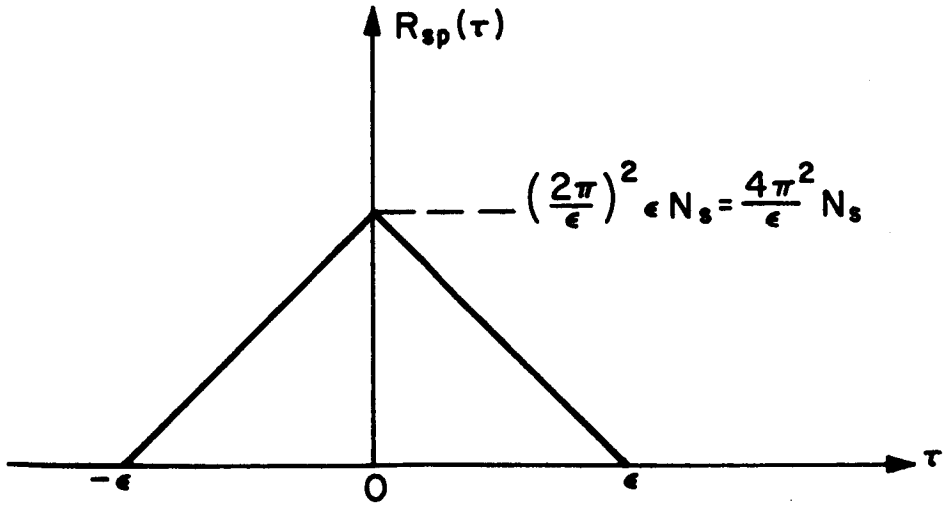

Fig. D.2 Autocorrelation function of a series of random pulses

APPENDIX E

Computer simulation of gaussian random noise

The gaussian random noise with a band limited spectrum is simulated by filtering a sequence of gaussian random numbers The gaussian random numbers are obtained by averaging a sequence of random numbers x_i generated by the following recursive scheme:

$$x_o = 1 \tag{E.1}$$

$$x_{i+1} = (2^{17} + 3)\, x_i \mod (2^{35}) \tag{E.2}$$

$$x_{i+1} = 131075\, x_i \mod (34, 359, 738, 368)$$

The period of this sequence is approximately 2^{33}.

By averaging 12 of these random numbers at a time, a good approximation to a gaussian random number is obtained as follows:

Let

$$\bar{x} = \frac{1}{n} \sum_{i=1}^{n} x_i \tag{E.3}$$

$$A = 2^{35} \tag{E.4}$$

$$y = \text{gaussian random number} = \frac{\bar{x} - E(\bar{x})}{\sqrt{E(\bar{x} - E(\bar{x}))^2}} \tag{E.5}$$

with zero mean, rms value = 1.

$$p(x_i) = \begin{cases} 1/A & O < x_i < A \\ O & \text{elsewhere} \end{cases} \tag{E.6}$$

$$E(x_i) = \int_0^A x_i p(x_i)\, dx_i = \int_0^A \frac{x}{A}\, dx = \frac{A}{2} \tag{E.7}$$

$$E(x_i - \tfrac{A}{2})^2 = \int_0^A (x_i - \tfrac{A}{2})^2 p(x_i)\, dx_i = \frac{A^2}{12} \tag{E.8}$$

$$E(\bar{x}) = E(x_i) = A/2 \tag{E.9}$$

$$E\left[\bar{x} - \frac{A}{2}\right]^2 = E\left[\frac{1}{n}\sum_{i=1}^{n}\left(x_i - \frac{A}{2}\right)\right]^2 \qquad \text{(E.10A)}$$

$$= \frac{1}{n^2}\left[\sum_{i=1}^{n} E\left(x_i - \frac{A}{2}\right)^2\right] = \frac{A^2}{12n} \qquad \text{(E.10B)}$$

Therefore,

$$y = \left[\frac{1}{n}\sum_{i=1}^{n} x_i - \frac{A}{2}\right]\frac{\sqrt{12n}}{A} \qquad \text{(E.11)}$$

For n = 12, the equation reduces to the simple form

$$y = \frac{1}{A}\left[\sum_{i=1}^{12} x_i\right] - 6 \qquad \text{(E.12)}$$

The ratio of the peak value to the rms value for this noise is

$$\frac{A}{2} \Big/ \frac{A}{\sqrt{12n}} = \sqrt{3n} = \sqrt{36} = 6 \qquad \text{(E.13)}$$

For n = 12, we have what is generally called "6σ" noise.

Filtering of the gaussian random noise was performed by making use of the sampling theorem to fill in intermediate values between the noise samples, y_i. According to the sampling theorem, the uncorrelated y_i can be assumed to be coming from the sampling of a process of bandwidth w_n at intervals $\Delta T = \pi / w_n$. If we let $Z_{5i} = y_i$, then the intermediate values, Z_i, are given by

$$Z_i = \sum_{j=-\infty}^{-\infty} Z_{5j} \frac{\sin(5j - i)\pi/5}{(5j - i)\pi/5} \qquad \text{(E.14)}$$

The new sequence Z_i has a bandwidth w_n but the samples are now $\Delta T/5 = \pi/5w_n$ apart. If we let this time interval equal 1 second, then the Z_i process has a bandwidth equal to $\pi/5$ radians/second.

The average power in the two processes, y and Z, are the same. The great usefulness of this technique is that, on the average, each gaussian random number produces 5 noise samples. Normally, with ordinary filtering on a computer, each gaussian random number produces only one noise sample. Since the computation of gaussian random numbers is relatively lengthy, this procedure reduces computer time. For the computer programs, using the six largest terms in the summation over j in Eq. (E. 14) was found to produce satisfactory results.

The Fortran IV program used for generating gaussian random numbers is given below:

```
901  FUNCTIΦN GRN(NR)
902  SRN = 0.
903  DΦ 905 JN = 1,12
904  NR = 131075 * NR
905  SRN = SRN + FLΦAT (NR)
906  GRN = 2.91038304 E - 11 * SRN - 6.
907  RETURN
     END
```

APPENDIX F

Computer simulation of the iterative procedure for solving the maximum likelihood equation

The computer program employed to solve the ML equation using the procedure developed in section 2.4.1 is given below. The program is written in FORTRAN IV. An explanation of the various symbols, constants and equations used is given after the complete program.

```
1.    DIMENSIΦN R(250), T(250), AS(250), AR(250), BS(250), BR(250),
      SCCS(250)
2.    DATA CNR, PR, PK, PM, PN/+3.0, 3.5355, .01578, .0040/
3.    DATA PW, PC, NR/.1257, 49.3, 1/
4.    DATA DB, DC/ -99., -99./
5.    DΦ 12  I = 1, 250
6.    X = .0444 * FLΦAT (I)
7.    S = SIN(X) + PR * GRN (NR)
8.    C = CΦS(X) + PR * GRN (NR)
9.    R(I) = SQRT (S * S + C * C)
10.   T(I) = ATAN 2 (S, C)
11.   AS(I) = O.
12.   BS(I) = O.
13.   DΦ 75  I = 1, 11
14.   IF (I. EQ. 1) GO TO 45
15.   DM1 = O.
16.   DM2 = O.
17.   DM3 = O.
18.   DΦ 21  IA = 1, 250
19.   DM1 = DM1 + AS(IA) * BS(IA)
20.   DM2 = DM2 + AS(IA) * BR(IA) + AR(IA) * BS(IA)
21.   DM3 = DM3 + AR(IA) * BR(IA)
23.   D2 = -98.
24.   DΦ39  IB = 1, 41
25.   E = .01 * FLΦAT (IA) - .21
26.   A = O.
27.   DN = O.
28.   DΦ 30 IC = 1, 250
29.   A = A + .1 * (AS(IC) + E * AR(IC))
30.   DN = DN + R(IC) * CΦS(T(IC) - A)
31.   DA = DB
32.   DB = DC
33.   DC = PN * DN - PM * (DM1 + E * (DM2 + E * DM3) )
34.   IF (D2. GE. DB) GΦ TΦ 39
35.   D1 = DA
36.   D2 = DB
37.   D3 = DC
```

```
38.   E2 = E - .01
39.   CΦNTINUE
40.   EB = E2 + .005 * (D3-D1)/(2. *D2 - D1 - D3)
41.   FL = D2 + .125 * (D3-D1) * (D3-D1)/(2. *D2-D1-D3)
42.   DΦ 44  ID = 1, 250
43.   AS(ID) = AS(ID) + EB * AR(ID)
44.   BS(ID) = BS(ID) + EB * BR(ID)
45.   A = O.
46.   SCC = O.
47.   DΦ 50  IE = 1, 250
48.   A = A + .1*AS(IE)
49.   SCC = SCC + R(IE) * SIN(T(IE) - A)
50.   SCCS(IE) = SCC
51.   U1 = O.
52.   V1 = O.
53.   DΦ 60  IF = 1, 250
54.   J = 251 -IF
55.   U2 = -PW*U1 + SCC - SCCS(IF)
56.   U1 = U1 + .1*U2
57.   AR(IF) = U1
58.   V2 = PW * V1 + SCCS(J) - SCC
59.   V1 = V1 - .1*V2
60.   BR(J) = V1
61.   ERR = O.
62.   TSE = O.
63.   DΦ 69  IG = 1, 250
64.   A1 = PK*(AR(IG) + BR(IG) )
65.   A4 = AS(IG)
66.   ERR = ERR + (A4 - .444) ** 2
67.   TSE = TSE + ABS (A1 - A4)
68.   AR(IG) = A1 - A4
69    BR(IG) = SCC-SCC(IG) - BS(IG)
70.   IF(I. EQ. 1) GΦ TΦ 75
71.   SNR = 10. * ALΦG1O(PC/ ERR)
72.   TSE = .1*TSE
73.   WRITE (6, 74) I, SNR, TSE, D2, FL, E2, EB
74.   FΦRMAT (1X,I3, F6. 2, F10. 3, 2F10. 5, 2F8. 5)
75.   CΦNTINUE
76.   DΦ 78  IH = 1, 25
77.   K = 10* IH-9
78.   AS(IH) = .1*(AS(K) + AS(K+1) + AS(K+2) +
      AS(K+3) + AS(K+4) +AS(K+5) + AS(K+6) +
      AS(A+7) + AS(K+8) + AS(K+9) )
79.   WRITE (6, 80) (AS(L), L=1, 25)
80.   FΦRMAT (1X, 5F10. 5)
81.   STΦP
82.   END
```

Given data:

$CNR = 2 = 3db$ (carrier-to-noise ratio)
$A = 1$ (carrier amplitude)
$w_m = \pi/25$ (modulation bandsidth, rad/sec.)
$w_n = \pi/5$ (noise bandsidth, rad/sec.)
$\beta = 5$ (modulation index)

$R_m(\tau) = \sigma^2 e^{-w_m|\tau|}$ (modulation autocorrelation function)

$R_n(\tau) = No\ \delta(\tau)$ (noise autocorrelation function)

$m(t) = \sigma = w_n/\sqrt{2}$ (modulation)

n(t) = gaussian random numbers (noise)
$\Delta t = .1$ (sampling interval, seconds)
$N = 250$ (number of samples)

Program constants:

$$PR = \sqrt{\frac{\pi}{2CNR\ w_n \Delta t}} = \text{noise coefficient}$$

$$PK = \frac{w_n^3\ CNR\ \Delta t}{\pi} = \text{ML equation coefficient}$$

$$PM = \frac{\Delta t}{2N} = \text{coefficient of } L_2 \text{ (likelihood function)}$$

$$PN = \frac{1}{N} = \text{coefficient of } L_1 \text{ (likelihood function)}$$

$PC = N\sigma^2$ = SNR coefficient

$PW = w_m$ = modulation bandwidth

NR = 1 = initial value for random number generator
Constant in step 6 = $.0444 = \sigma\Delta t$
Constant in step 66 = $.444 = \sigma$
DB = -99.
DC = -99. } initial values
D2 = -98.

$\Delta t = .1$; used in steps 29, 48, 56, 59 and 72

Program symbols:

AS ( ) = $a_i(t)$ = approximate solution of the ML equation
AR ( ) = $a_R(t) - a_i(t)$ = solution error

$$BS(\ ) = \frac{\pi}{2\beta^3 CNR w_m^4\ \Delta t}\ (w_m^2 a_i - \ddot{a}_i)$$

$$BR(\ ) = \frac{\pi}{2\beta^3 CNR\, w_m^4 \Delta t}\left(w_m^2(a_R - a_i) - (\dot{a}_R - \dot{a}_i)\right)$$

E = ϵ ; range: - . 21 to +. 21

DA, DB, DC
D1, D2, D3 } = consecutive values of the likelihood function

EB = value of ϵ corresponding to the peak of the likelihood function; step 40 estimates location of the peak based on a parabola being passed thru the points (E-. 02, D1), (E-. 01, D2), and (E, D3)

FL = estimated balue of the likelihood function at the peak of the parabola noted above (see step 41)

A = $\int a$ = approximate modulation angle

SCC - SCCS ( ) = $b_1(t)$; see Eq. (2.66)

U1 = $b_2(t)$; see Eq. (2.67A)

V1 = $b_4(t)$; see Eq. (2.67C)

ERR = squared error
TSE = total solution error
A1 = $a_R(t)$; see step 64 and Eq. (2.68)

SNR = output signal-to-noise ratio in db

BIBLIOGRAPHY

Chapter 1

1.1 Optimum Demodulation
F. Lehan, R. Parks IRE Conv Rec. IT 3/53

1.2 The use of the method of maximum likelihood in estimating continuous - modulated intelligence which has been corrupted by noise.
D. Youla IRE Trans. IT 3/54

1.3 Results of Investigations of analog and digital communication techniques
H. Becker, J. Lawton, A. Kobos IEEE Conv. Rec. Part 6 3/64

1.4 Maximum a posteriori demodulation of analogue-type signals through random fading media
M. Schwartz Res. Rep. PIBMRI - 1244-64 12/64

1.5 The structure of efficient demodulators for multidimensional phase modulated signals
H. Van Trees IEEE Trans. CS 9/63

1.6 Error Rates for digital signals demodulated by an FM discriminator
D. Schilling, E. Hoffman, E. Nelson IEEE Trans. CT 6/67

1.7 Noise in FM Receivers
S. Rice Time Series Analysis Chapter 25 1963

1.8 The spectrum of a carrier frequency modulated by gaussian noise
J. Stewart Proc. IRE Vol. 42 10/54

1.9 A comparison of the threshold performance of the frequency demodulator using feedback and the pahse locked loop
D. Schilling, J. Billig Res. Report PIBMRI-1207-64 2/64

Chapter 2

2.1 The Fourier Integral and its applications
A. Papoulis McGraw-Hill p. 274, eq. I-23 1962

2.2 Probability, random variables, and stochastic processes
A. Papoulis McGraw-Hill p. 405, eq. 11-44 1965

2.3 Synthesis of Passive Networks
E. Guillemin John Wiley and Sons p. 588-591 1957

2.4 A special method of successive approximations for Fredholm Integral Equations
H. Buckner Duke Math. Jnl. Vol. 15, p. 197 1946

2.5 On the solution of Fredholm Integral Equations of the second kind by iteration
C. Wagner Journal of Math. and Phys. Vol. 31, p. 23 1952

2.6 Rapidly converging solutions to integral equations
P. Samuelson Journal of Math. and Phys. Vol. 31, p. 276 1952

Chapter 3

3.1 A new approach to the analysis of FM threshold reception
J. Cohn Proc. N.E.C. p. 221-236 1956

Chapter 4

5.1 Threshold Comparison of Phase-lock, Frequency-lock, and Maximum Likelihood types of FM Discriminators
J. Spilker IRE Weson Conv. Record Part 14 1963

Appendix B

B.1 Rhinehart Mathematical Tables, Formulas and Curves
H. Larsen Rhinehart and Co. Inc., N.Y. p. 266, Eq. 442 1953